nature synthesis

Article

https://doi.org/10.1038/s44160-023-00292-9

Catalytic production of ammonia from dinitrogen employing molybdenum complexes bearing N-heterocyclic carbene-based PCP-type pincer ligands

In the format provided by the authors and unedited

Table of Contents

1. General Methods

^{1}H NMR (400 MHz), ^{13}C NMR (101 MHz), ^{19}F NMR (376 MHz), ^{31}P NMR (162 MHz), and ^{77}Se NMR (76 MHz) spectra were recorded on a JEOL JMN-ECS400 spectrometer in suitable solvents, and spectra were referenced to residual solvent (^{1}H, ^{13}C{^{1}H}) or external standard (^{31}P: 85% H_3PO_4, ^{19}F: C_6F_6, ^{77}Se: $SePh_2$). Magnetic susceptibility was measured in CD_2Cl_2 or THF-d_8 using the Evans method.[S1] IR spectra were recorded on a JASCO FT/IR 4100 Fourier Transform infrared spectrometer. Ultraviolet–visible (UV–vis) absorption spectra were recorded on a Shimadzu MultiSpec-1500 and a Shimadzu UV-1850. Evolved dihydrogen was quantified by a gas chromatography using a Shimadzu GC-8A with a TCD detector and a SHINCARBON ST (6 m x 3 mm). Mass spectra were measured on a JEOL JMS-700 mass spectrometer. Elemental analyses were performed at Microanalytical Center of The University of Tokyo.

All manipulations were carried out under an atmosphere of nitrogen or argon by using standard Schlenk techniques or glovebox techniques unless otherwise stated. Solvents were dried by general methods and degassed before use. [MoI_3(PCP)],[S2] [MoI_3(CF_3-PCP)],[S3] KC_8,[S4] $FeCp_2OTf$,[S5] $CoCp^*_2$,[S6] 4,5-bis(trifluoromethyl)-*o*-phenylenediamine,[S7] [$MoCl_3$(thf)$_3$],[S8] [$Mo(CO)_3$(η^6–toluene)],[S9] SmI_2(thf)$_2$,[S10] **1a**,[S11] and **1b**[S11] were prepared according to the literature methods. All the other reagents were commercially available.

2. Experimental procedures

Preparation of [Mo(N)I(PCP)]OTf.

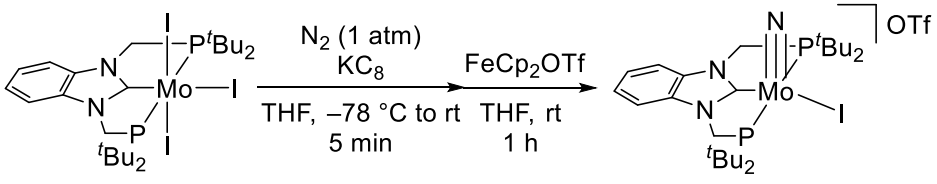

To a solution of [MoI_3(PCP)] (456 mg, 0.500 mmol) in THF (20 mL) at -78 ˚C was added a suspension of KC_8 (149 mg, 1.10 mmol) in THF (5 mL) at -78 ˚C under N_2, and the mixture was stirred at room temperature for 3 h. The dark brown solution was filtered through Celite, and the filter cake was washed with THF (2 mL x 3). To the combined extract was added [$FeCp_2$]OTf (160 mg, 0.4 mmol), and the mixture was stirred at room temperature for 1 h. Volatiles were removed in vacuo, and the residue was washed with hexane (5 mL x 3). The residue was extracted with CH_2Cl_2 (25 mL+2 mL x 5), and slow addition of hexane (40 mL) to the extract gave

[Mo(N)I(PCP)]OTf as orange crystals, which were collected by filtration, washed with cold THF (1 mL x 2) and hexane (1 mL x 3), and dried in vacuo (199 mg, 0.243 mmol, 51% yield). Anal Calcd for $C_{26}H_{44}F_3IMoN_3O_3P_2S$ + 0.5CH_2Cl_2: C, 36.88; H, 5.26; N, 4.87. Found: C, 36.83; H, 5.28; N, 4.83.

Preparation of [Mo(N)I(PCP)]BAr^F_4.

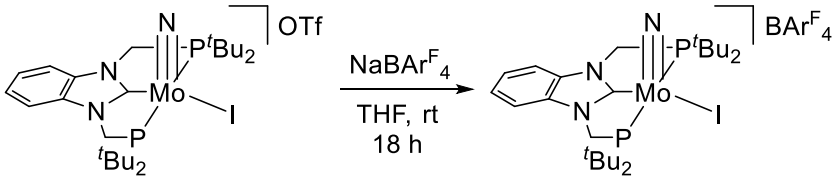

A mixture of [Mo(N)I(PCP)]OTf (100 mg, 0.122 mmol) and $NaBAr^F_4$ (108 mg, 0.122 mmol) in THF was stirred at room temperature for 18 h. The resultant orange solution was dried in vacuo, and the Et_2O (5 mL) was added to the residue. The solution was filtered through Celite, and filter cake was washed with Et_2O (2 mL x 3). Slow addition of hexane (15 mL) to the extract gave [Mo(N)I(PCP)]BAr^F_4 as orange crystals, which were collected by filtration, washed with hexane (1 mL x 3), and dried in vacuo (154 mg, 0.101 mmol, 83% yield). Anal Calcd for $C_{57}H_{56}F_{24}IMoN_3P_2$: C, 44.61; H, 3.68; N, 2.74. Found: C, 44.98; H, 3.27; N, 2.78.

Preparation of [Mo(N)I(PCP)] (2a).

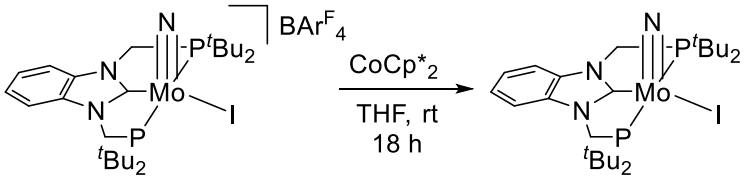

To a solution of [Mo(N)I(PCP)]BAr^F_4 (144 mg, 0.0941 mmol) in THF (8 mL) was added a solution of CoCp*$_2$ (32.4 mg, 0.0984 mmol) in THF (2 mL), the mixture and was stirred at room temperature for 18 h. After the resultant yellow-green solution was dried in *vacuo*, and the residue was washed with Et_2O (2 mL x 4) and dried in vacuo. Recrystallization from THF-hexane afforded **2a** as brown crystals (34.0 mg, 0.0506 mmol, 54% yield). Anal Calcd for $C_{25}H_{44}IMoN_3P_2$+C_4H_8O: C, 46.84; H, 7.05; N, 5.65. Found: C, 47.12; H, 7.01; N, 5.76. ^{1}H NMR (C_4D_8O): δ 7.78-7.74 (m, 2H), 7.42-7.37 (m, 2H), 4.79 (d, J = 13.6 Hz, 2H), 4.66 (d, J = 13.6 Hz, 2H), 1.61 (s, 18H), 1.17 (s, 18H). ^{31}P{^{1}H} NMR (C_4D_8O): δ 111.2 (s).

Preparation of 7c–7f

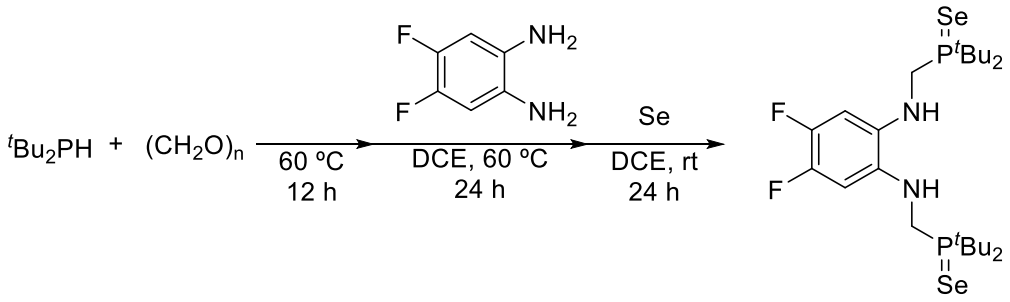

A typical procedure for the preparation of **7c** is described below. A mixture of $^{t}Bu_2PH$ (1.12 g, 7.41 mmol) and paraformaldehyde (225 mg, 7.49 mmol) in 50 mL of Schlenk flask was stirred at 60 °C for 17 h. 1,2-Dichloroethane (50 mL) and 4,5-difluoro-1,2-diaminobenzene (432 mg, 3.00 mmol) were added to the resulting liquid and stirred at 60 °C for 11 h. Elemental selenium (671 mg, 8.50 mmol) was added to the resulting mixture and stirred 60 °C for 16 h. The solvent was removed *in vacuo*, and then the crude mixture was purified by column chromatography (SiO_2) with hexane/CH_2Cl_2 (33/66 to 20/80) to give **7c** as a pale brown solid (1.16 g, 1.83 mmol, 61 %). **7c**: M.p. = 187.5–189.2 °C. ^{1}H NMR ($CDCl_3$): δ 6.50 (t, J = 9.8 Hz, 2H), 4.76 (br, 2H), 3.31 (d, J = 6.8 Hz, 4H), 1.42 (d, J = 15.6 Hz, 36H). $^{13}C\{^{1}H\}$ NMR ($CDCl_3$): δ 143.5 (dd, J = 238.6, 15.3 Hz), 134.2–134.0 (m), 101.4–100.8 (m), 37.2 (d, J = 32.6 Hz), 35.6 (d, J = 40.3 Hz), 28.0 (s). ^{19}F NMR ($CDCl_3$): δ –150.6 (t, J = 11.7 Hz). $^{31}P\{^{1}H\}$ NMR ($CDCl_3$): δ 79.6 (s with Se satellites, J = 702.0 Hz). HRMS (FAB) Calcd. for $C_{24}H_{45}N_2F_2P_2Se_2$ $[M+H]^+$: 621.1356. Found 621.1356.

Isolated yields and spectroscopic data of **7d**–**7f** are summarized below:

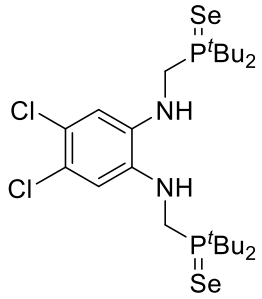

7d: 66% yield. A white solid. M.p. = 195.4 – 196.5 °C. ^{1}H NMR ($CDCl_3$): δ 6.64 (s, 2H), 4.77 (dt, 2H, J = 8.8 and 5.1 Hz), 3.28 (dd, 4H, J = 6.4 and 5.1 Hz), 1.42 (d, J = 15.6 Hz, 36H). $^{13}C\{^{1}H\}$ NMR ($CDCl_3$): δ 137.4 (d, J = 11.5 Hz)), 121.6 (s), 112.1 (s), 37.2 (d, J = 32.6 Hz), 34.8 (d, J = 40.3 Hz), 28.0 (s). $^{31}P\{^{1}H\}$ NMR ($CDCl_3$): δ 79.7 (s with Se satellites, J = 706.2 Hz). HRMS (FAB) Calcd. for $C_{24}H_{44}N_2Cl_2P_2Se_2$ $[M]^+$: 652.0687. Found: 652.0679.

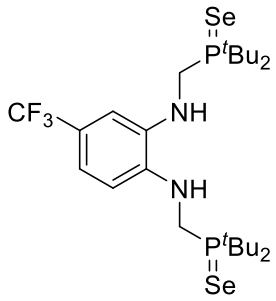

7e: 63% yield. A white solid. M.p. = 198.1– 199.6 °C. ^{1}H NMR ($CDCl_3$): δ 7.07 (d, *J* = 7.8 Hz, 1H, Ar*H*), 6.81 (s, 1H), 6.65 (d, *J* = 7.8 Hz, 1H), 5.02–4.98 (m, 1H), 4.80–4.76 (m, 1H), 3.39–3.33 (m, 4H), 1.44 (d, *J* = 15.2 Hz, 18H), 1.43 (d, *J* = 14.8 Hz, 18H). ^{13}C{^{1}H} NMR ($CDCl_3$): δ 140.4 (d, *J* = 10.6 Hz), 136.8 (d, *J* = 10.5 Hz), 125.0 (q, *J* = 271.2 Hz), 120.9 (q, *J* = 32.3 Hz), 117.3 (s), 110.2 (s), 108.1 (s), 37.32 (d, *J* = 32.6 Hz), 37.29 (d, *J* = 32.8 Hz), 34.9 (d, *J* = 39.3 Hz), 34.8 (d, *J* = 40.2 Hz), 28.11 (s), 28.07 (s). ^{19}F NMR ($CDCl_3$): δ –60.8 (s). ^{31}P{^{1}H} NMR ($CDCl_3$): δ 80.0 (s with Se satellites, *J* = 706.1 Hz), 79.6 (s with Se satellites, *J* = 706.1 Hz). HRMS (FAB) Calcd. for $C_{25}H_{45}N_2F_3P_2Se_2$ $[M]^+$: 652.1341. Found 652.1373.

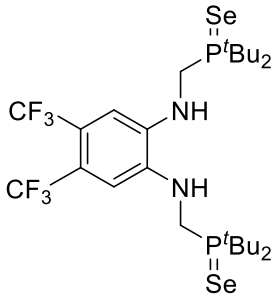

7f: 49% yield. A white solid. M.p. = 225.0– 226.7 °C. ^{1}H NMR ($CDCl_3$): δ 6.92 (s, 2H), 5.21 (br, 2H), 3.35 (d, 4H, *J* = 7.2 Hz), 1.44 (d, *J* = 15.6 Hz). ^{13}C{^{1}H} NMR ($CDCl_3$): δ 138.8 (d, *J* = 10.6 Hz), 123.6 (q, *J* = 273.2 Hz), 119.0–118.0 (m), 108.8 (s), 37.4 (d, *J* = 33.6 Hz), 33.7 (d, *J* = 39.3 Hz), 28.0 (s). ^{19}F NMR ($CDCl_3$): δ –57.9 (s). ^{31}P{^{1}H} NMR ($CDCl_3$): δ 80.3 (s with Se satellites, *J* = 710.6 Hz). HRMS (FAB) Calcd. for $C_{26}H_{45}N_2F_6P_2Se_2$ $[M+H]^+$: 721.1293. Found 721.1275.

Preparation of 8c–8e

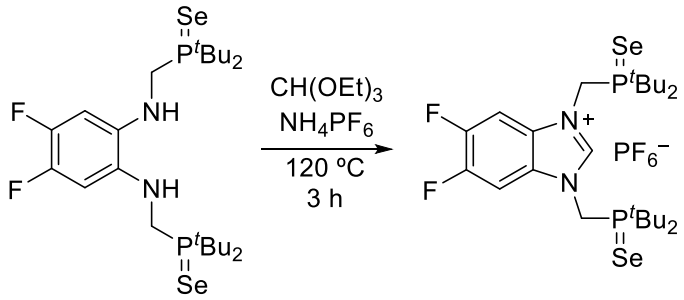

A typical procedure for the preparation of **8c** is described below. To a mixture of **7c** (583 mg, 0.922 mmol) and NH_4PF_6 (153 mg, 0.938 mmol) was added $CH(OEt)_3$ (3 mL), and the mixture in 200 mL of Schlenk flask was stirred at 120 °C for 3 h. The volatiles were removed *in vacuo*. The resultant solid was washed with CH_2Cl_2/Et_2O = 1/2 (v/v, 12 mL x 3) and Et_2O (7 mL x 1) and dried under vacuum to give **8c** as a white solid (596 mg, 0.769 mmol, 83 %).

8c: M.p. > 200 °C (decomp.). ^{1}H NMR (Acetone–d_6): δ 10.66 (s), 8.47 (t, J = 8.2 Hz, 2H), 5.53 (d, J = 3.2 Hz, 4H), 1.49 (d, J = 16.0 Hz, 36H). ^{13}C{^{1}H} NMR (Acetone–d_6): δ 151.0 (dd, J = 251.6, 16.8 Hz), 144.6 (s), 128.6 (t, J = 6.2 Hz), 104.8–104.3 (m), 41.1 (d, J = 25.8 Hz), 39.4 (d, J = 31.7 Hz), 28.2 (s). ^{19}F NMR (Acetone–d_6): δ –72.5 (d, J = 705.3 Hz), –135.6 (s).^{31}P{^{1}H} NMR (Acetone–d_6): δ 82.7 (s with Se satellites, J = 732.4 Hz), –144.0 (sep, J = 708.4 Hz). HRMS (FAB) Calcd. for $C_{25}H_{43}N_2F_2P_2Se_2$ [M]$^+$: 631.1200. Found 631.1187.

Isolated yields and spectroscopic data of **8d** and **8e** are summarized below:

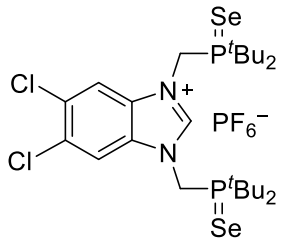

8d: 81% yield. A white solid. M.p. > 200 °C (decomp.). ^{1}H NMR (Acetone–d_6): δ 10.69 (s), 8.69 (s, 2H), 5.57 (d, J = 2.8 Hz, 4H), 1.50 (d, J = 16.4 Hz, 36H). ^{13}C{^{1}H} NMR (Acetone–d_6): δ 144.6 (s), 132.1 (s), 131.7 (s), 117.0 (s), 40.8 (d, J = 26.8 Hz), 39.2 (d, J = 30.7 Hz), 28.0 (s). ^{31}P{^{1}H} NMR (Acetone–d_6): δ 83.1 (s with Se satellites, J = 732.4 Hz), –143.9 (sep, J = 708.4 Hz). HRMS (FAB) Calcd. for $C_{25}H_{43}N_2Cl_2P_2Se_2$ [M]$^+$: 663.0609. Found 663.0620.

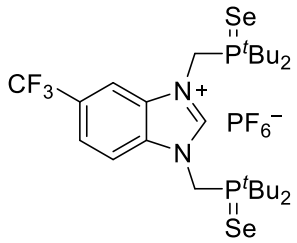

8e: 90% yield. A white solid. M.p. > 190 °C (decomp.). ^{1}H NMR (Acetone–d_6): δ 10.70 (s, 1H), 8.81 (s, 1H), 8.60 (d, J = 8.8, 1H), 8.13 (dd, J = 8.6 and 1.0 Hz, 1H), 5.71 (d, J = 2.8 Hz, 2H), 5.63 (d, J = 2.8 Hz, 2H), 1.52 (d, J = 16.0 Hz, 18H), 1.51 (d, J = 16.0 Hz, 18H). ^{13}C{^{1}H} NMR (Acetone–d_6): δ 145.1 (s), 134.5 (s), 132.2 (s), 129.3 (q, J = 33.5 Hz), 124.8 (q, J = 3.7 Hz), 124.6 (q, J = 268.7 Hz), 116.7 (s), 113.7 (q, J = 3.9 Hz), 40.8 (d, J = 25.8 Hz), 40.6 (d, J = 26.8 Hz), 39.3 (d, J = 31.7 Hz), 39.2 (d, J = 31.7 Hz), 28.0 (s). ^{19}F NMR (Acetone–d_6): δ –61.9 (s), –72.3 (d, J = 711.0 Hz, PF_6^-). ^{31}P{^{1}H} NMR (Acetone–d_6): δ 83.7 (s with Se satellites, J = 736.8 Hz), 83.2 (s with Se satellites, J = 736.8 Hz), –143.9 (sep, J = 710.6 Hz). HRMS (FAB) Calcd. for $C_{26}H_{44}N_2F_3P_2Se_2$ [M]$^+$: 663.1262. Found 663.1258.

Preparation of 8f

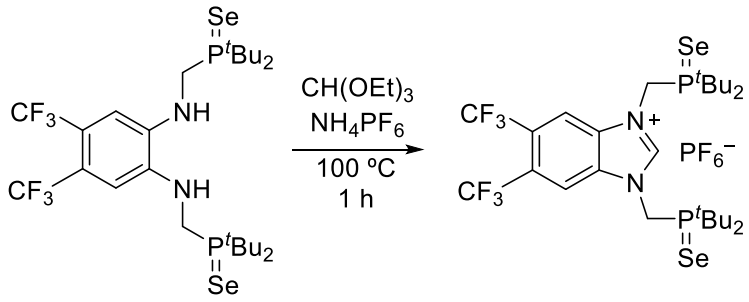

To a mixture of **7f** (3.10 g, 4.31 mmol) and NH_4PF_6 (703 mg, 4.31 mmol) was added $CH(OEt)_3$ (12 mL), and the mixture in 200 mL of Schlenk flask was stirred at 100 °C for 1 h. The volatiles were removed *in vacuo*. The resultant solid was washed with CH_2Cl_2/hexane = 1/4 (v/v, 10 mL x 3) and boiled EtOH (20 mL) and dried under vacuum to give **8f** as a white solid (2.44 g, 2.79 mmol, 65 %). M.p. > 180 °C (decomp.). ^{1}H NMR (Acetone–d_6): δ 10.76 (s, 1H), 9.05 (s, 2H), 5.80 (d, J = 3.6 Hz, 4H), 1.53 (d, J = 16.0 Hz, 36H). ^{13}C{^{1}H} NMR (Acetone–d_6): δ 147.3 (s), 134.3 (s), 127.1–125.9 (m), 123.7 (q, J = 273.8 Hz), 117.9 (s), 41.6 (d, J = 25.8 Hz), 39.6 (d, J = 31.7 Hz), 28.2 (s). ^{19}F NMR (Acetone–d_6): δ –59.1 (s), –72.7 (d, J = 704.9 Hz). ^{31}P{^{1}H} NMR (Acetone–d_6): δ 83.4 (s with Se satellites, J = 736.8 Hz), –144.0 (sep, J = 708.4 Hz). HRMS (FAB) Calcd. for $C_{27}H_{43}N_2F_6P_2Se_2$ [M]$^+$: 731.1136. Found 731.1141.

Preparation of 5c–5f

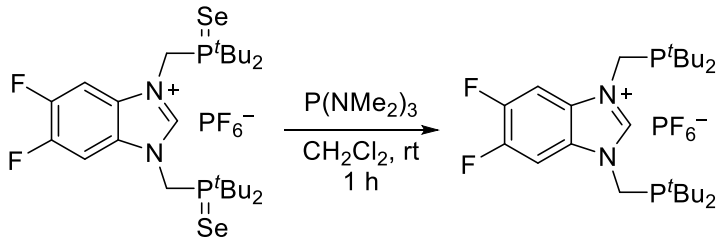

A typical procedure for the preparation of **5c** is described below. In a 50 mL Schlenk flask were placed **8c** (468 mg, 0.604 mmol) and CH_2Cl_2 (25 mL), and then tris(dimethylamino)phosphine (250 μL, 1.38 mmol) was added. The reaction mixture was stirred at room temperature for 1 h, and then the volatiles were removed under reduced pressure. The resultant solid was washed with toluene (10 mL x 3) and dried under vacuum to give **5c** as a white solid (257 mg, 0.417 mmol, 69 %). The suitable sample for elemental analysis was obtained from recrystallization from CH_2Cl_2/hexane.

5c: ^{1}H NMR (THF–d_8): δ 9.82 (s, 1H), 8.17 (t, J = 8.2 Hz, 2H), 4.77 (s, 4H), 1.21 (d, J = 11.6 Hz, 36H). ^{13}C{^{1}H} NMR (THF–d_8): δ 150.8 (dd, J =251.6, 16.6 Hz), 145.1 (t, J = 12.9 Hz), 129.2 (s), 104.1–104.0 (m), 43.7 (d, J = 27.8 Hz), 32.8 (d, J = 19.2 Hz), 29.6 (d, J = 13.5 Hz). ^{19}F NMR (THF–d_8): δ –74.9 (d, J = 716.6 Hz), –137.9 (s). ^{31}P{^{1}H} NMR (THF–d_8): δ 24.0 (s), –146.0 (sep, J = 710.6 Hz). Anal. Calcd. for $C_{25}H_{43}F_8N_2P_3$: C, 48.70, H, 7.03, N, 4.54. Found: C, 48.88, H, 6.75, N, 4.67.

Isolated yields and spectroscopic data of **5d**–**5f** are summarized below:

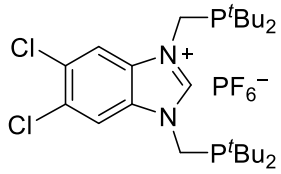

5d: 88% yield. A white solid. ^{1}H NMR (THF–d_8): 9.86 (s, 1H), 8.42 (s, 2H), 4.82 (s, 4H), 1.23 (d, J = 12.0 Hz, 36H). ^{13}C{^{1}H} NMR (THF–d_8): δ 145.9 (t, J = 11.5 Hz), 132.5 (s), 131.8 (s), 117.2 (d, J = 6.7 Hz), 43.7 (d, J = 27.8 Hz), 32.9 (d, J = 20.1 Hz), 29.6 (d, J = 17.6 Hz). ^{31}P{^{1}H} NMR (THF–d_8): δ 24.7 (s), –146.0 (sep, J = 712.1 Hz). Anal. Calcd. for $C_{25}H_{43}Cl_2F_6N_2P_3$: C, 46.24, H, 6.67, N, 4.31. Found: C, 46.11, H, 6.58, N, 4.68.

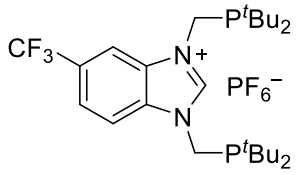

5e: 80% yield. A white solid. The suitable sample for elemental analysis was obtained from recrystallization from CH_2Cl_2/hexane. ^{1}H NMR (THF–d_8): δ 9.90 (s, 1H), 8.50 (s, 1H), 8.37 (d, J = 9.0 Hz, 1H), 7.92 (d, J = 9.0 Hz, 1H), 4.87 (s, 2H), 4.83 (s, 2H), 1.20 (d, J = 12.0 Hz, 18H), 1.18 (d, J = 12.0 Hz, 18H). ^{13}C{^{1}H} NMR (THF–d_8): δ 146.1 (t, J = 11.5 Hz), 135.5 (s), 132.9 (s), 129.2 (q, J = 32.9 Hz), 124.9 (q, J = 272.5 Hz), 124.3 (q, J = 3.7 Hz), 117.1 (d, J = 5.7 Hz), 113.7–113.5 (m), 43.9 (d, J = 28.7 Hz), 43.7 (d, J = 27.8 Hz), 32.94 (d, J = 19.2 Hz), 32.88 (d, J = 20.1 Hz), 29.64 (d, J = 13.4 H), 29.60 (d, J = 13.5 Hz). ^{19}F NMR (THF–d_8): δ –64.3 (s), –75.2 (d, J = 716.6 Hz). ^{31}P{^{1}H} NMR (THF–d_8): δ 25.2 (s), 24.1 (s), –145.9 (sep, J = 710.6 Hz). Anal. Calcd. for $C_{26}H_{44}F_9N_2P_3$: C, 48.15, H, 6.84, N, 4.32. Found: C, 48.54 H, 6.68, N, 3.96.

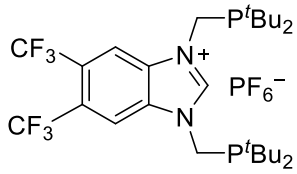

5f: 55% yield. A white solid. The suitable sample for elemental analysis was obtained from recrystallization from THF/Et_2O at –30 °C. ^{1}H NMR (THF–d_8): δ 10.13 (s, 1H), 8.83 (s, 2H), 4.99 (s, 4H), 1.26 (d, J = 12.0 Hz, 36H). ^{13}C{^{1}H} NMR (THF–d_8): δ 148.2 (t, J = 11.1 Hz), 134.7 (s), 126.8–125.6 (m), 123.7 (q, J = 275.4 Hz), 117.4 (s), 44.4 (d, J = 28.8 Hz), 33.0 (d, J = 19.1 Hz), 29.6 (d, J = 12.5 Hz). ^{19}F NMR (THF–d_8): δ –61.2 (s), –75.6 (d, J = 711.0 Hz). ^{31}P{^{1}H} NMR (THF–d_8): δ 25.5 (s), –145.8 (sep, J = 711.4 Hz). Anal. Calcd. for $C_{27}H_{43}F_{12}N_2P_3$: C, 45.26, H, 6.05, N, 3.91. Found: C, 45.25, H, 5.86, N, 3.66.

Preparation of 4a and 4b

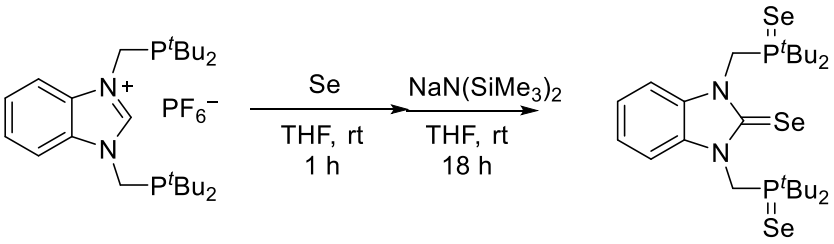

A typical procedure for the preparation of **4a** is described below. In a 20 mL Schlenk flask were placed **5a** (56.3 mg, 0.100 mmol) and elemental selenium (39.5 mg, 0.500 mmol), and then THF (5 mL) was added. The mixture was stirred at room temperature for 1 h. $KN(SiMe_3)_2$ (20.2 mg, 0.110 mmol) was added to the resulting suspension and stirred at room temperature for 18 h. The solvent was removed under vacuum and the residue was dissolved in CH_2Cl_2 (10 mL). After the resultant suspension was filtrated over Celite, the solvent was removed under vacuum. The residue was washed with hexane (5 mL x 2) and dried under vacuum to afford **4a** (58.1 mg, 0.0865 mmol, 87%) as a white solid. M.p. = 230.5–232.0 °C. ^{1}H NMR (THF–d_8): δ 8.59–8.56 (m, 2H), 7.22–7.19 (m, 2H), 5.69 (br, 4H), 1.47 (d, J = 15.6 Hz, 36H). ^{13}C{^{1}H} NMR (THF–d_8): δ 171.7 (s), 135.1 (s), 123.6 (s), 115.7 (s), 48.9 (d, J = 32.6 Hz), 39.5 (d, J = 30.7 Hz), 28.7 (s). ^{31}P{^{1}H} NMR (THF–d_8): δ 71.6 (s with Se satellites, J = 732.4 Hz). ^{77}Se{^{1}H} NMR (THF–d_8): δ 147.1 (s), –384.5 (d, J = 733.5 Hz). HRMS(FAB) Calcd. for $C_{25}H_{44}N_2P_2Se_3$ $[M]^+$: 674.0475. Found 674.0488.

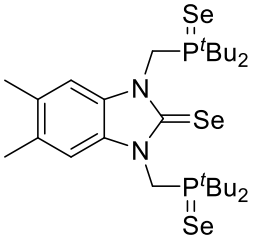

4b: A white solid. 45% yield. M.p. = 239.5–240.7 °C. ^{1}H NMR (THF–d_8): δ 8.44 (s, 2H), 5.68 (br, 4H), 2.33 (s, 6H), 1.46 (d, J = 15.6 Hz, 36H). ^{13}C{^{1}H} NMR (THF–d_8): δ 170.3 (s), 133.4 (s), 132.6 (s), 116.0 (s), 49.15 (d, J = 31.7 Hz), 39.4 (d, J = 30.8 Hz), 28.7 (s), 20.0 (s). ^{31}P{^{1}H} NMR (THF–d_8): δ 71.2 (s with Se satellites, J = 732.3 Hz). ^{77}Se{^{1}H} NMR (THF–d_8): δ 135.2 (s), –381.0 (d, J = 733.5 Hz). HRMS(FAB) Calcd. for $C_{27}H_{48}N_2P_2Se_3$ $[M]^+$: 702.0788. Found 702.0809.

Preparation of 4c–4f

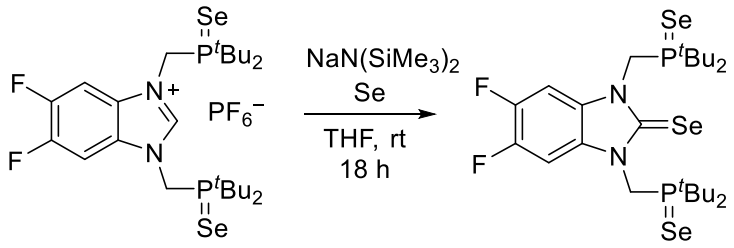

A typical procedure for the preparation of **4c** is described below. In a 20 mL Schlenk flask were placed **8c** (77.4 mg, 0.100 mmol), $NaN(SiMe_3)_2$ (560 mg, 2.81 mmol) and elemental selenium (39.5 mg, 0.500 mmol), and then toluene (5 mL) was added. The mixture was stirred at room temperature for 18 h. The solvent was removed under vacuum and the residue was dissolved in CH_2Cl_2. After the resultant suspension was filtrated over Celite, the solvent of the filtrate was removed under vacuum. The residue was washed with hexane (5 mL x 2) and dried under vacuum to afford **4c** (19.8 mg, 0.0279 mmol, 28%) as a white solid. M.p. = 239.7–240.4 °C. ^{1}H NMR (THF–d_8): δ 8.65 (t, J = 8.6 Hz), 5.68 (br, 4H), 1.47 (d, J = 15.6 Hz, 36H). ^{13}C{^{1}H} NMR (THF–d_8): δ 172.9 (s), 147.8 (dd, J = 245.4, 16.3 Hz), 130.7 (t, J = 6.2 Hz), 104.9–104.4 (m), 48.4 (d, J = 31.6 Hz), 39.5 (d, J = 30.7 Hz), 28.5 (s). ^{19}F NMR (THF–d_8): δ –145.5 (s). ^{31}P{^{1}H} NMR (THF–d_8): δ 71.3 (s with Se satellites, J = 728.1 Hz). ^{77}Se{^{1}H} NMR (THF–d_8): 170.2 (s), –382.0 (d, J = 727.6 Hz). HRMS(FAB) Calcd. for $C_{25}H_{43}N_2F_2P_2Se_3$ $[M+H]^+$: 711.0365. Found 711.0358.

Isolated yields and analytical data of **4d**–**4f** are summarized below:

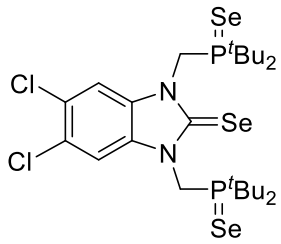

4d: 76% yield. A white solid. M.p. = 226.3–227.8 °C. ^{1}H NMR (THF–d_8): δ 8.84 (s, 2H), 5.68 (br, 4H), 1.47 (d, J = 15.2 Hz, 36H). ^{13}C{^{1}H} NMR (THF–d_8): δ 173.2 (s), 134.2 (s), 127.3 (s), 116.9 (s), 47.9 (d, J = 30.8 Hz), 39.5 (d, J = 29.8 Hz), 28.5 (s). ^{31}P{^{1}H} NMR (THF–d_8): δ 71.6 (s with Se satellites, J = 732.4 Hz). ^{77}Se{^{1}H} NMR (THF–d_8): 177.3 (s), –383.2 (d, J = 733.6 Hz). HRMS(FAB) Calcd. for $C_{25}H_{43}N_2Cl_2P_2Se_3$ $[M+H]^+$: 742.9780. Found 742.9774.

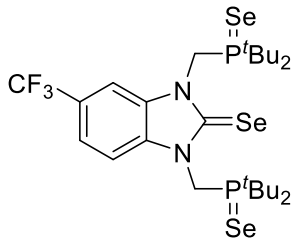

4e: >99% yield. A white solid. M.p. = 182.0–183.0 °C. ^{1}H NMR (THF–d_8): δ 8.92 (s, 1H), 8.64 (d, J = 8.8 Hz, 1H), 7.47 (dd, J = 8.8, 0.8 Hz, 1H), 5.68 (br, 4H), 1.43 (d, J = 15.6 Hz, 36H). ^{13}C{^{1}H} NMR (THF–d_8): δ 173.8 (s), 137.3 (s), 134.8 (s), 125.5 (q, J = 270.3 Hz), 125.3 (q, J = 30.7 Hz), 120.4 (s), 116.2 (s), 113.5 (s), 48.0 (d, J = 30.7 Hz), 47.8 (d, J = 31.7 Hz), 39.6 (d, J = 34.3 Hz), 28.6 (s). ^{19}F NMR (THF–d_8): δ –63.7 (s). ^{31}P{^{1}H} NMR (THF–d_8): δ 72.3 (s with Se satellites, J = 732.4 Hz), 72.1 (s with Se satellites, J = 732.3 Hz). ^{77}Se{^{1}H} NMR (THF–d_8): 174.3 (s), –387.2 (d, J = 733.5 Hz), –387.9 (d, J = 733.5 Hz). HRMS(FAB) Calcd. for $C_{26}H_{43}N_2F_3P_2Se_3$ [M]$^+$: 742.0349. Found 742.0351.

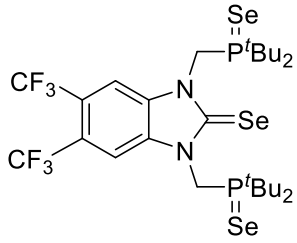

4f: 91% yield. A white solid. M.p. > 180 °C (decomp). ^{1}H NMR (THF–d_8): δ 9.10 (s, 2H), 5.74 (br, 4H), 1.49 (d, J = 15.6 Hz, 36H). ^{13}C{^{1}H} NMR (THF–d_8): δ 175.1 (s), 136.4 (s), 124.3 (q, J = 275.4 Hz), 122.6–121.6 (m), 116.4 (s), 46.7 (d, J = 30. 7 Hz), 39.6 (d, J = 30.7), 28.5 (s). ^{19}F NMR (THF–d_8): δ –60.8 (s). ^{31}P{^{1}H} NMR (THF–d_8): δ 72.8 (s with Se satellites, J = 732.4 Hz). ^{77}Se{^{1}H} NMR (THF–d_8): 196.6 (s), –391.2 (d, J = 733.6 Hz). HRMS(FAB) Calcd. for $C_{27}H_{42}N_2F_6P_2Se_3$ [M]$^+$: 810.0223. Found 810.0199.

Preparation of 6a–6f

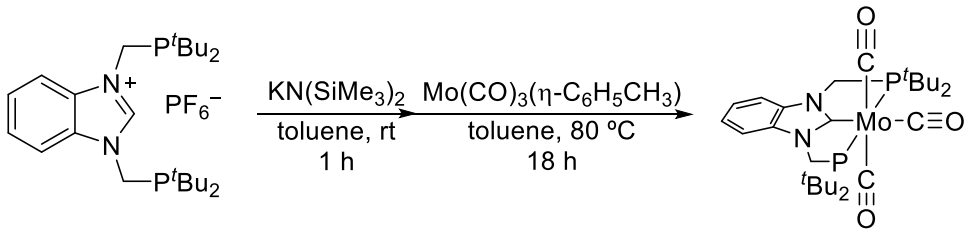

A typical procedure for the preparation of **6a** is described below. In a 20 mL Schlenk flask were placed **5a** (112.4 mg, 0.200 mmol) and $KN(SiMe_3)_2$ (43.5 mg, 0.218 mmol), and then toluene (4 mL) was added. The mixture was stirred at room temperature for 1 h. The resulting suspension was filtered through Celite. $[Mo(CO)_3(\eta^6–C_6H_5CH_3)]$ (49.5 mg, 0.182 mmol) was added to the filtrate and the mixture was stirred at 80 °C for 18 h. The solvent of mixture was removed under vacuum to give a yellow solid. The solid was recrystallized from Et_2O in –30 °C to afford **6a** (26.7 mg, 0.0414 mmol, 23%) as yellow crystals. ^{1}H NMR (THF–d_8): δ 7.45–7.42 (m, 2H), 7.21–7.19 (m, 2H), 4.35 (d, J = 1.6 Hz, 4H), 1.37–1.33 (m, 36H). ^{31}P{^{1}H} NMR (THF–d_8): δ 115.3 (s). IR (KBr, cm^{-1}) 1814 (s, ν_{CO}), 1826 (s, ν_{CO}), 1926 (s, ν_{CO}). IR (THF, cm^{-1}) 1833 (s, ν_{CO}), 1936 (s, ν_{CO}). Anal. Calcd. for $C_{28}H_{44}MoN_2O_3P_2$: C, 54.72; H, 7.22; N, 4.56. Found : C, 54.75; H, 6.99; N, 4.55.

Isolated yields and analytical data of **6b**–**6f** are summarized below:

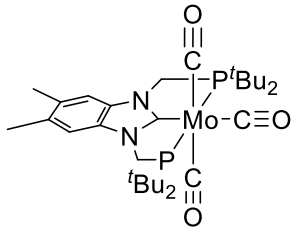

6b: Recrystallization from toluene/hexane gave as yellow crystals. 20% yield. The suitable sample for elemental analysis were obtained by freeze drying in benzene as **6b**·0.1C_6H_6. ^{1}H NMR (THF–d_8): δ 7.22 (s, 2H), 4.29 (br, 4H), 2.35 (s, 6H), 1.34 (pseudo t, J = 6.2 Hz, 36H). ^{31}P{^{1}H} NMR (THF–d_8): δ 115.3 (s). IR (KBr, cm^{-1}) 1811 (s, ν_{CO}), 1819 (s, ν_{CO}), 1924 (s, ν_{CO}). IR (THF, cm^{-1}) 1831 (s, ν_{CO}), 1935 (s, ν_{CO}). Anal. Calcd. for $C_{30}H_{48}MoN_2O_3P_2$ + 0.1C_6H_6: C, 56.51; H, 7.53; N, 4.31. Found: C, 56.88; H, 7.35; N, 3.98.

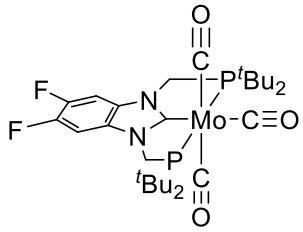

6c: Recrystallization from Et_2O in –30 °C gave **6c** as yellow crystals. 26% yield. ^{1}H NMR (THF–d_8): δ 7.50 (t, J = 8.4 Hz, 2H), 4.33 (s, 4H), 1.34 (pseudo t, J = 6.2 Hz, 36H). ^{19}F NMR (THF–d_8): δ –147.8 (s). ^{31}P{^{1}H} NMR (THF–d_8): δ 115.5 (s). IR (KBr, cm^{-1}) 1820 (s, ν_{CO}), 1833 (s, ν_{CO}), 1938 (s, ν_{CO}). IR (THF, cm^{-1}) 1836 (s, ν_{CO}), 1939 (s, ν_{CO}). Anal. Calcd. for $C_{28}H_{42}F_2MoN_2O_3P_2$: C, 51.70; H, 6.51; N, 4.31. Found: C, 51.80; H, 6.36; N, 4.36.

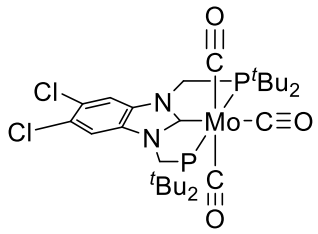

6d: Recrystallization from Et_2O in –30 °C gave **6d** as yellow crystals. 8% yield. ^{1}H NMR (THF–d_8): δ 7.70 (s, 2H), 4.35 (s, 4H), 1.34 (pseudo t, J = 6.2 Hz, 36H). ^{31}P{^{1}H} NMR (THF–d_8): δ 115.5 (s). IR (KBr, cm^{-1}) 1811 (s, ν_{CO}), 1832 (s, ν_{CO}), 1923 (s, ν_{CO}), 1940 (s, ν_{CO}). IR (THF, cm^{-1}) 1838 (s, ν_{CO}), 1940 (s, ν_{CO}). Anal. Calcd. for $C_{28}H_{42}MoCl_2N_2O_3P_2$: C, 49.21; H, 6.19; N, 4.10. Found: C, 48.95; H, 5.91; N, 4.10.

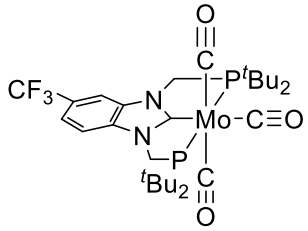

6e: Recrystallization from Et_2O in –30 °C gave **6e** as yellow crystals. 25% yield. ^{1}H NMR (THF–d_8): δ 7.83 (s, 1H), 7.60 (d, J = 8.4 Hz, 1H), 7.54 (d, J = 8.4 Hz, 1H), 4.45 (s, 2H), 4.41 (s, 2H), 1.38–1.33 (m, 36H). ^{19}F NMR (THF–d_8): δ –63.3 (s). ^{31}P{^{1}H} NMR (THF–d_8): δ 115.4 (s). IR (KBr, cm^{-1}) 1812 (s, ν_{CO}), 1826 (s, ν_{CO}), 1938 (s, ν_{CO}). IR (THF, cm^{-1}) 1837 (s, ν_{CO}), 1940 (s, ν_{CO}). Anal. Calcd. for $C_{29}H_{43}F_3MoN_2O_3P_2$: C, 51.03; H, 6.35; N, 4.10. Found: C, 50.85; H, 6.07; N, 3.71.

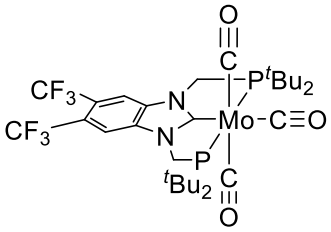

6f: Recrystallization from toluene/hexane gave **6f** as orange crystals. 21% yield. ^{1}H NMR (THF–d_8): δ 8.06 (s, 2H), 4.51 (pseudo t, 4H, J = 1.6 Hz), 1.36 (pseudo t, J = 6.2 Hz, 36H). ^{19}F NMR (THF–d_8): δ –60.3 (s). ^{31}P{^{1}H} NMR (THF–d_8): δ 115.7 (s). IR (KBr, cm^{-1}) 1830 (s, ν_{CO}), 1935 (s, ν_{CO}). IR (THF, cm^{-1}) 1843 (s, ν_{CO}), 1942 (s, ν_{CO}). Anal. Calcd. for $C_{30}H_{42}F_6MoN_2O_3P_2$: C, 48.01; H, 5.64; N, 3.73. Found: C, 48.21; H, 5.51; N, 3.48.

Supplementary Table 1. The ν_{CO} of molybdenum carbonyl complexes **6a-6f**.

Mo complex	IR (THF, ν_{CO}, cm^{-1})
6a	1833, 1936
6b	1831, 1935
6c	1836, 1939
6d	1838, 1940
6e	1837, 1940
6f	1842, 1942

Preparation of 1c-1f

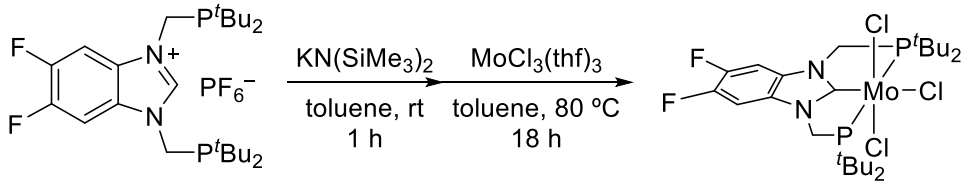

A typical procedure for the preparation of **1c** is described below. In a 50 mL Schlenk flask were placed **5c** (1.23 g, 2.00 mmol) and $KN(SiMe_3)_2$ (561 mg, 2.81 mmol), and then toluene (50 mL) was added. The suspension was stirred at room temperature for 1 h, and then the mixture was filtered through Celite and the filter cake was washed with toluene (5 mL x 3). The solvent was removed under reduced pressure to give brown solid. $[MoCl_3(thf)_3]$ (753.5 mg, 1.80 mmol) and toluene (50 mL) were added to the residue and the mixture was stirred at 80 °C for 19 h. The solution was evaporated to about 5 mL under reduced pressure and the resultant suspension was filtered through filter paper. The residue was washed with toluene (5 ml x 3) and the resultant solid was extracted with CH_2Cl_2 (5mL x 4), then slow addition of hexane (30 mL) to the extract afforded **1c** (391 mg, 0.580 mmol, 32%) as brown crystals. Analytically pure sample was prepared by recrystallization from THF at –30 °C as **1c**·THF. Magnetic susceptibility (Evans method) μ_{eff} = 3.75 μ_B in CD_2Cl_2 at 292 K. Anal. Calcd. for $C_{25}H_{42}Cl_3F_2MoN_2P_2 + C_4H_8O$: C, 46.76; H, 6.77; N, 3.76. Found: C, 46.48; H, 6.58; N, 3.82.

Isolated yields and analytical data of **1d**–**1f** are summarized below:

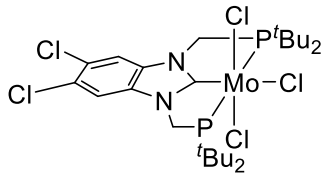

1d: Recrystallization from CH_2Cl_2–hexane gave **1d** as brown crystals. 13% yield. Analytically pure sample was prepared by recrystallization from THF at –30 °C as **1d**·THF. Magnetic susceptibility (Evans method) μ_{eff} = 3.53 μ_B in CD_2Cl_2 at 293 K. Anal. Calcd. for $C_{25}H_{42}Cl_5MoN_2P_2 + C_4H_8O$: C, 44.78; H, 6.48; N, 3.60. Found: C, 44.48; H, 6.46; N, 3.43.

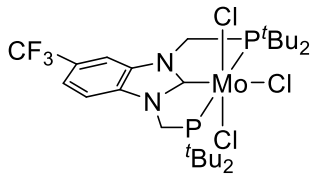

1e: Recrystallization from CH_2Cl_2–hexane gave **1e** as brown crystals. 30% yield. Magnetic

susceptibility (Evans method) μ_{eff} = 3.81 μ_B in CD_2Cl_2 at 293 K. Anal. Calcd. for $C_{26}H_{43}Cl_3F_3MoN_2P_2$: C, 44.30; H, 6.15; N, 3.97. Found: C, 44.16; H, 6.01; N, 3.88.

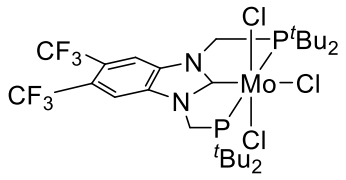

1f: Recrystallization from CH_2Cl_2–hexane gave **1f** as brown crystals. 50% yield. Magnetic susceptibility (Evans method) μ_{eff} = 3.86 μ_B in CD_2Cl_2 at 293 K. Anal. Calcd. for $C_{27}H_{42}Cl_3F_6MoN_2P_2$: C, 41.96; H, 5.48; N, 3.62. Found: C, 42.27; H, 5.29; N, 3.78.

Synthesis of [Mo(N)I(CF$_3$-PCP)] (2e).

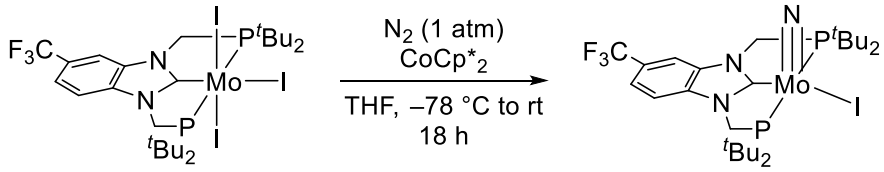

To a solution of [MoI_3(CF$_3$-PCP)] (197 mg, 0.20 mmol) in THF (10 mL) was added a solution of CoCp*$_2$ (145 mg, 0.44 mmol) in THF (10 mL) at -78 °C, and the mixture was stirred at room temperature for 18 h. Volatiles were removed in vacuo, and the resultant yellow-brown solid was washed with hexane (5 mL × 3). The residue was extracted with THF (15 mL). Slow addition of hexane (45 mL) to the extract afforded **2e** as yellow-brown crystals, which were collected by filtration, washed with hexane (3 mL × 3), and dried in vacuo (88.8 mg, 0.12 mmol, 60%). ^{1}H NMR (THF-d_8): δ 8.14 (s, 1H), 7.94 (d, J = 8.0 Hz, 1H), 7.72 (dd, J = 1.2, 8.0 Hz, 1H), 4.93-4.67 (m, 4H), 1.62 (d, J = 12.4 Hz, 9H), 1.60 (d, J = 12.8 Hz, 9H), 1.20 (d, J = 12.0 Hz, 9H), 1.14 (d, J = 12.4 Hz, 9H). ^{19}F NMR (THF-d_8): δ -63.0 (s). ^{31}P{^{1}H} NMR (THF-d_8): δ 114.0 (d, J = 99.7 Hz), 112.0. (d, J = 99.7 Hz). Anal Calcd for $C_{26}H_{43}F_3IMoN_3P_2$: C, 42.23; H, 5.86; N, 5.68. Found: C, 42.16; H, 5.81; N, 5.66.

Reaction of 1a with 5 equivalents of $SmI_2(thf)_2$ under N_2

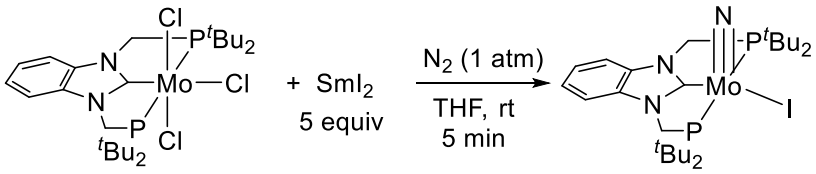

A mixture of **1a** (6.4 mg, 0.010 mmol) and $SmI_2(thf)_2$ (27.4 mg, 0.050 mmol) in THF (2 ml) placed in a 20 ml Schlenk flask was stirred at room temperature for 5 min under N_2 (1 atm). After volatiles were removed in vacuo, formation of **2a** was confirmed by ^{1}H NMR (THF–d_8). The NMR yield of **2a** (0.0073 mmol, 72%) in the residual solid was determined with hexamethylbenzene as an internal standard. The reaction mixture was also analyzed with ESI–TOF–MS (THF): m/z = 673.3 ([MoI(N)(PCP)] = 673.1).

Stoichiometric reaction of 2a with 5 equivalents of $SmI_2(thf)_2$ and H_2O under Ar

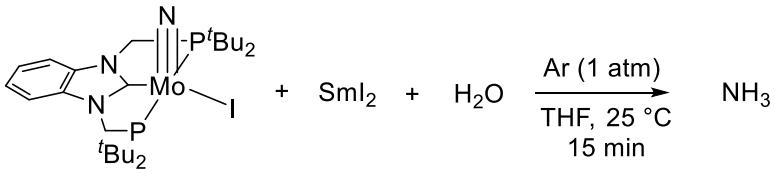

To a 50 mL Schlenk flask were added **2a** (20.2 mg, 0.301 mmol), $SmI_2(thf)_2$ (82.4 mg, 0.150 mmol) and THF (5 mL) under Ar. Then THF solution (1 mL) containing H_2O (0.150 mmol) was added to the stirred solution in the Schlenk flask in one portion. After the addition of the water, the mixture was further stirred at 25 °C for 3 min. After the reaction, aqueous potassium hydroxide solution (30 wt%, 5 mL) was added to the reaction mixture. The mixture was evaporated under reduced pressure, and the distillate was trapped in a dilute H_2SO_4 solution (0.5 M, 10 ml). The amount of ammonia (0.0284 mmol, 94% yield) present in the H_2SO_4 solution was determined by the indophenol method.[S12]

Catalytic reduction of dinitrogen to ammonia with 1a–1f, [Mo(N)I(PCP)]OTf, and 2a

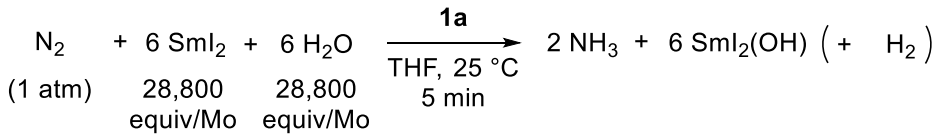

A typical experimental procedure for catalytic reduction with **1a** is described below. In a 50 mL Schlenk flask was placed a CH_2Cl_2 solution of **1a** (0.05 mM, 500 μL, 25 nmol) and the solvent was removed under reduced pressure. To the flask were added $SmI_2(thf)_2$ (395 mg, 0.720 mmol) and THF (5 mL) under N_2. Then THF solution (1 mL) containing H_2O (0.72 mmol) was added to the stirred solution in the Schlenk flask in one portion. After the addition of the water, the mixture was further stirred at 25 °C for 5 min. After the reaction, the amount of generated dihydrogen (0.0043 mmol, 170 equiv. based on the molybdenum atom, 1.2% yield based on $SmI_2(thf)_2$) of the catalytic reaction was quantified by GC. Aqueous potassium hydroxide solution (30 wt%, 5 mL) was added to the reaction mixture. The mixture was evaporated under reduced pressure, and the distillate was trapped in a dilute H_2SO_4 solution (0.5 M, 10 ml). The amount of ammonia (0.0756 mmol, 3030 equiv. based on the molybdenum atom, 32% yield based on $SmI_2(thf)_2$) present in the H_2SO_4 solution was determined by the indophenol method.[S12] The results of catalytic reactions for each catalyst are shown in **Supplementary Table 2**.

Supplementary Table 2. Results of catalytic reactions using molybdenum catalysts bearing substituted PCP-type pincer ligand in catalytic reduction of dinitrogen.

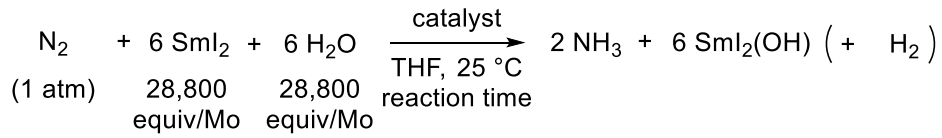

catalyst	reaction time	NH_3 (equiv/Mo)*	NH_3 (%)*	H_2 (equiv/Mo)*	H_2 (%)*
1a	5 min	2950 ± 110	31 ± 1	180 ± 10	1 ± 0
1a	15 min	4130 ± 140	43 ± 1	1000 ± 210	7 ± 1
1a	30 min	4690 ± 330	49 ± 3	900 ± 450	6 ± 3
1a	1 h	7020 ± 120	73 ± 1	1340 ± 70	9 ± 0
1a	2 h	8050 ± 300	84 ± 3	880 ± 570	6 ± 4
1a	4 h	8410 ± 480	88 ± 5	570 ± 140	4 ± 1
1b	5 min	1600 ± 60	17 ± 1	180 ± 10	1 ± 0
1b	15 min	2520 ± 850	26 ± 9	930 ± 900	6 ± 6
1b	30 min	3580 ± 20	37 ± 0	1410 ± 30	10 ± 0
1b	1 h	5350 ± 560	56 ± 6	1460 ± 220	10 ± 2
1b	2 h	6330 ± 440	66 ± 5	1980 ± 620	14 ± 4
1b	4 h	5960 ± 560	62 ± 6	3020 ± 150	21 ± 1
1c	5 min	3170 ± 10	33 ± 0	150 ± 20	1 ± 0
1c	15 min	5730 ± 600	60 ± 6	360 ± 180	3 ± 1
1c	30 min	7420 ± 280	77 ± 3	390 ± 100	3 ± 1
1c	1 h	7310 ± 80	76 ± 1	650 ± 10	5 ± 0
1c	2 h	9120 ± 70	95 ± 1	480 ± 140	3 ± 1
1c	4 h	8990 ± 100	94 ± 1	550 ± 240	4 ± 2
1d	5 min	3100 ± 400	32 ± 4	240 ± 40	2 ± 0
1d	15 min	6900 ± 120	72 ± 1	320 ± 100	2 ± 1
1d	30 min	8220 ± 200	86 ± 2	620 ± 260	4 ± 2
1d	1 h	8170 ± 230	85 ± 2	670 ± 70	5 ± 0
1d	2 h	8770 ± 550	91 ± 6	860 ± 70	6 ± 1
1d	4 h	8360 ± 410	87 ± 4	810 ± 140	6 ± 1
1e	5 min	3990 ± 240	42 ± 2	200 ± 40	1 ± 0
1e	15 min	7400 ± 80	77 ± 1	290 ± 40	2 ± 0
1e	30 min	7760 ± 410	81 ± 4	380 ± 60	3 ± 0
1e	1 h	8480 ± 340	88 ± 4	750 ± 120	5 ± 1
1e	2 h	8940 ± 80	93 ± 1	850 ± 320	6 ± 2
1e	4 h	8800 ± 110	92 ± 1	1190 ± 430	8 ± 3
1f	5 min	3560 ± 140	37 ± 1	310 ± 30	2 ± 0
1f	15 min	6650 ± 520	69 ± 5	290 ± 60	2 ± 0
1f	30 min	8430 ± 160	88 ± 2	460 ± 10	3 ± 0
1f	1 h	8660 ± 600	90 ± 6	600 ± 160	4 ± 1
1f	2 h	9240 ± 420	96 ± 4	340 ± 170	2 ± 1
1f	4 h	8610 ± 290	90 ± 3	560 ± 540	4 ± 4
[Mo(N)I(PCP)]OTf	4 h	6080 ± 990	63 ± 10	740 ± 180	5 ± 1
2a	4 h	8230 ± 30	86 ± 0	760 ± 0	5 ± 0

*Data are means of multiple individual experiments (two to four times) with error bars based on standard deviation (s.d.)

Catalytic reduction of dinitrogen to ammonia with larger amount of $SmI_2(thf)_2$ and H_2O

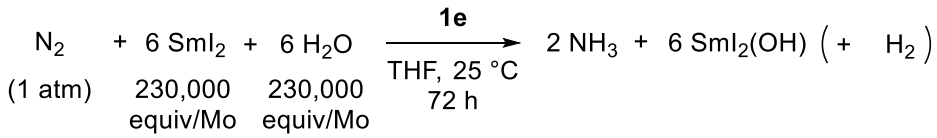

In a 50 mL Schlenk flask was placed a CH_2Cl_2 solution of **1e** (0.05 mM, 500 μL, 25 nmol) and the solvent was removed under reduced pressure. To the flask were added $SmI_2(thf)_2$ (1.05 g, 1.92 mmol) and THF (6 mL) under N_2. Then THF solution (1 mL) containing H_2O (1.92 mmol) was added to the stirred solution in the Schlenk flask in one portion. After the addition of the water, the mixture was further stirred at 25 °C for 24 h. To the flask were added $SmI_2(thf)_2$ (1.05 g, 1.92 mmol) and THF solution (1 mL) containing H_2O (1.92 mmol), and the mixture was further stirred at 25 °C for 24 h. To the flask were added $SmI_2(thf)_2$ (1.05 g, 1.92 mmol) and THF solution (1 mL) containing H_2O (1.92 mmol), and the mixture was further stirred at 25 °C for 24 h. Aqueous potassium hydroxide solution (30 wt%, 5 mL) was added to the reaction mixture. The mixture was evaporated under reduced pressure, and the distillate was trapped in a dilute H_2SO_4 solution (0.5 M, 10 ml). The amount of ammonia (1.42 mmol, 56,800 equiv. based on the molybdenum atom, 74% yield based on $SmI_2(thf)_2$) present in the H_2SO_4 solution was determined by the indophenol method.[S12]

3. Kinetic studies.

Catalytic reduction of dinitrogen to ammonia with various concentration of 1a

Based on a typical experimental procedure for catalytic reduction of dinitrogen with **1a**, the catalytic reactions at various initial concentration of **1a** were carried out. The reaction order of **1a** was analyzed by method of initial rates and regression analysis. The analysis showed the reaction rates of **1a** were 1.3 and 1.9, respectively, at high concentration of **1a** (over 1.5 μM) and low concentration (below 1.0 μM). The experimental results were shown in **Supplementary Table 3**.

Supplementary Table 3. Experimental data for the analysis on the reaction order of **1a.**

[**1a**] (10^{-6} M)	log[**1a**]	reaction time (min)	NH_3 (μmol)*	H_2 (μmol)*	v_{NH3} (10^{-3} M·h^{-1})*	log(v_{NH3})*
0.5	–6.30	60	33.8	12.9	5.63	–2.25
		60	31.3	12.0	5.22	–2.28
		(average)	32.6 ± 1.8	12.5 ± 0.6	5.43 ± 0.29	–2.27 ± 0.02
0.7	–6.15	20	19.8	6.0	9.9	–2.00
		20	20.2	8.2	10.1	–2.00
		20	24.0	7.5	12.0	–1.92
		(average)	21.3 ± 2.3	7.2 ± 1.1	10.6 ± 1.2	–1.97 ± 0.05
0.8	-6.10	20	37.9	5.7	19.0	–1.72
		20	24.0	10.8	12.0	–1.92
		20	23.9	11.4	12.0	–1.92
		(average)	28.6 ± 8.1	9.3 ± 3.1	14.3 ± 4.0	–1.86 ± 0.12
1.0	–6.00	20	53.9	6.1	27.0	–1.57
		20	36.8	8.7	18.4	–1.74
		20	34.4	12.4	17.2	–1.76
		(average)	41.7 ± 10.6	9.1 ± 3.2	20.9 ± 5.3	–1.69 ± 0.11
1.5	–5.82	10	44.9	7.7	44.9	–1.35
		10	46.6	4.6	46.6	–1.33
		(average)	45.8 ± 1.2	6.2 ± 2.2	45.8 ± 1.2	–1.34 ± 0.01
2.0	–5.70	5	26.5	2.3	53.0	–1.28
		5	30.5	3.6	61.0	–1.21
		(average)	28.5 ± 2.8	3.0 ± 0.9	57.0 ± 5.7	–1.25 ± 0.04
3.0	–5.52	5	52.7	5.2	105	–0.977
		5	57.5	5.6	115	–0.939
		(average)	55.1 ± 3.4	5.4 ± 0.3	110 ± 7	–0.958 ± 0.027
4.2	–5.38	5	71.8	4.5	144	–0.843
		5	75.6	4.3	151	–0.820
		(average)	73.7 ± 2.7	4.4 ± 0.1	147 ± 5	–0.832 ± 0.016
6.0	-5.22	2	45.8	2.2	229	–0.640
		2	62.2	3.0	311	–0.507
		(average)	54.0 ± 11.6	2.6 ± 0.6	270 ± 58	–0.574 ± 0.094

*The mean values are shown with error bars based on standard deviation (s.d.)

Catalytic reduction of dinitrogen to ammonia with various concentration of $SmI_2(thf)_2$

Based on a typical experimental procedure for catalytic reduction of dinitrogen with **1a**, the catalytic reactions at various initial concentrations of SmI_2 were carried out. The reaction order of SmI_2 was analyzed by method of initial rates and regression analysis. The analysis showed the reaction order of SmI_2 were 1.0 and 0.3, respectively, at the high concentration of **1a** ([**1a**] = 4.2 μM) and the low concentration ([**1a**] = 0.7 μM). The experimental results were shown in **Supplementary Tables 4** and **5**.

Supplementary Table 4. Experimental data for the analysis on the reaction order of SmI_2 at the high concentration of **1a** ([**1a**] = 4.2 μM).

[SmI_2] (M)	log[SmI_2]	reaction time (min)	NH_3 (μmol)*	H_2 (μmol)*	v_{NH3} (10^{-2} M·h^{-1})*	log(v_{NH3})*
0.03	–1.52	5	14.9	9.4	2.98	–1.53
		5	23.0	6.8	4.60	–1.34
		5	25.8	3.9	5.16	–1.29
		(average)	21.2 ± 5.7	6.7 ± 2.8	4.25 ± 1.13	–1.38 ± 0.13
0.06	–1.22	5	33.5	12.4	6.70	–1.17
		5	42.6	5.7	8.52	–1.07
		(average)	38.1 ± 6.4	9.1 ± 4.7	7.61 ± 1.29	–1.12 ± 0.07
0.09	–1.05	5	60.6	4.1	12.1	–0.916
		5	64.7	5.6	12.9	–0.888
		(average)	62.7 ± 2.9	4.9 ± 1.1	12.5 ± 0.6	–0.902 ± 0.020
0.12	–0.92	5	71.8	4.5	14.4	–0.843
		5	75.6	4.3	15.1	–0.820
		(average)	73.7 ± 2.7	4.4 ± 0.1	14.7 ± 0.5	–0.832 ± 0.016

*The mean values are shown with error bars based on standard deviation (s.d.)

Supplementary Table 5. Experimental data for the analysis on the reaction order of SmI_2 at the low concentration of **1a** ([**1a**] = 0.7 μM).

[SmI_2] (M)	log[SmI_2]	reaction time (min)	NH_3 (μmol)*	H_2 (μmol)*	v_{NH3} (10^{-2} M·h^{-1})*	log(v_{NH3})*
0.03	–1.53	20	15.9	14.2	0.795	–2.10
		20	10.4	10.6	0.520	–2.28
		20	14.0	6.6	0.700	–2.15
		(average)	13.4 ± 2.8	10.5 ± 3.8	0.672 ± 0.140	–2.18 ± 0.09
0.06	–1.22	20	19.0	7.9	0.950	–2.02
		20	13.6	12.8	0.680	–2.17
		20	21.5	8.6	1.08	–1.97
		(average)	18.0 ± 4.0	9.8 ± 2.7	0.902 ± 0.202	–2.05 ± 0.10
0.09	–1.05	20	19.6	10.4	0.980	–2.01
		20	18.1	9.8	0.905	–2.04
		(average)	18.9 ± 1.1	10.1 ± 0.4	0.943 ± 0.053	–2.03 ± 0.02
0.12	–6.15	20	19.8	6.0	0.990	–2.00
		20	20.2	8.2	1.01	–2.00
		20	24.0	7.5	1.20	–1.92
		(average)	21.3 ± 2.3	7.2 ± 1.1	1.07 ± 0.12	–1.97 ± 0.05

*The mean values are shown with error bars based on standard deviation (s.d.)

Catalytic reduction of dinitrogen to ammonia with various concentration of H_2O

Based on a typical experimental procedure for catalytic reduction of dinitrogen with **1a**, the catalytic reactions at various initial concentrations of H_2O were carried out. The reaction order of H_2O was analyzed by method of initial rates and regression analysis. The analysis showed the reaction order of SmI_2 were 0.8 and 0.4, respectively, at the high concentration of **1a** ([**1a**] = 4.2 μM) and the low concentration ([**1a**] = 0.7 μM). The experimental results were shown in **Supplementary Tables 6** and **7**.

Supplementary Table 6. Experimental data for the analysis on the reaction order of H_2O at the high concentration of **1a** ([**1a**] = 4.2 μM).

[H_2O] (M)	log[H_2O]	reaction time (min)	NH_3 (μmol)*	H_2 (μmol)*	v_{NH3} (10^{-2} M·h^{-1})*	log(v_{NH3})*
0.03	–1.52	10	48.1	0.9	4.81	–1.32
		10	56.4	0.5	5.64	–1.25
		(average)	52.3 ± 5.9	0.7 ± 0.3	5.23 ± 0.59	–1.28 ± 0.05
0.06	–1.22	5	42.7	0.8	8.54	–1.07
		5	55.5	0.9	11.1	–0.95
		5	52.0	0.7	10.4	–0.98
		(average)	50.1 ± 6.6	0.8 ± 0.1	10.0 ± 1.3	–1.00 ± 0.06
0.09	–1.05	5	73.6	1.8	14.7	–0.832
		5	71.5	1.6	14.3	–0.845
		(average)	72.6 ± 1.5	1.7 ± 0.1	14.5 ± 0.3	–0.838 ± 0.009
0.12	–0.92	5	71.8	4.5	14.4	–0.843
		5	75.6	4.3	15.1	–0.820
		(average)	73.7 ± 2.7	4.4 ± 0.1	14.7 ± 0.5	–0.832 ± 0.016

*The mean values are shown with error bars based on standard deviation (s.d.)

Supplementary Table 7. Experimental data for the analysis on the reaction order of H_2O at the low concentration of **1a** ([**1a**] = 0.7 μM).

[H_2O] (M)	log[H_2O]	reaction time (min)	NH_3 (μmol)*	H_2 (μmol)*	v_{NH3} (10^{-2} M·h^{-1})*	log(v_{NH3})*
0.03	–1.53	20	10.7	1.0	0.535	–2.27
		20	13.5	1.1	0.675	–2.17
		(average)	12.1 ± 2.0	1.0 ± 0.1	0.605 ± 0.099	–2.22 ± 0.07
0.06	–1.22	20	16.9	2.0	0.845	–2.07
		20	17.3	2.5	0.865	–2.06
		(average)	17.1 ± 0.3	2.2 ± 0.3	0.855 ± 0.014	–2.07 ± 0.01
0.09	–1.05	20	18.4	6.1	0.920	–2.04
		20	16.2	5.9	0.810	–2.09
		(average)	17.3 ± 1.6	6.0 ± 0.1	0.865 ± 0.078	–2.06 ± 0.04
0.12	–6.15	20	19.8	6.0	0.990	–2.00
		20	20.2	8.2	1.01	–2.00
		20	24.0	7.5	1.20	–1.92
		(average)	21.3 ± 2.3	7.2 ± 1.1	1.07 ± 0.12	–1.97 ± 0.05

*The mean values are shown with error bars based on standard deviation (s.d.)

Catalytic reduction of dinitrogen to ammonia with D_2O

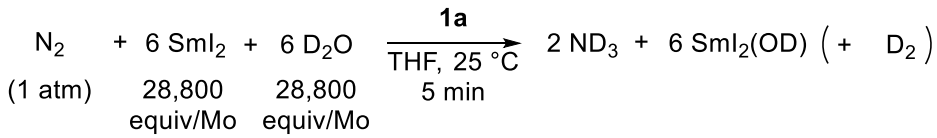

A typical experimental procedure for catalytic reduction with **1a** is described below. In a 50 mL Schlenk flask was placed a CH_2Cl_2 solution of **1a** (0.05 mM, 500 μL, 25 nmol) and the solvent was removed under reduced pressure. To the flask were added $SmI_2(thf)_2$ (395 mg, 0.720 mmol) and THF (5 mL) under N_2. Then THF solution (1 mL) containing D_2O (0.72 mmol) was added to the stirred solution in the Schlenk flask in one portion. After the addition of the water, the mixture was further stirred 25 °C for 5 min. After the reaction, the amount of generated deuterated–dihydrogen (0.0038 mmol, 150 equiv. based on the molybdenum atom, 1.1% yield based on $SmI_2(thf)_2$) of the catalytic reaction was quantified by GC. Aqueous potassium hydroxide solution (30 wt%, 5 mL) was added to the reaction mixture. The mixture was evaporated under reduced pressure, and the distillate was trapped in a dilute H_2SO_4 solution (0.5 M, 10 ml). The amount of deuterated–ammonia (0.0284 mmol, 1120 equiv. based on the molybdenum atom, 12% yield based on $SmI_2(thf)_2$) present in the H_2SO_4 solution was determined by the indophenol method.[S12] The detailed results of determination of kinetic isotope effects are shown in **Supplementary Table 8**.

Supplementary Table 8. Experimental data for the determination of kinetic isotope effects.

[**1a**] (10^{-6} M)	reaction time (min)	ND_3 (μmol)*	D_2 (μmol)*	v_{ND3} (10^{-3} M·h^{-1})*	k_H/k_D (NH_3)*
4.2	5	28.3 ± 0.4	3.3 ± 0.8	56.5 ± 0.7	2.61 ± 0.13
0.7	20	15.0 ± 2.0	3.4 ± 1.1	7.50 ± 1.0	1.57 ± 0.62

*Data are means of multiple individual experiments with error bars based on standard deviation (s.d.)

4. Electrochemical studies.

Cyclic voltammograms and differential pulse voltammograms were recorded on a potentiostat/galvanostat (GAMRY INSTRUMENTS, Interface 1000) with glassy carbon working electrode and Pt wire counter electrode in THF containing 1 mM of sample and 0.1 M of [^{n}Bu$_4$N][PF$_6$] as a supporting electrolyte at a scan rate of 0.1 V/s at room temperature under N_2 atmosphere. All potentials were measured against an $Ag^{0/+}$ electrode and converted to the values *vs*. ferrocene/ferrocenium ($FeCp_2^{+/0}$) referenced to external standard ($FeCp_2^{+/0}$). $E_{1/2}$ values for the irreversible waves were calculated according to the peak potential in differential pulse voltammetry measurements. Cyclic voltammograms and differential pulse voltammograms of [Mo(N)I(PCP)] (**2a**) and [Mo(N)I(CF$_3$-PCP)] (**2e**) are shown in **Supplementary Figure 1**.

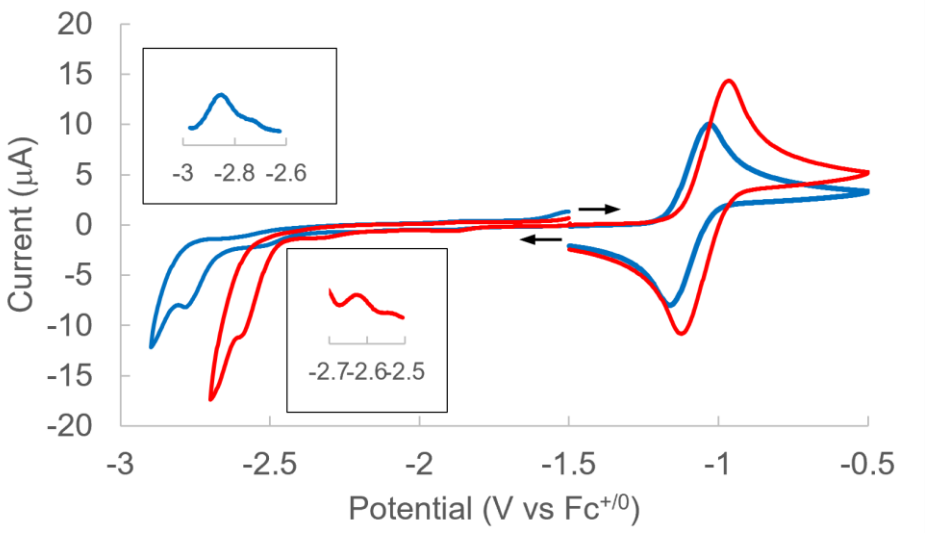

Supplementary Figure 1. Cyclic voltammograms and differential pulse voltammograms of **2a** (blue line) and **2e** (red line). **2a**: $E_{1/2(red)}$ = -2.85 V, $E_{1/2(ox)}$ = -1.10 V (vs $FeCp_2^{+/0}$). **2e**: $E_{1/2(red)}$ = -2.63 V, $E_{1/2(ox)}$ = -1.05 V (vs $FeCp_2^{+/0}$).

5. X-ray crystallographic studies

Crystallographic data of **1c**·CH_2Cl_2, **1d**·1/2CH_2Cl_2, **1e**, **1f**, [Mo(N)I(PCP)]OTf, **2a**, **2e**, **6a**, **6b**, **6c**, **6d**, **6e**·C_4H_4O and **6f** are summarized in **Supplementary Tables 9–13**. Their ORTEP drawings are shown in **Supplementary Figures 2–14**. Diffraction data were collected for the 2θ range of 4˚ to 55˚ on a Rigaku RAXIS RAPID imaging plate area detector with graphite-monochromated Mo *K*α radiation (λ = 0.71075 Å), with VariMax optics. Intensity data were corrected for Lorenz-polarization effects and for empirical absorption (ABSCOR). The structure solution and refinements were carried out by using the *CrystalStructure* crystallographic software package.[S13] The positions of non-hydrogen atoms were determined by direct methods (SIR 97[S14] for **1c**, **1d**, **1e**, **1f**, [Mo(N)I(PCP)]OTf, **6a**, **6b** and **6f**, SHELXS[S15] for **2a**, **2e**, **6d** and **6e**·C_4H_4O and SHELXT[S16] for **6c**) and subsequent Fourier syntheses (SHELXL Version 2016/6[S17]) and were refined on F_o^2 using all unique reflections by full-matrix least-squares with anisotropic thermal parameters. All the hydrogen atoms were placed at the calculated positions with fixed isotropic parameters. For the crystal of [Mo(N)I(PCP)]OTf, the molybdenum center (Mo(1) and Mo(2)) is disordered among two positions in a ratio of 9:1. For the crystal of **2a**, the molybdenum center (Mo(2A) and Mo(2B)) is disordered among two positions in a ratio of 9:1.

According to the International Union of Crystallography checkCIF reports, the following Alert level B errors are reported for crystallographic data of **1e**:

PLAT242_ALERT_2_B Low 'MainMol' Ueq as Compared to Neighbors of C19.

The alert (PLAT242_ALERT_2_B) is due to the disorder of the ligand. However, some carbon atoms could not be fixed and solving these disorders could not refine the data, thus disorders were ignored.

According to the International Union of Crystallography checkCIF reports, the following Alert level B errors are reported for crystallographic data of **2a**:

PLAT201_ALERT_2_B Isotropic non-H Atoms in Main Residue(s) C9.

PLAT315_ALERT_2_B Singly Bonded Carbon Detected (H-atoms Missing) C46.

The alerts (PLAT201_ALERT_2_B and PLAT315_ALERT_2_B) are due to the disorders of the ligands. However, some hydrogen atoms could not be fixed and solving these disorders could not refine the data, thus disorders were ignored.

PLAT971_ALERT_2_B Check Calcd Resid. Dens. 0.92Ang From I2 2.53 eA-3

PLAT972_ALERT_2_B Check Calcd Resid. Dens. 0.77Ang From I2 -2.59 eA-3

The alerts (PLAT971_ALERT_2_B and PLAT972_ALERT_2_B) are due to the disorders of the iodide ligand (I2).

PLAT973_ALERT_2_B Check Calcd Positive Resid. Density on Mo2 1.74 eA-3

The alert (PLAT973_ALERT_2_B) is due to the disorders of the molybdenum atom (Mo2).

According to the International Union of Crystallography checkCIF reports, the following Alert level B errors are reported for crystallographic data of **2e**:

PLAT971_ALERT_2_B Check Calcd Resid. Dens. 0.80Ang From I1 3.19 eA-3

The alert (PLAT971_ALERT_2_B) is due to the disorders of the iodide ligand (I1).

According to the International Union of Crystallography checkCIF reports, the following Alert level B errors are reported for crystallographic data of **6a**:

PLAT043_ALERT_1_B Calculated and Reported Mo1. Weight Differ by 20.18.

PLAT241_ALERT_2_B High 'MainMol" Ueq as Compared to Neighbors of C23.

PLAT315_ALERT_2_B Singly Bonded Carbon Detected (H-atoms Missing) C19.

PLAT315_ALERT_2_B Singly Bonded Carbon Detected (H-atoms Missing) C21.

PLAT315_ALERT_2_B Singly Bonded Carbon Detected (H-atoms Missing) C23.

PLAT315_ALERT_2_B Singly Bonded Carbon Detected (H-atoms Missing) C25.

The alerts (PLAT043_ALERT_1_B, PLAT241_ALERT_2_B and PLAT315_ALERT_2_B) are due to the disorders of the ligands. However, some hydrogen atoms could not be fixed and solving these disorders could not refine the data, thus disorders were ignored.

The unit cell of **1e**, **1f**, [Mo(N)I(PCP)]OTf, **2a** or **2e** contains solvent accessible voids of 4466 $Å^3$, 912 $Å^3$, 318 $Å^3$, 949 $Å^3$ or 2517 $Å^3$, respectively. The electron density associated with some solvent molecules was removed by the SQUEEZE routine of PLATONS[S18] for crystal data of **1e**, **1f**, [Mo(N)I(PCP)]OTf, **2a** and **2e**.

Supplementary Table 9. X-ray crystallographic data for **1c**, **1d** and **1e**.

	1c·CH_2Cl_2	**1d·0.5CH_2Cl_2**	**1e**
CCDC number	2069962	2069963	2069964
chemical formula	$C_{26}H_{44}Cl_5F_2MoN_2P_2$	$C_{25.5}H_{43}Cl_6MoN_2P_2$	$C_{26}H_{43}Cl_3F_3MoN_2P_2$
formula weight	757.80	748.24	704.88
dimensions of crystals, mm^3	0.20 × 0.10 × 0.10	0.20 × 0.20 × 0.10	0.33 × 0.33 × 0.30
crystal color, habit	brown, block	brown, block	brown, block
crystal system	triclinic	monoclinic	orthorhombic
space group	*P-1*	*P2₁/n*	*Pbca*
a, Å	13.3594(4)	22.4049(4)	14.4397(3)
b, Å	15.0448(5)	11.7325(2)	31.5536(6)
c, Å	19.3873(6)	25.1980(5)	35.1843(7)
α, deg	74.865(5)	90	90
β, deg	71.918(5)	91.113(6)	90
γ, deg	69.087(5)	90	90
V, $Å^3$	3410.2(2)	6622.4(2)	16030.9(6)
Z	4	8	16
ρ_{calcd}, g cm^{-3}	1.476	1.501	1.168
F(000)	1556.00	3072.00	5808.00
μ, cm^{-1}	8.994	9.949	6.352
temperature, °C	–95	–90	–95
trans. factors range	0.641 – 0.914	0.644 – 0.905	0.520 – 0.826
no. reflections measured	15563	60922	207815
no. unique reflections	15563 (R_{int} = 0.0616)	15110 (R_{int} = 0.0416)	18301 (R_{int} = 0.0876)
no. parameters refined	685	682	687
*R*1 ($I > 2\ \sigma(I)$)[a]	0.0862	0.0329	0.1433
*wR*2 (all data)[b]	0.1665	0.0589	0.2372
GOF (all data)[c]	1.158	1.000	1.000
max diff peak / hole, e $Å^{-3}$	+1.25 / –1.22	+0.89 / –0.92	+1.10 / –0.75

[a] $R1 = \Sigma||F_o|-|F_c||/\Sigma|F_o|$. [b] $wR2 = [\Sigma w(F_o^2-F_c^2)^2/\Sigma w(F_o^2)^2]^{1/2}$, $w = 1/[\sigma^2(F_o^2) + (qP)^2 + rP]$, $P = (\mathrm{Max}(F_o^2, 0) + 2\ F_c^2)/3$ [q = 0.0289 (**1c**), 0 (**1d**), 0 (**1e**); r = 24.5563 (**1c**), 9.5000 (**1d**), 257.0000 (**1e**)]. [c] GOF = $[\Sigma w(F_o^2-F_c^2)^2/(N_o-N_{params})]^{1/2}$.

Supplementary Table 10. X-ray crystallographic data for **1f** and [Mo(N)I(PCP)]OTf.

	1f	[Mo(N)I(PCP)]OTf
CCDC number	2069965	2069966
chemical formula	$C_{27}H_{42}Cl_3F_6MoN_2P_2$	$C_{26}H_{44}F_3IMoN_3O_3P_2S$
formula weight	772.88	820.50
dimensions of crystals, mm^3	0.65 × 0.53 × 0.39	0.10 × 0.10 × 0.08
crystal color, habit	brown, block	yellow, block
crystal system	orthorhombic	triclinic
space group	$P2_12_12_1$	*P-1*
a, Å	15.0732(3)	8.5806(5)
b, Å	15.4195(3)	12.5836(6)
c, Å	16.7982(3)	17.7606(8)
α, deg	90	84.944(6)
β, deg	90	80.943(6)
γ, deg	90	86.677(6)
V, $Å^3$	3904.26(13)	1884.52(16)
Z	4	2
ρ_{calcd}, g cm^{-3}	1.315	1.446
F(000)	1580.00	826.00
μ, cm^{-1}	6.690	13.495
temperature, °C	–180	–150
trans. factors range	0.127 – 0.771	0.600 – 0.898
no. reflections measured	28806	17503
no. unique reflections	10691 (R_{int} = 0.0734)	8470 (R_{int} = 0.0309)
no. parameters refined	382	372
*R*1 ($I > 2\ \sigma(I)$)[a]	0.0455	0.0564
*wR*2 (all data)[b]	0.1060	0.1319
GOF (all data)[c]	0.978	1.078
max diff peak / hole, e $Å^{-3}$	+1.05 / –0.77	+1.45 / –1.38

[a] $R1 = \Sigma||F_o|-|F_c||/\Sigma|F_o|$. [b] $wR2 = [\Sigma w(F_o^2-F_c^2)^2/\Sigma w(F_o^2)^2]^{1/2}$, $w = 1/[\sigma^2(F_o^2) + (qP)^2 + rP]$, $P = (\mathrm{Max}(F_o^2, 0) + 2F_c^2)/3$ [q = 0.0465 (**1f**), 0.0460 ([Mo(N)I(PCP)]OTf); r = 0 (**1f**), 6.8500 ([Mo(N)I(PCP)]OTf)]. [c] GOF = $[\Sigma w(F_o^2-F_c^2)^2/(N_o-N_{params})]^{1/2}$.

Supplementary Table 11. X-ray crystallographic data for **2a** and **2e**.

	2a	**2e**
CCDC number	2069967	2222890
chemical formula	$C_{25}H_{44}IMoN_3P_2$	$C_{26}H_{43}F_3IMoN_3P_2$
formula weight	671.44	739.43
dimensions of crystals, mm^3	0.16 × 0.13 × 0.08	0.34 × 0.26 × 0.19
crystal color, habit	Light-yellow, block	Yellow, block
crystal system	monoclinic	trigonal
space group	*P2₁/n*	*R-3*
a, Å	20.0923(4)	27.2353(4)
b, Å	13.0128(2)	27.2353(4)
c, Å	24.7556(5)	24.2398(5)
α, deg	90	90
β, deg	96.2844(19)	90
γ, deg	90	90
V, $Å^3$	6433.6(2)	15571.3(6)
Z	4	18
ρ_{calcd}, g cm^{-3}	1.386	1.419
F(000)	2720.00	6696.00
μ, cm^{-1}	14.824	13.972
temperature, °C	–180	–180
trans. factors range	0.242 – 0.893	0.480 – 0.770
no. reflections measured	56484	24836
no. unique reflections	16987 (R_{int} = 0.0948)	8505 (R_{int} = 0.0310)
no. parameters refined	587	325
*R*1 ($I > 2\ \sigma(I)$)[a]	0.0909	0.0545
*wR*2 (all data)[b]	0.1951	0.1250
GOF (all data)[c]	1.006	1.012
max diff peak / hole, e $Å^{-3}$	+2.61 / –2.78	+3.15 / –1.64

[a] $R1 = \Sigma||F_o|-|F_c||/\Sigma|F_o|$. [b] $wR2 = [\Sigma w(F_o^2-F_c^2)^2/\Sigma w(F_o^2)^2]^{1/2}$, $w = 1/[\sigma^2(F_o^2) + (qP)^2 + rP]$, $P = (\mathrm{Max}(F_o^2, 0) + 2F_c^2)/3$ [q = 0 (**2a**), 0.0376 (**2e**); r = 75.0000 (**2a**), 252.5977 (**2e**)]. [c] $\mathrm{GOF} = [\Sigma w(F_o^2-F_c^2)^2/(N_o-N_{params})]^{1/2}$.

Supplementary Table 12. X-ray crystallographic data for **6a**, **6b** and **6c**.

	6a	**6b**	**6c**
CCDC number	2069968	2069969	2069970
chemical formula	$C_{28}H_{44}MoN_2O_3P_2$	$C_{30}H_{48}MoN_2O_3P_2$	$C_{32}H_{52}F_2MoN_2O_4P_2$
formula weight	614.55	642.61	724.66
dimensions of crystals, mm^3	0.19 × 0.05 × 0.04	0.15 × 0.10 × 0.05	0.25 × 0.10 × 0.10
crystal color, habit	yellow, plate	yellow, block	yellow, block
crystal system	monoclinic	monoclinic	orthorhombic
space group	*Cc*	*P2₁/n*	*P2₁/n*
a, Å	8.9621(3)	19.3547(4)	12.8624(4)
b, Å	31.4256(9)	11.5359(2)	16.2151(4)
c, Å	11.0080(3)	29.3538(6)	17.7821(4)
α, deg	90	90	90
β, deg	105.5340(74)	92.469(7)	106.884(8)
γ, deg	90	90	90
V, $Å^3$	2987.0(2)	6547.8(2)	3548.9(2)
Z	4	8	4
ρ_{calcd}, g cm^{-3}	1.366	1.304	1.356
F(000)	1288.00	2704.00	1520.00
μ, cm^{-1}	5.759	5.285	5.057
temperature, °C	–100	–75	–100
trans. factors range	0.857 – 0.977	0.809 – 0.974	0.934 – 0.951
no. reflections measured	14385	61407	31160
no. unique reflections	6590 (R_{int} = 0.0260)	14653 (R_{int} = 0.0865)	8024 (R_{int} = 0.0583)
no. parameters refined	376	711	402
*R*1 ($I > 2\ \sigma(I)$)[a]	0.0302	0.0487	0.0648
*wR*2 (all data)[b]	0.0636	0.0817	0.1195
GOF (all data)[c]	1.002	1.009	1.000
max diff peak / hole, e $Å^{-3}$	+0.41 / –0.31	+0.71 / –0.50	+0.66 / –0.48

[a] $R1 = \Sigma||F_o|-|F_c||/\Sigma|F_o|$. [b] $wR2 = [\Sigma w(F_o^2-F_c^2)^2/\Sigma w(F_o^2)^2]^{1/2}$, $w = 1/[\sigma^2(F_o^2) + (qP)^2 + rP]$, $P = (\mathrm{Max}(F_o^2, 0) + 2\ F_c^2)/3$ [q = 0 (**6a**), 0.0339 (**6b**), 0 (**6c**); r = 8.5000 (**6a**), 0 (**6b**), 16.9000 (**6c**)]. [c] GOF = $[\Sigma w(F_o^2-F_c^2)^2/(N_o-N_{params})]^{1/2}$.

Supplementary Table 13. X-ray crystallographic data for **6d**, **6e** and **6f**.

	6d	**6e**·C_4H_4O	**6f**
CCDC number	2069971	2069972	2069973
chemical formula	$C_{28}H_{42}Cl_2MoN_2O_3P_2$	$C_{33}H_{53}F_3MoN_2O_4P_2$	$C_{30}H_{42}F_6MoN_2O_3P_2$
formula weight	683.44	756.68	750.55
dimensions of crystals, mm^3	0.10 × 0.05 × 0.05	0.20 × 0.05 × 0.05	0.20 × 0.10 × 0.05
crystal color, habit	yellow, block	brown, block	yellow, block
crystal system	monoclinic	monoclinic	monoclinic
space group	$P2_1/n$	$P2_1/c$	$P2_1/n$
a, Å	13.3948(4)	15.6266(10)	13.4331(3)
b, Å	14.6553(4)	15.1914(10)	15.1511(3)
c, Å	17.2580(5)	16.7554(11)	17.3972(4)
α, deg	90	90	90
β, deg	109.880(8)	111.687(8)	107.359(8)
γ, deg	90	90	90
V, $Å^3$	3185.9(2)	3696.0(5)	3379.54(19)
Z	4	4	4
ρ_{calcd}, g cm^{-3}	1.425	1.360	1.475
$F(000)$	1416.00	1584.00	1544.00
μ, cm^{-1}	7.097	4.924	5.481
temperature, °C	–180	–100	–90
trans. factors range	0.772 – 0.965	0.069 – 0.976	0.819 – 0.973
no. reflections measured	30147	28674	32476
no. unique reflections	7260 (R_{int} = 0.0518)	8275 (R_{int} = 0.1549)	7722 (R_{int} = 0.0526)
no. parameters refined	355	420	409
$R1$ ($I > 2\ \sigma(I)$)[a]	0.0379	0.1168	0.0444
$wR2$ (all data)[b]	0.0664	0.2495	0.0992
GOF (all data)[c]	1.000	1.007	1.069
max diff peak / hole, e $Å^{-3}$	+0.70 / –0.55	+2.07 / –0.68	+0.39 / –0.46

[a] $R1 = \Sigma||F_o|-|F_c||/\Sigma|F_o|$. [b] $wR2 = [\Sigma w(F_o^2-F_c^2)^2/\Sigma w(F_o^2)^2]^{1/2}$, $w = 1/[\sigma^2(F_o^2) + (qP)^2 + rP]$, $P = (\mathrm{Max}(F_o^2, 0) + 2\ F_c^2)/3$ [q = 0 (**6d**), 0 (**6e**), 0.0564 (**6f**); r = 6.0000 (**6d**), 28.0000 (**6e**), 0 (**6f**)]. [c] GOF = $[\Sigma w(F_o^2-F_c^2)^2/(N_o-N_{params})]^{1/2}$.

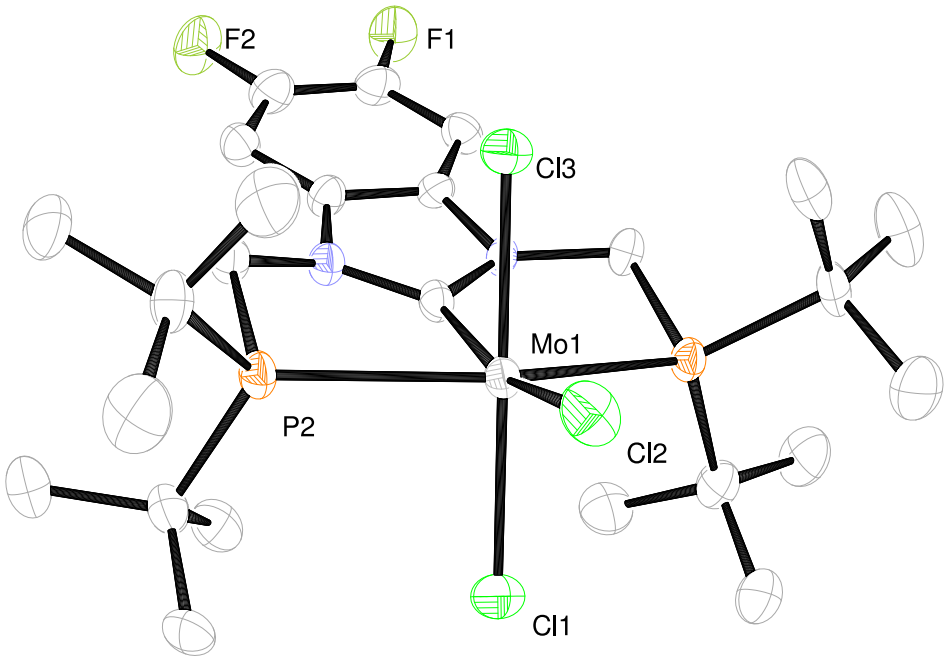

Supplementary Figure 2. Molecular structure of 1c·CH_2Cl_2. Thermal ellipsoids are shown at the 50% probability level. Hydrogen atoms and solvent atoms are omitted for clarity.

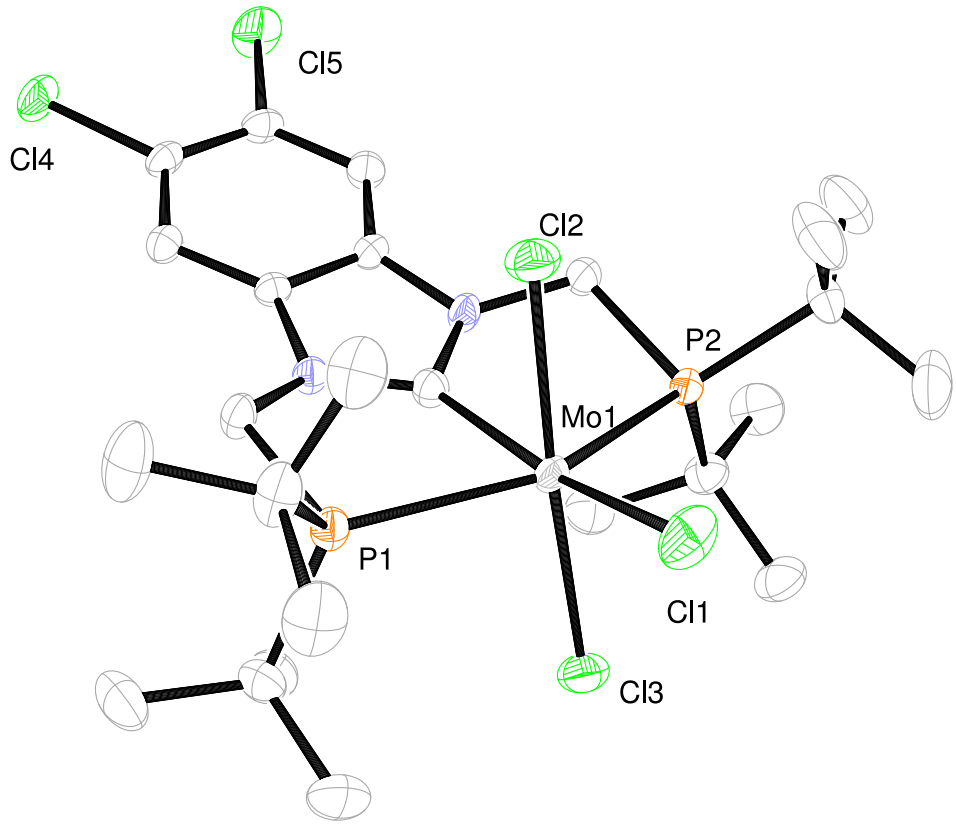

Supplementary Figure 3. Molecular structure of 1d·0.5CH_2Cl_2. Thermal ellipsoids are shown at the 50% probability level. Hydrogen atoms and solvent atoms are omitted for clarity.

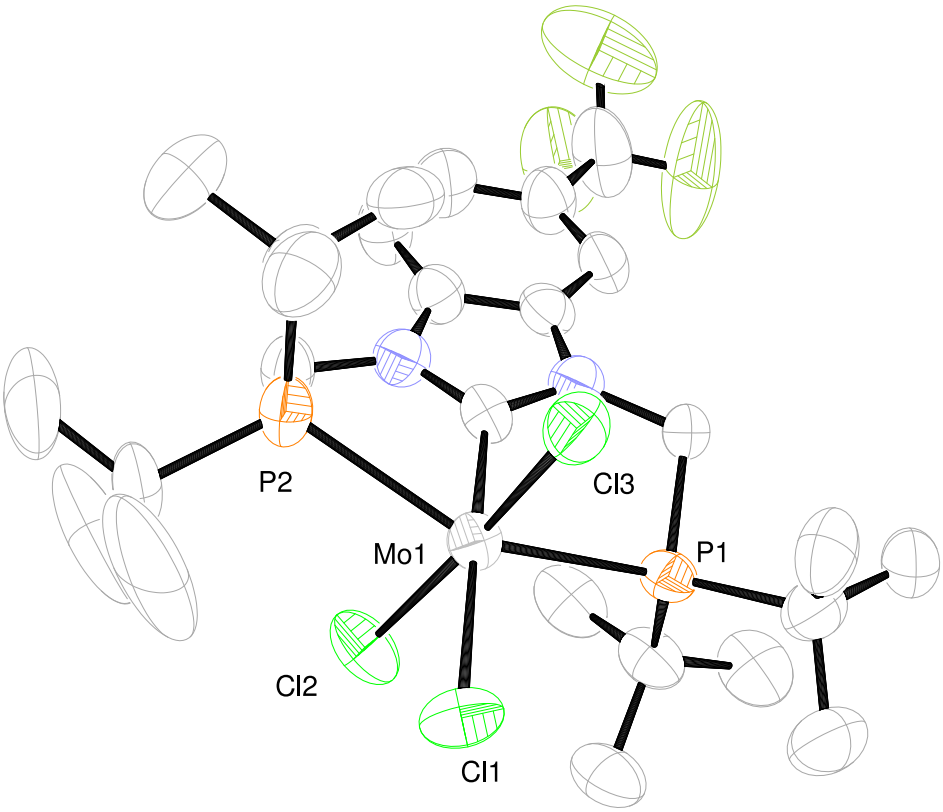

Supplementary Figure 4. Molecular structure of 1e. Thermal ellipsoids are shown at the 50% probability level. Hydrogen atoms are omitted for clarity.

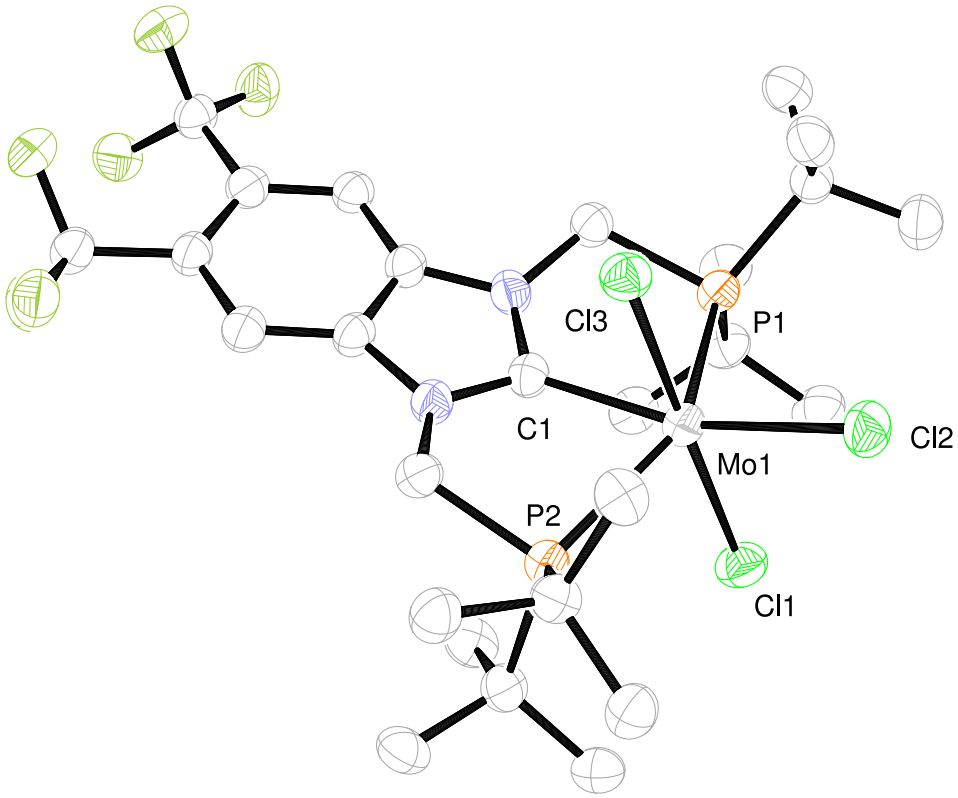

Supplementary Figure 5. Molecular structure of 1f. Thermal ellipsoids are shown at the 50% probability level. Hydrogen atoms are omitted for clarity.

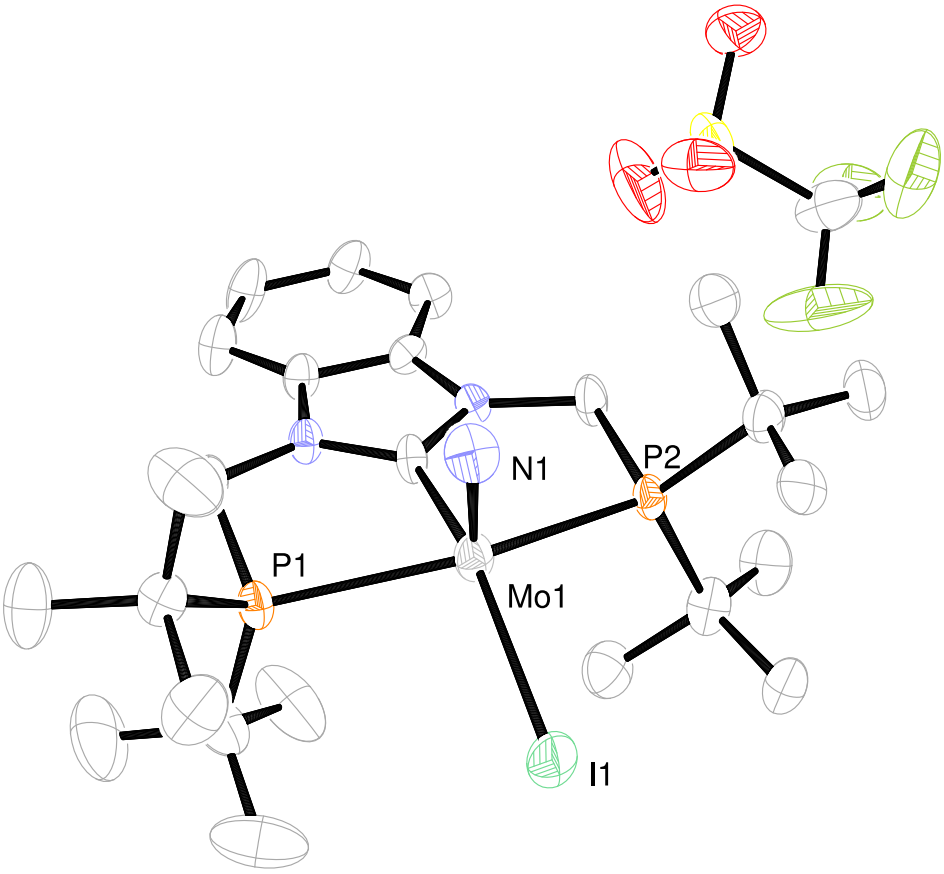

Supplementary Figure 6. Molecular structure of [Mo(N)I(PCP)]OTf. Thermal ellipsoids are shown at the 50% probability level. Hydrogen atoms are omitted for clarity.

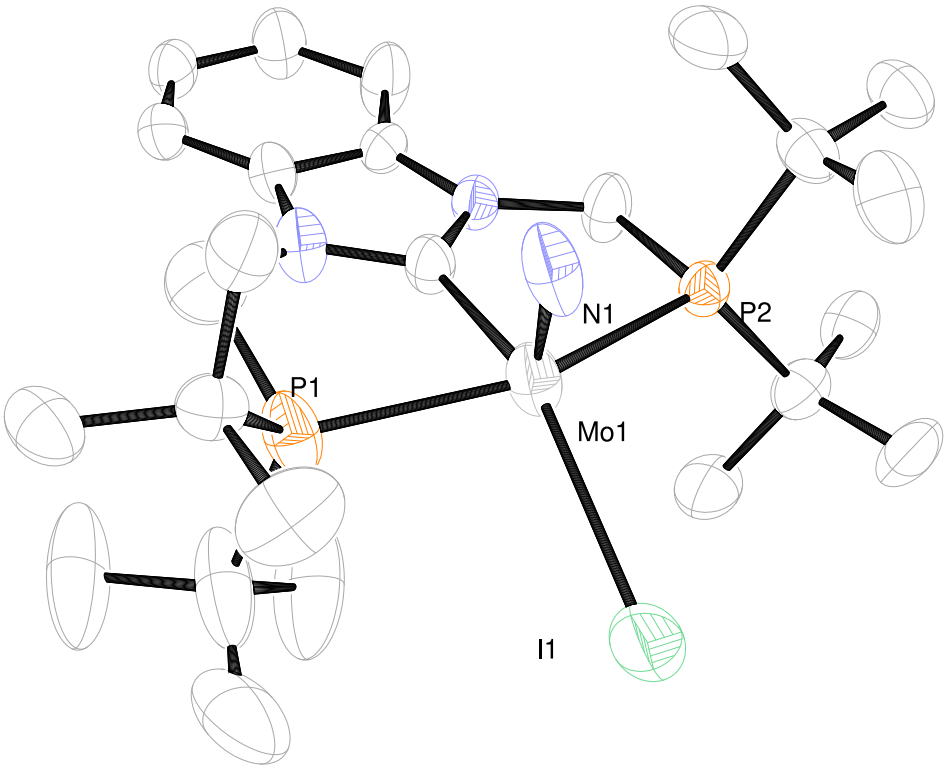

Supplementary Figure 7. Molecular structure of 2a. Thermal ellipsoids are shown at the 50% probability level. Hydrogen atoms are omitted for clarity.

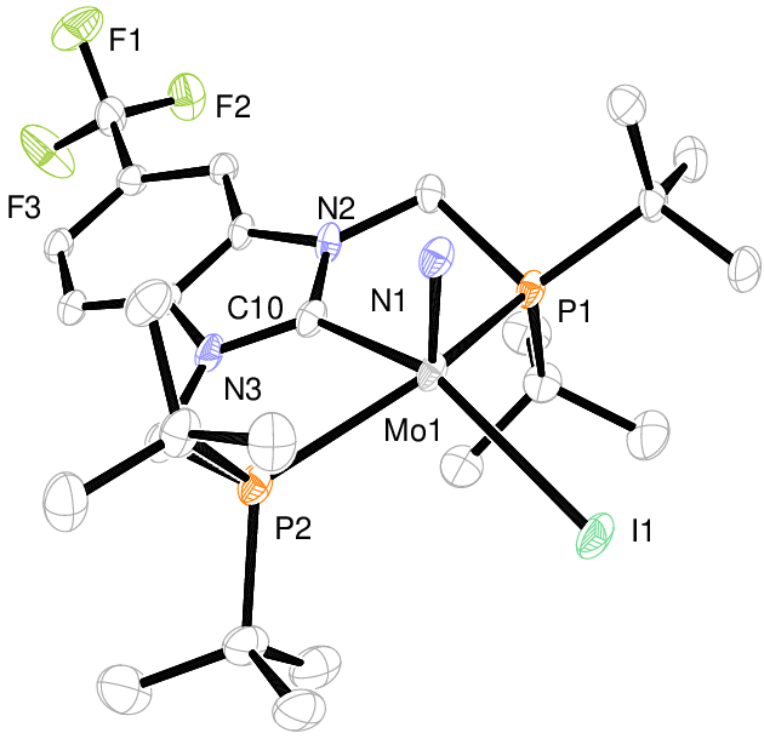

Supplementary Figure 8. Molecular structure of 2e. Thermal ellipsoids are shown at the 50% probability level. Hydrogen atoms are omitted for clarity.

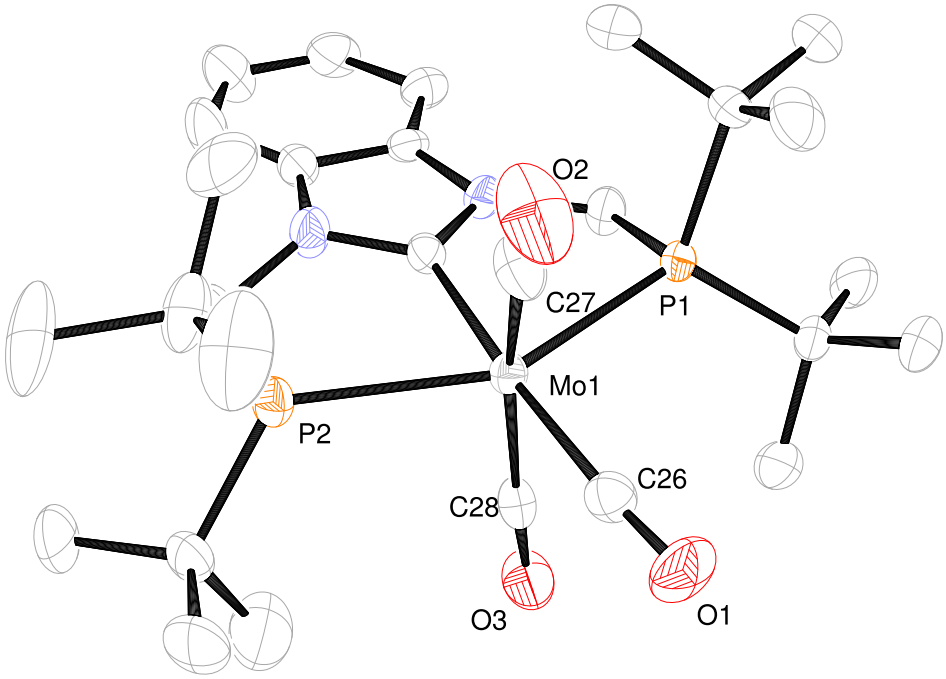

Supplementary Figure 9. Molecular structure of 6a. Thermal ellipsoids are shown at the 50% probability level. Hydrogen atoms are omitted for clarity.

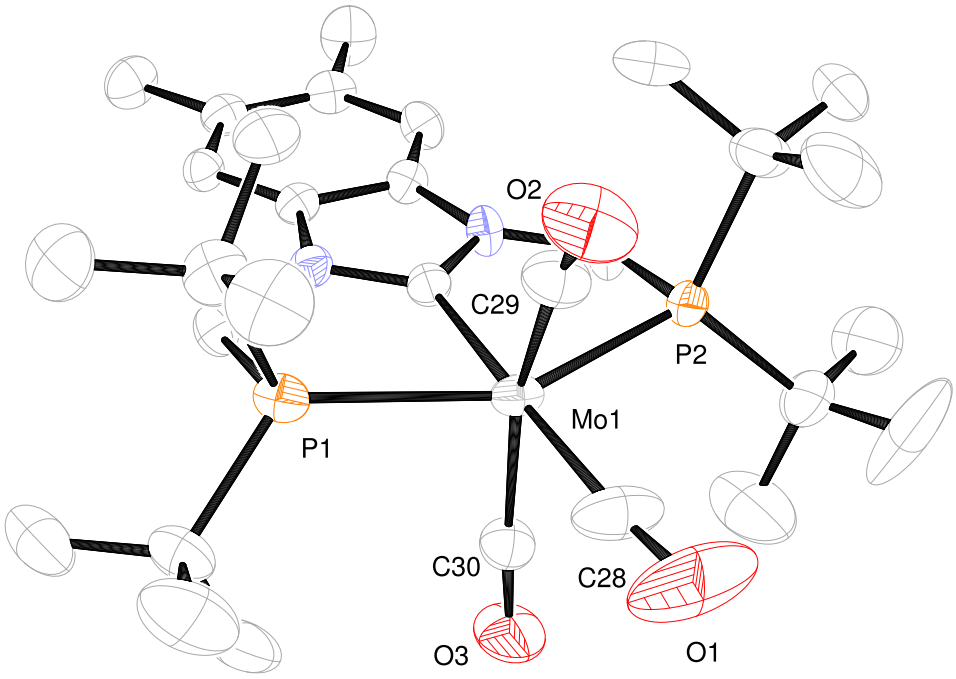

Supplementary Figure 10. Molecular structure of 6b. Thermal ellipsoids are shown at the 50% probability level. Hydrogen atoms are omitted for clarity.

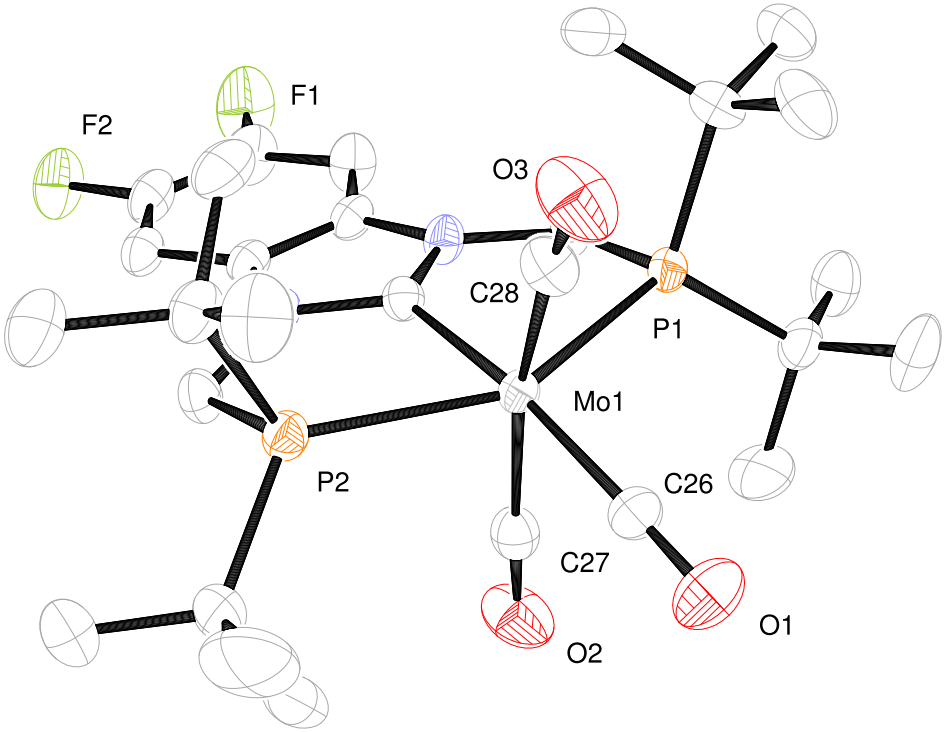

Supplementary Figure 11. Molecular structure of 6c. Thermal ellipsoids are shown at the 50% probability level. Hydrogen atoms are omitted for clarity.

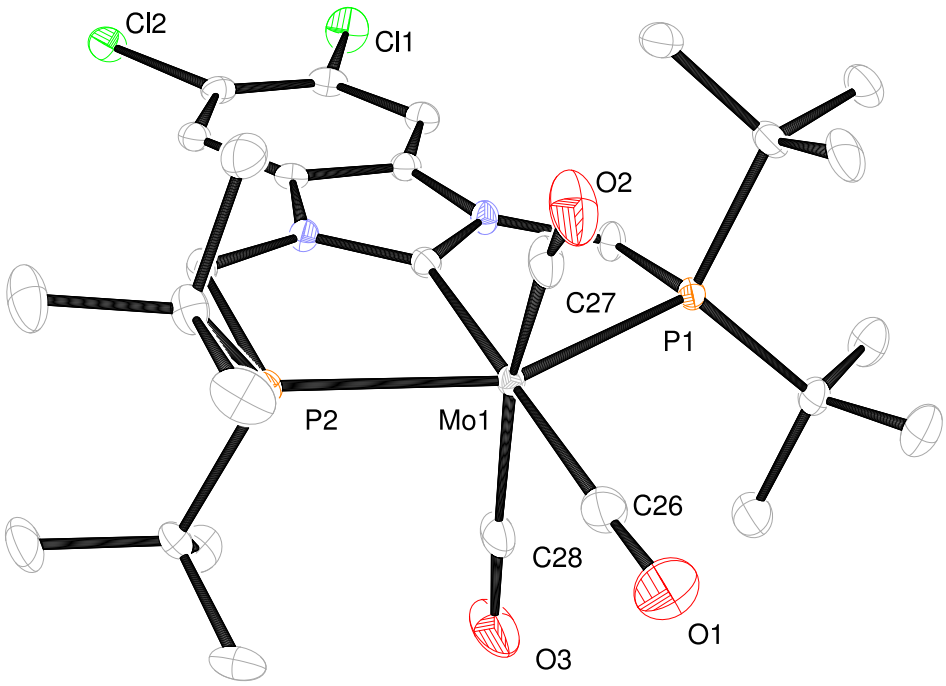

Supplementary Figure 12. Molecular structure of 6d. Thermal ellipsoids are shown at the 50% probability level. Hydrogen atoms are omitted for clarity.

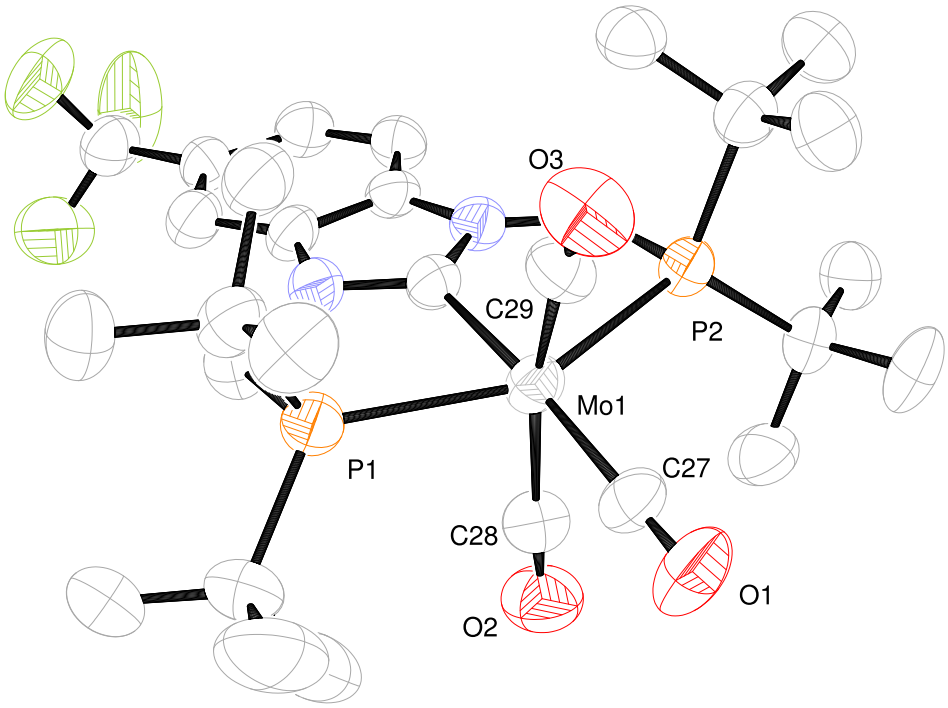

Supplementary Figure 13. Molecular structure of 6e·C_2H_4O. Thermal ellipsoids are shown at the 50% probability level. Hydrogen atoms and solvent atoms are omitted for clarity.

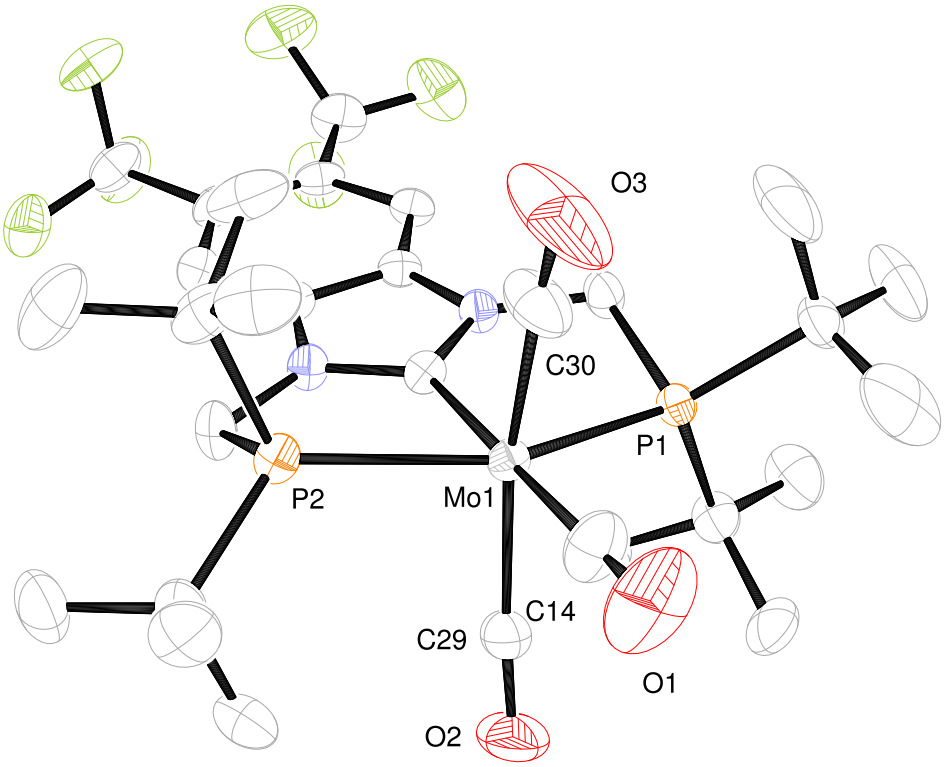

Supplementary Figure 14. Molecular structure of 6f. Thermal ellipsoids are shown at the 50% probability level. Hydrogen atoms are omitted for clarity.

6. Calculation details

DFT calculations were performed with the Gaussian09 program (Rev. E.01).[S19] Geometry optimizations were carried out with the B3LYP-D3 functional, which is the B3LYP hybrid functional[S20–S23] combined with an empirical dispersion correction developed by Grimme.[S24] In the present calculations, the SDD (Stuttgart/Dresden pseudopotentials) basis sets[S25,S26] are employed for the molybdenum and iodine atoms. The 6-31G(d) basis sets[S27–S30] are employed for the other atoms. All stationary-point structures were confirmed to have the appropriate number of imaginary frequencies by vibrational analysis. To determine the free energy profiles, single-point energy calculations were performed at the optimized geometries using the SDD and 6-311+G(d,p) basis sets.[S31–S33] In the single-point calculations, solvation effects of THF (ε = 7.4257) were taken into account by using the polarizable continuum model (PCM).[S34] All optimized structures of nitride-, imide-, amide-, and ammine intermediates are shown in **Supplementary Figures 15-20**. **Supplementary Table 14** lists the HOMO and LUMO energies of **2a** and 5,6-substituted Mo-nitride complexes (**2b**-**2d**, **2f**) plotted in **Figure 2(a)**.

Detailed data on SCF energies, thermal energy corrections at 298 K, and SCF energies in THF are summarized in **Supplementary Table 15**. Cartesian coordinates of all optimized structures are given in a separated .xyz file.

Supplementary Table 14. The HOMO and LUMO energies of [MoI(N)($PCP^{R1,R2}$)] (**2a**-**2d**, **2f**)

(R^1, R^2)	HOMO (eV)	LUMO (eV)
(H, H) (**2a**)	–3.77	–1.41
(Me, Me) (**2b**)	–3.69	–1.29
(F, F) (**2c**)	–3.89	–1.64
(Cl, Cl) (**2d**)	–3.99	–1.78
(CF_3, CF_3) (**2f**)	–4.11	–1.94

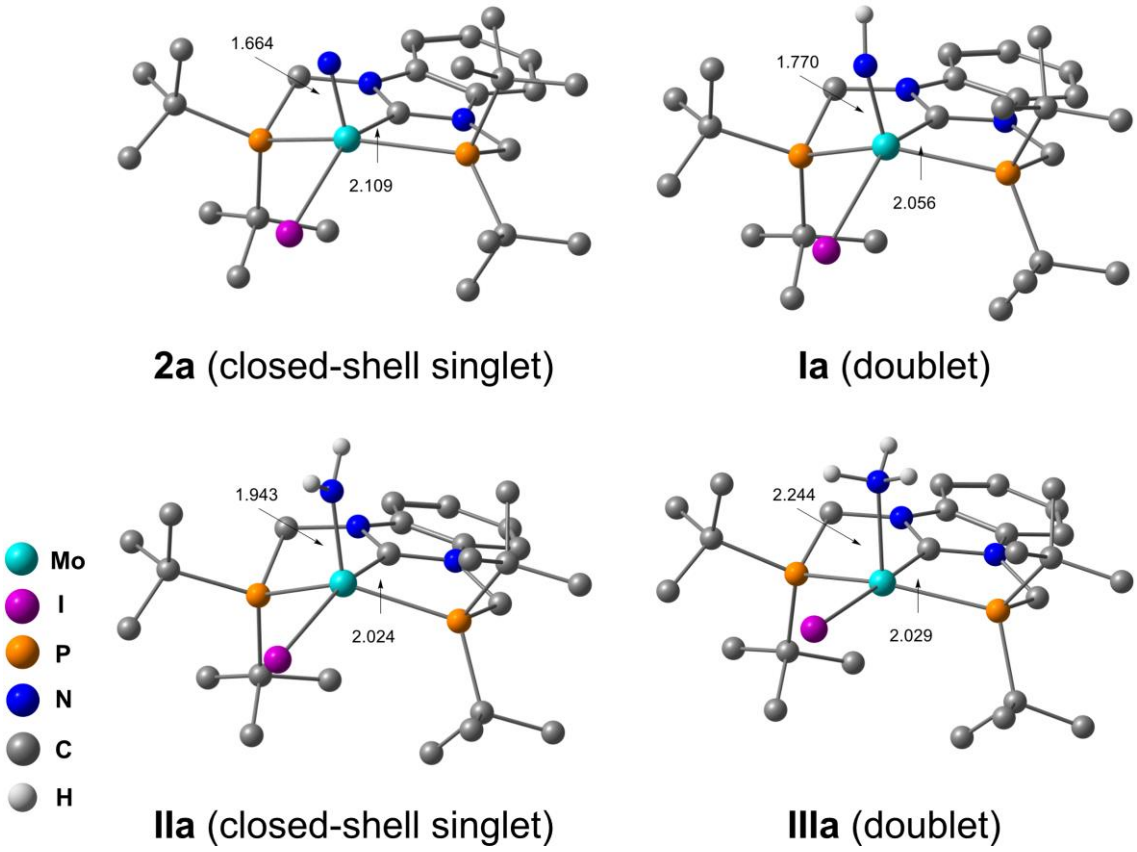

Supplementary Figure 15. Optimized structures of non-substituted nitride- (**2a**), imide- (**Ia**), amide- (**IIa**), and ammine (**IIIa**) intermediates in the ground spin state. Selected interatomic distances are presented in Å. Hydrogen atoms attached to carbon atoms are omitted for clarity.

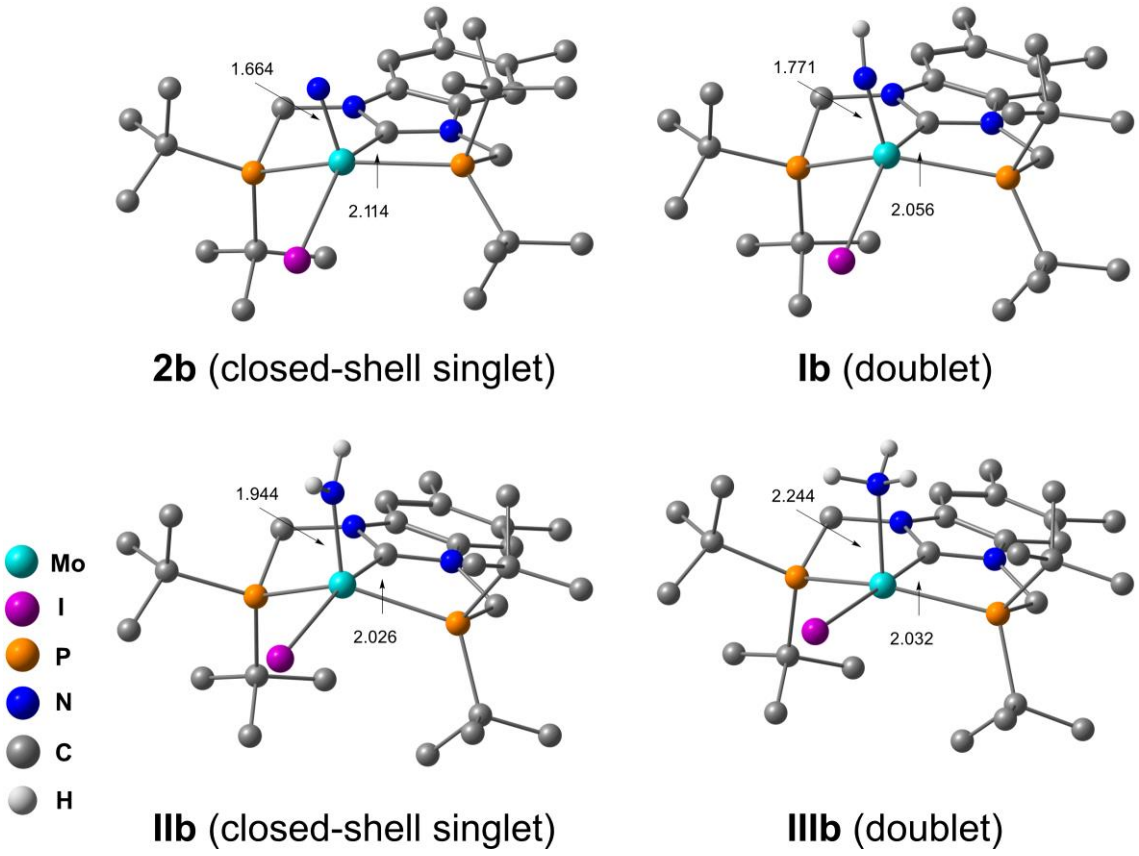

Supplementary Figure 16. Optimized structures of nitride- (**2b**), imide- (**Ib**), amide- (**IIb**), and ammine (**IIIb**) intermediates with a 5,6-dimethyl-substituted PCP-type ligand in the ground spin state. Selected interatomic distances are presented in Å. Hydrogen atoms attached to carbon atoms are omitted for clarity.

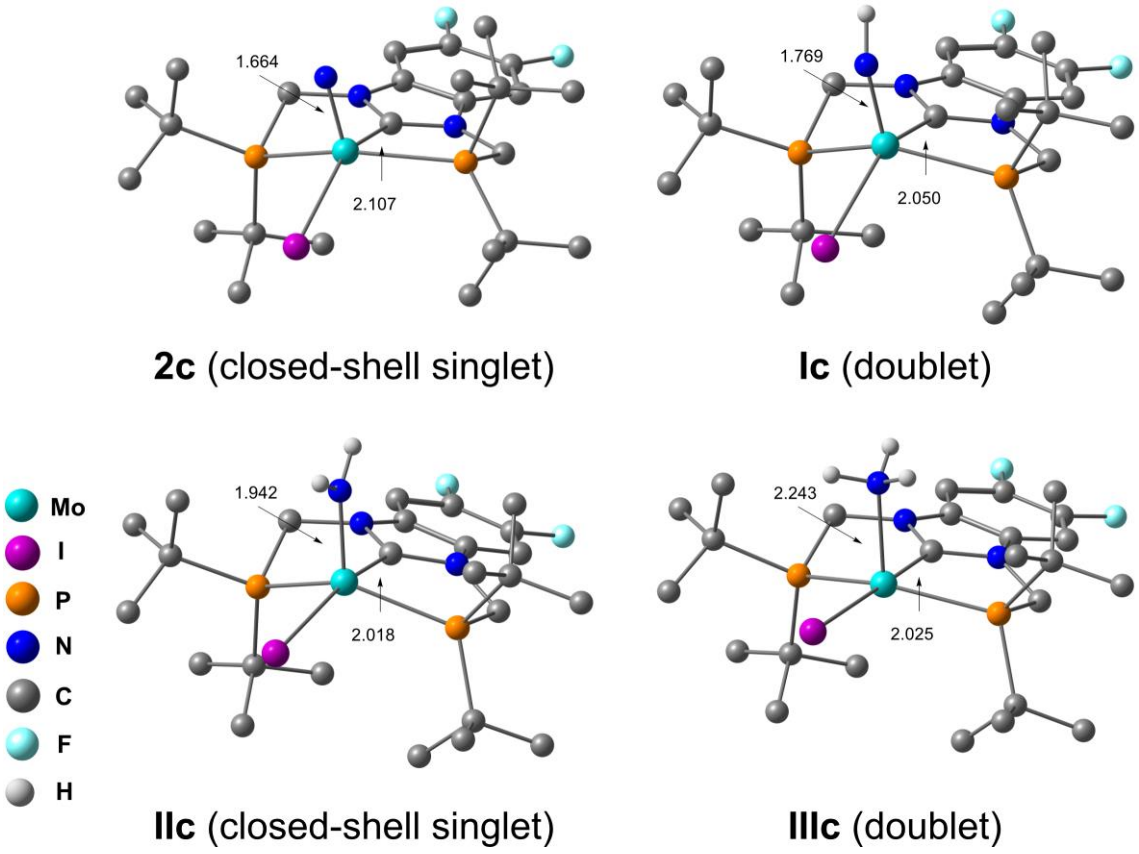

Supplementary Figure 17. Optimized structures of nitride- (**2c**), imide- (**Ic**), amide- (**IIc**), and ammine (**IIIc**) intermediates with a 5,6-difluoro-substituted PCP-type ligand in the ground spin state. Selected interatomic distances are presented in Å. Hydrogen atoms attached to carbon atoms are omitted for clarity.

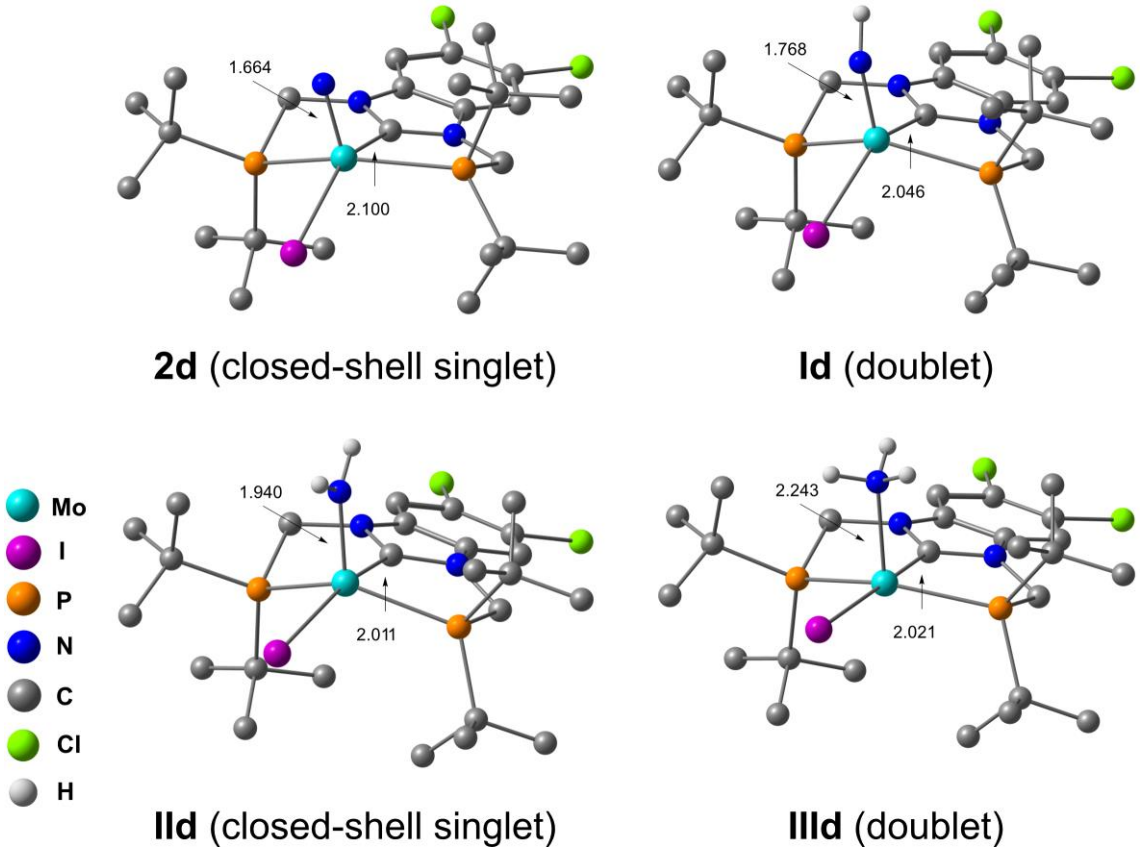

Supplementary Figure 18. Optimized structures of nitride- (**2d**), imide- (**Id**), amide- (**IId**), and ammine (**IIId**) intermediates with a 5,6-dichloro-substituted PCP-type ligand in the ground spin state. Selected interatomic distances are presented in Å. Hydrogen atoms attached to carbon atoms are omitted for clarity.

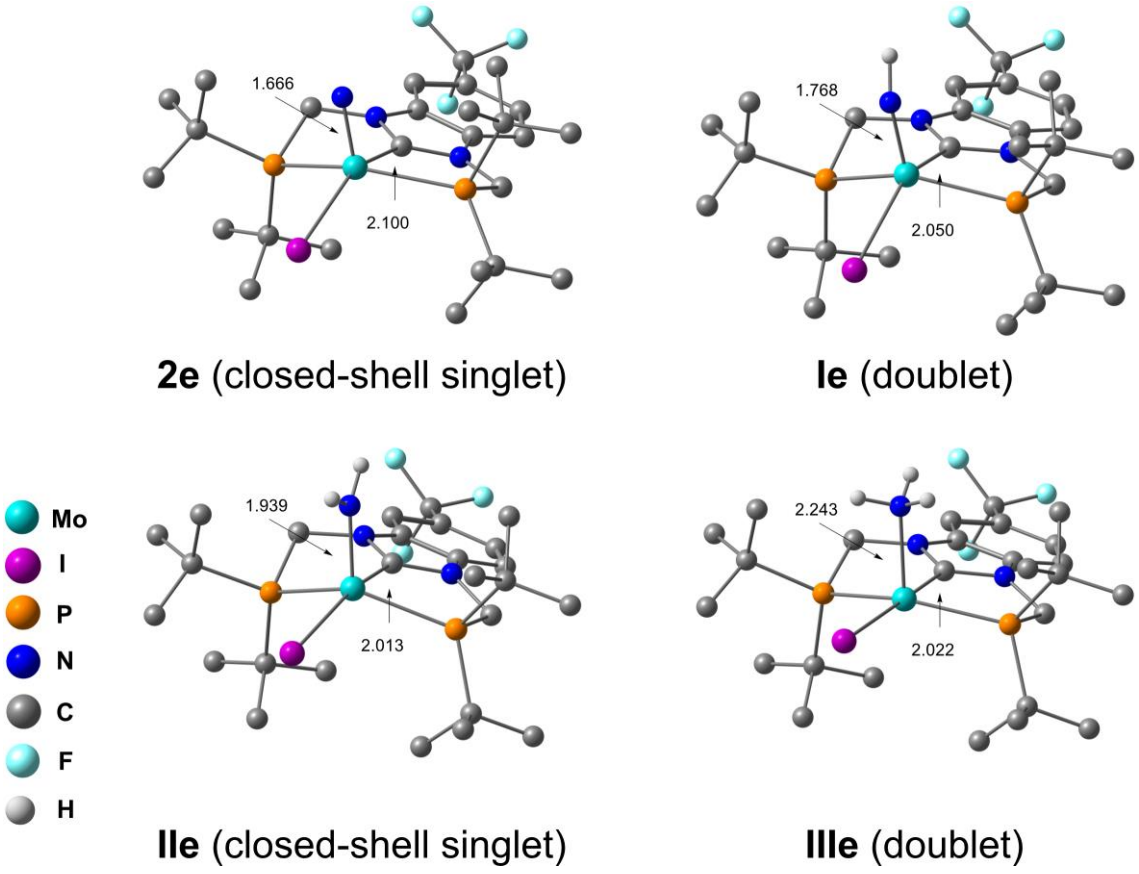

Supplementary Figure 19. Optimized structures of nitride- (**2e**), imide- (**Ie**), amide- (**IIe**), and ammine (**IIIe**) intermediates with a 5-trifluoromethyl-substituted PCP-type ligand in the ground spin state. Selected interatomic distances are presented in Å. Hydrogen atoms attached to carbon atoms are omitted for clarity.

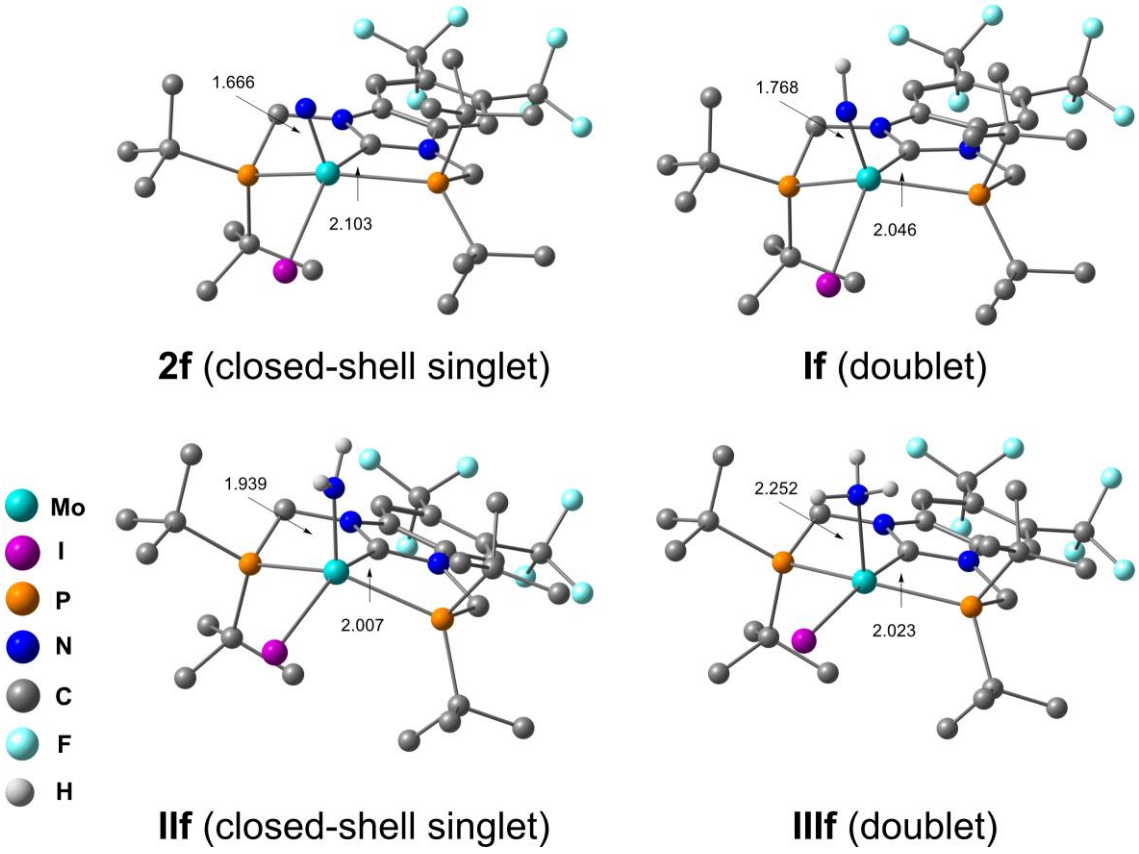

Supplementary Figure 20. Optimized structures of nitride- (**2f**), imide- (**If**), amide- (**IIf**), and ammine (**IIIf**) intermediates with a 5,6-bis(trifluoromethyl)-substituted PCP-type ligand in the ground spin state. Selected interatomic distances are presented in Å. Hydrogen atoms attached to carbon atoms are omitted for clarity.

Supplementary Table 15. SCF energies (SCFE), thermal correction at 298.15 K (TC_{298}), and single-point energies in THF (E_{solv}) calculated for all species in the present study. Units are given in Hartree.

Species (spin state)	SCFE	TC_{298}	E_{solv}
2a (closed-shell singlet)	-1905.97046849	0.59383800	-1906.37660205
Ia (doublet)	-1906.54515352	0.60242200	-1906.95198928
IIa (closed-shell singlet)	-1907.15242717	0.61449600	-1907.56092654
IIIa (doublet)	-1907.73584891	0.62501900	-1908.14998301
2b (closed-shell singlet)	-1984.61041904	0.64490000	-1985.03692409
Ib (doublet)	-1985.18449957	0.65398500	-1985.61126114
IIb (closed-shell singlet)	-1985.79136074	0.66619400	-1986.21936669
IIIb (doublet)	-1986.37492271	0.67710900	-1986.80824840
2c (closed-shell singlet)	-2104.42528807	0.57312500	-2104.90548342
Ic (doublet)	-2105.00088052	0.58308500	-2105.48197922
IIc (closed-shell singlet)	-2105.60903515	0.59510800	-2106.09230778
IIIc (doublet)	-2106.19330511	0.60621300	-2106.68228749
2d (closed-shell singlet)	-2825.15003041	0.56796800	-2825.61819113
Id (doublet)	-2825.72696533	0.57888700	-2826.19577968
IId (closed-shell singlet)	-2826.33578494	0.58989300	-2826.80683851
IIId (doublet)	-2826.92058365	0.60155500	-2827.39735557
2e (closed-shell singlet)	-2243.00884232	0.59357800	-2243.53215975
Ie (doublet)	-2243.58532893	0.60123900	-2244.10976183
IIe (closed-shell singlet)	-2244.19387419	0.61560000	-2244.72046872
IIIe (doublet)	-2244.77847166	0.62487200	-2245.31087645
2f (closed-shell singlet)	-2580.04105277	0.59194700	-2580.67596325
If (doublet)	-2580.61803637	0.60179700	-2581.25468551
IIf (closed-shell singlet)	-2581.22265080	0.61574300	-2581.86270059
IIIf (doublet)	-2581.80880539	0.62470700	-2582.45193683

7. NMR and IR spectra

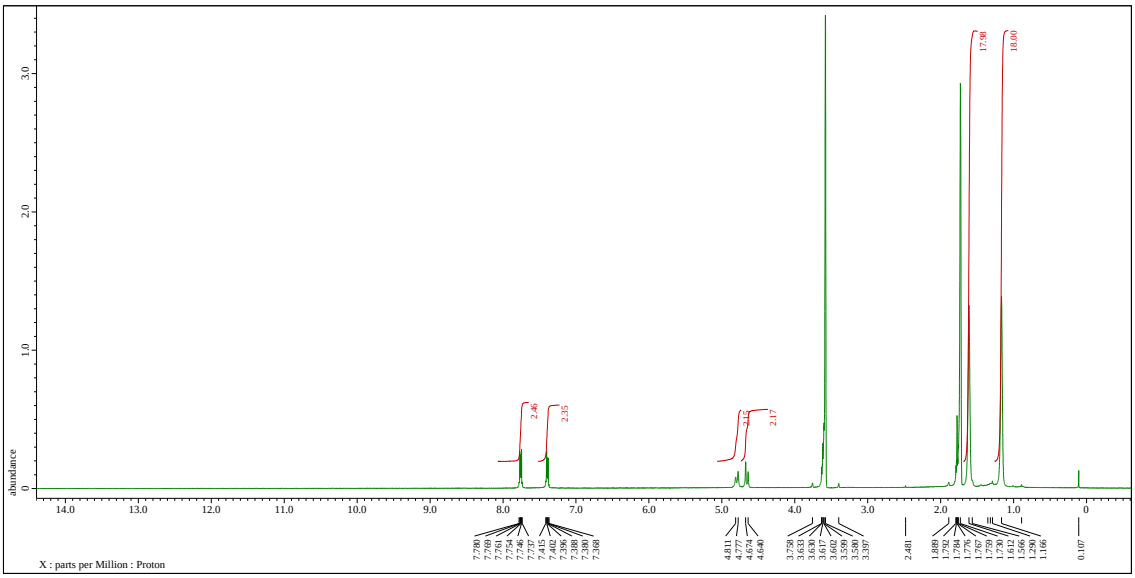

Supplementary Figure 21. ^{1}H NMR of **2a**.

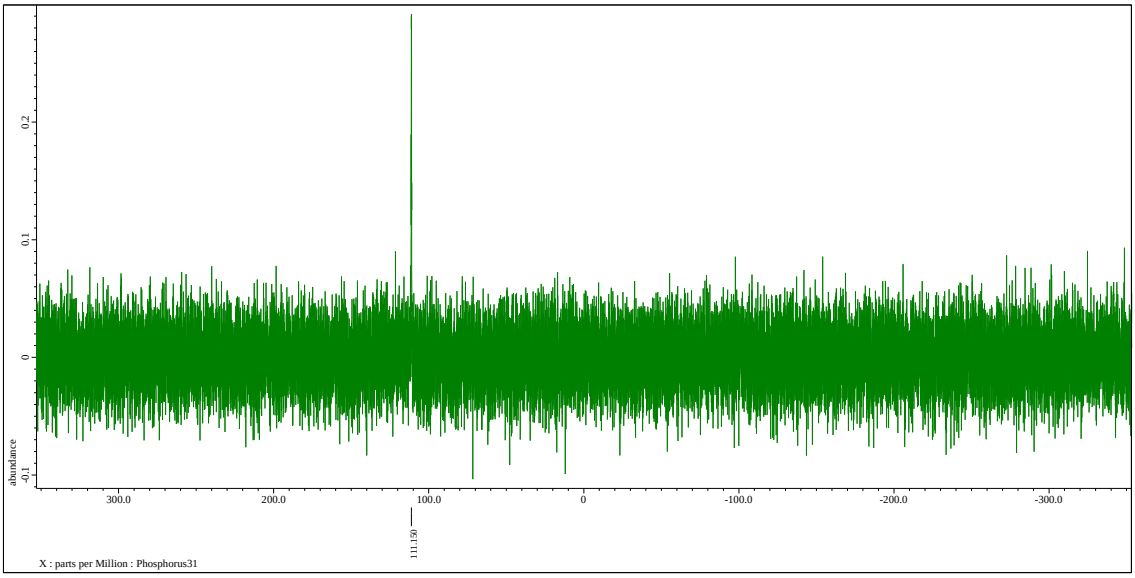

Supplementary Figure 22. ^{31}P{^{1}H} NMR of **2a**.

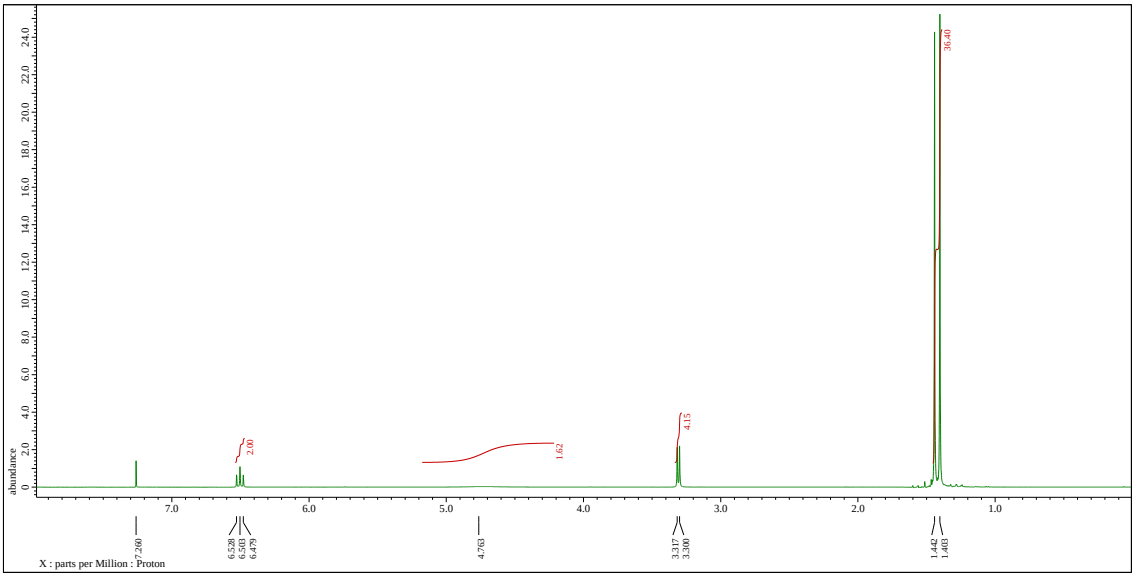

Supplementary Figure 23. ^{1}H NMR of **7c**.

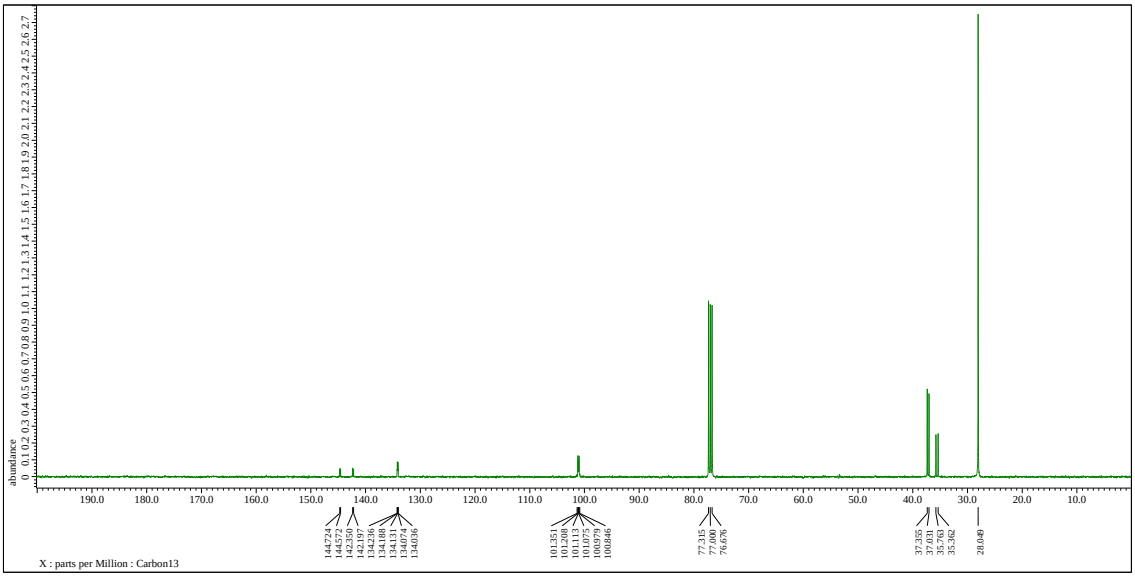

Supplementary Figure 24. $^{13}C\{^{1}H\}$ NMR of **7c**.

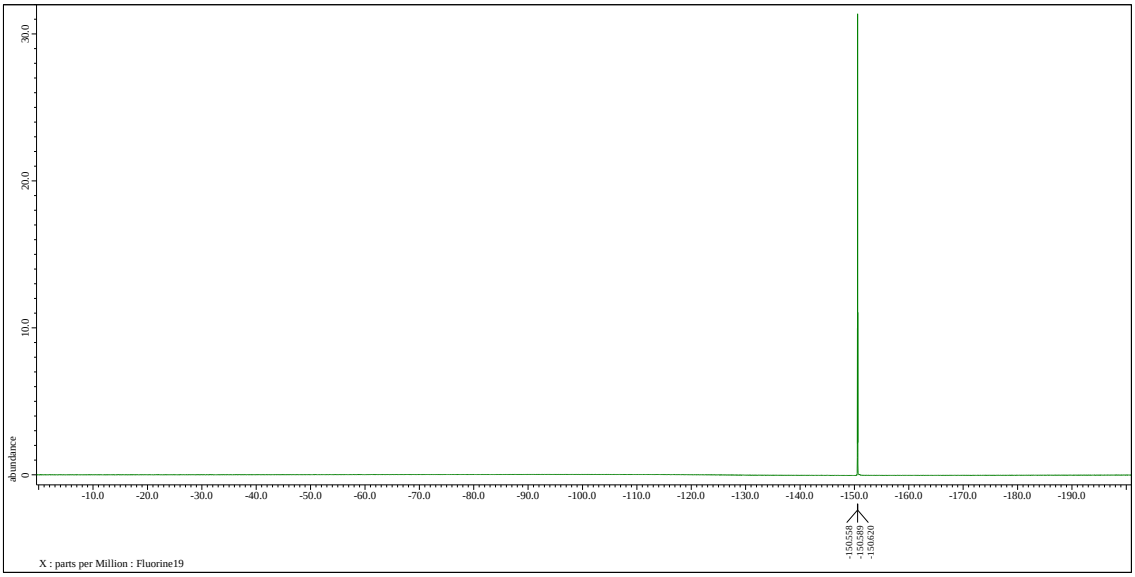

Supplementary Figure 25. ^{19}F NMR of **7c**.

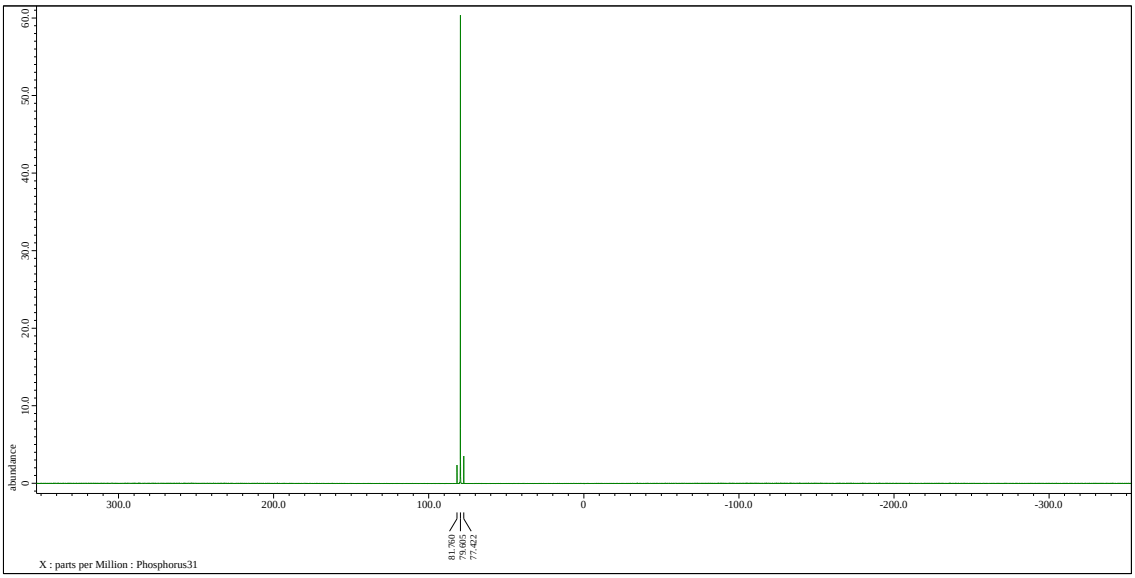

Supplementary Figure 26. $^{31}P\{^{1}H\}$ NMR of **7c**.

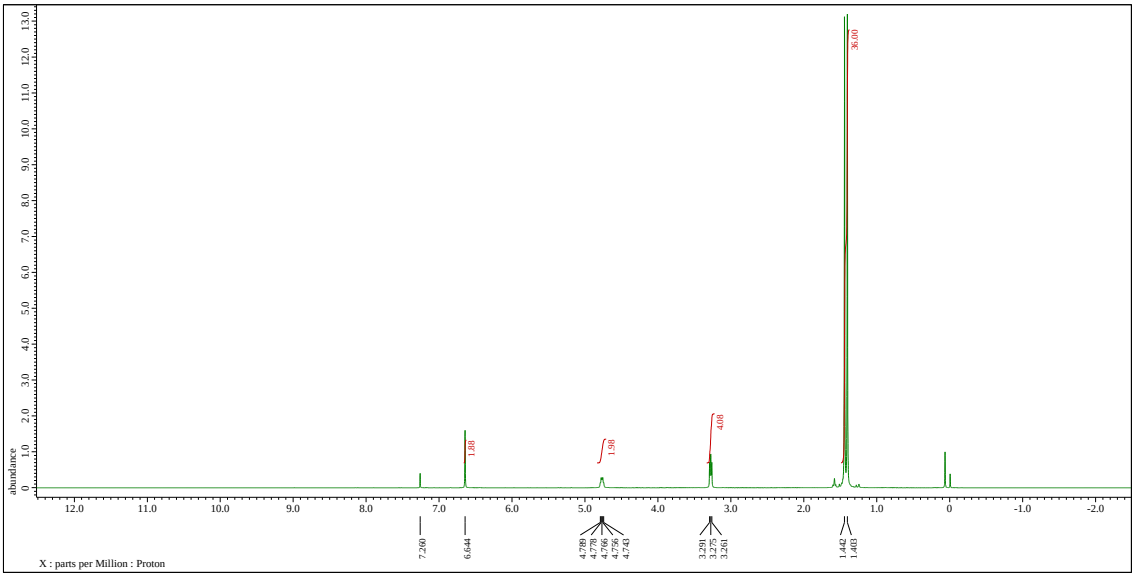

Supplementary Figure 27. ^{1}H NMR of **7d**.

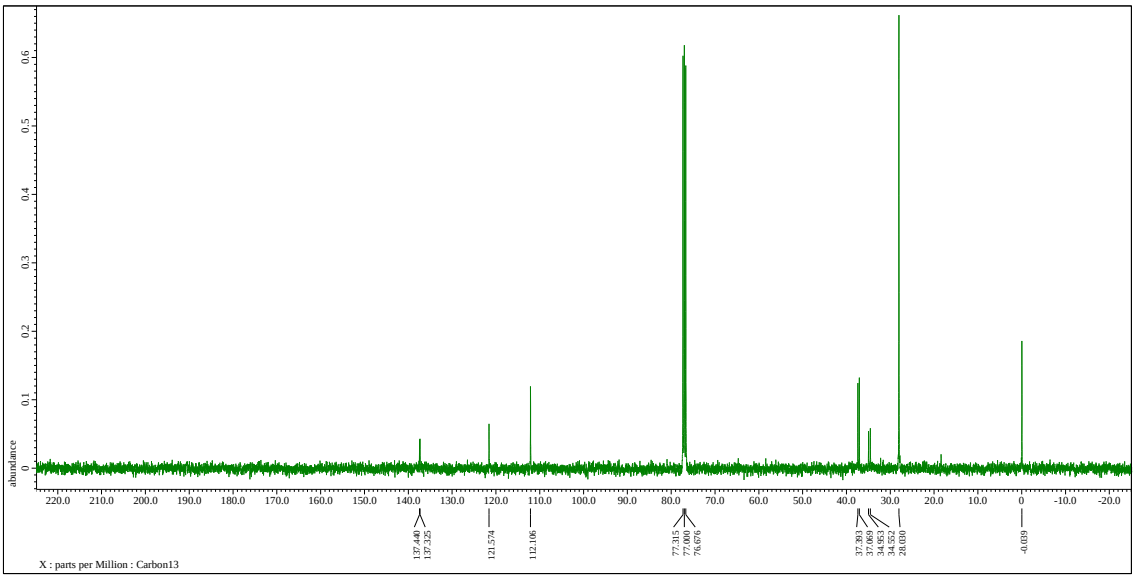

Supplementary Figure 28. ^{13}C{^{1}H} NMR of **7d**.

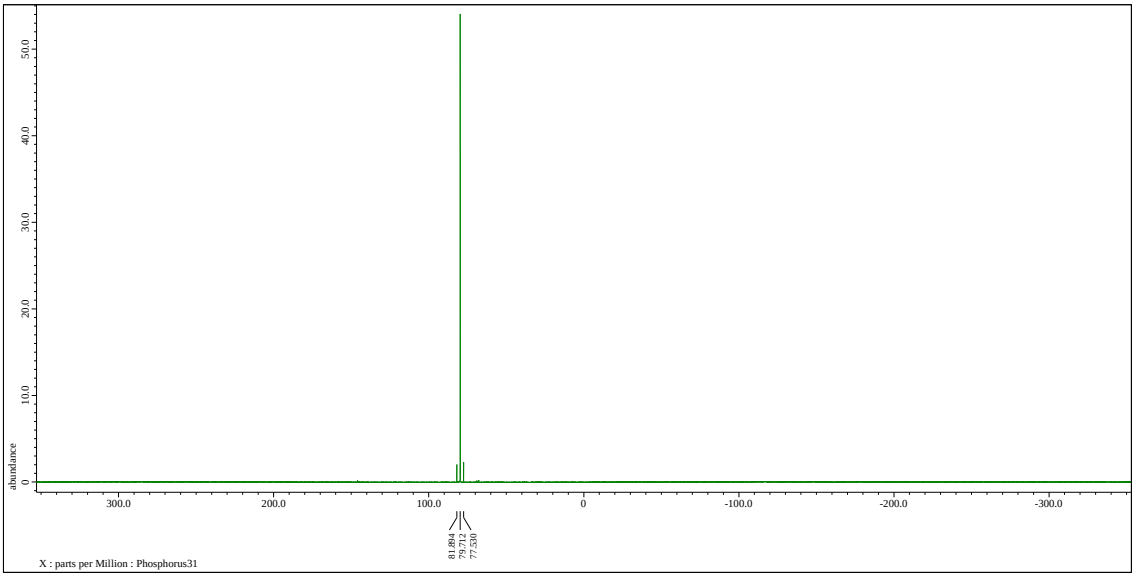

Supplementary Figure 29. $^{31}P\{^{1}H\}$ NMR of **7d**.

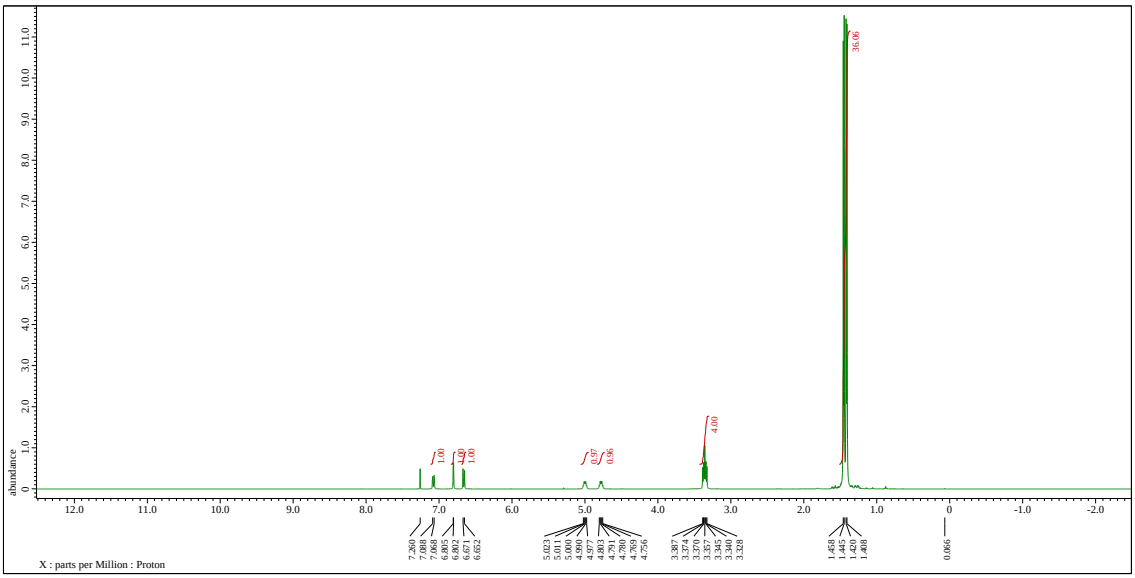

Supplementary Figure 30. ^{1}H NMR of **7e**.

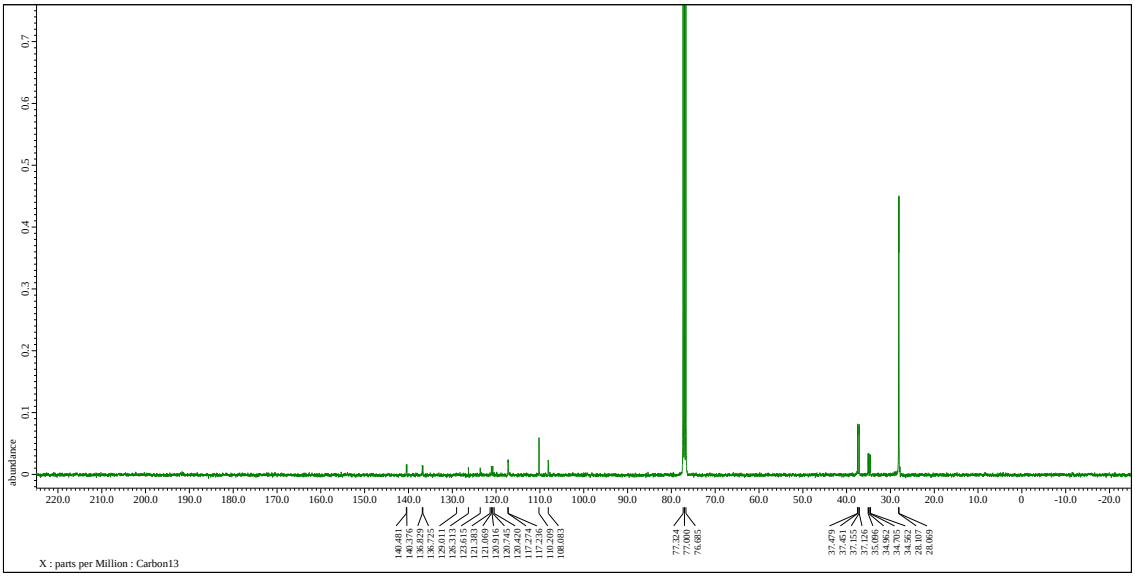

Supplementary Figure 31. $^{13}C\{^{1}H\}$ NMR of **7e**.

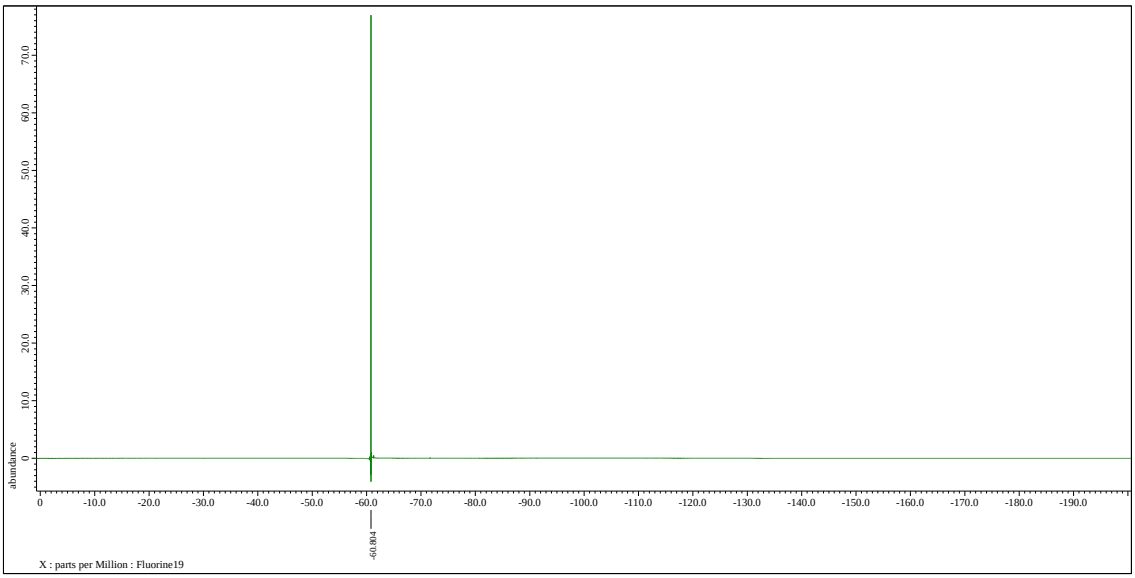

Supplementary Figure 32. ^{19}F NMR of **7e**.

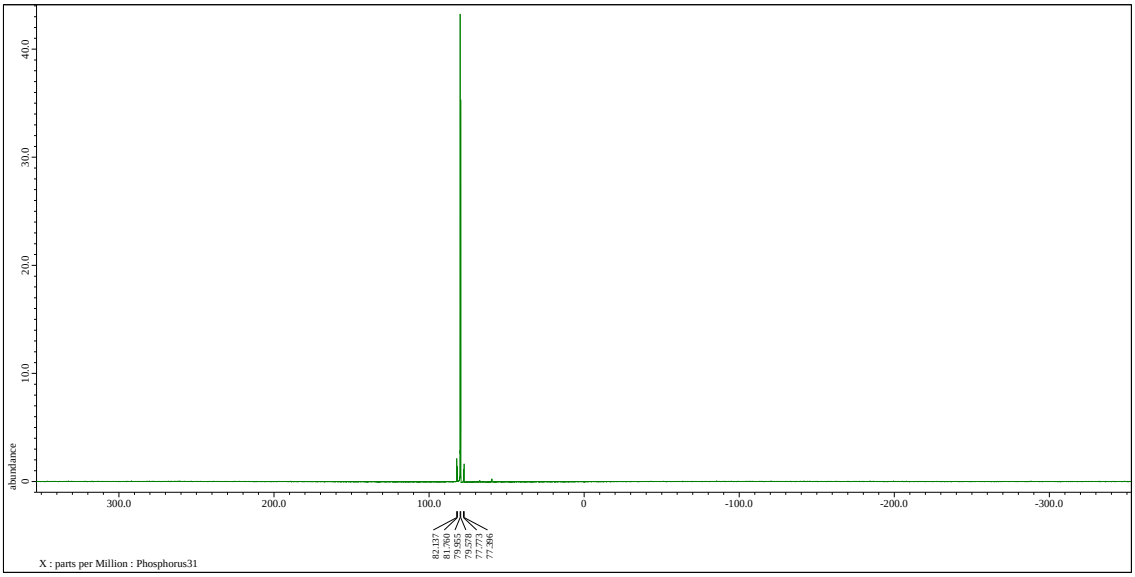

Supplementary Figure 33. $^{31}P\{^{1}H\}$ NMR of **7e**.

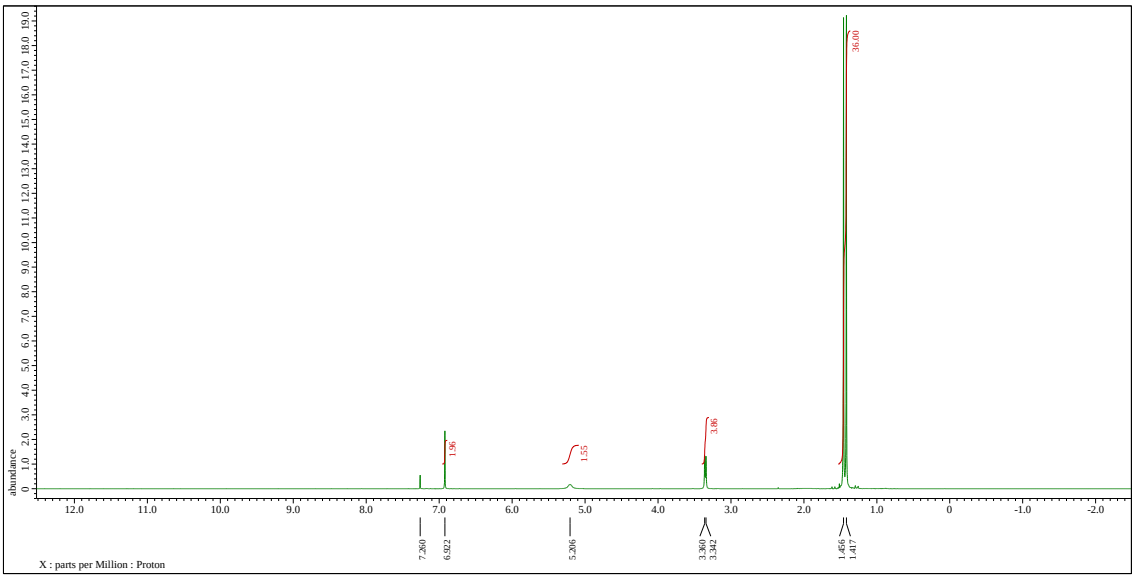

Supplementary Figure 34. ^{1}H NMR of **7f**.

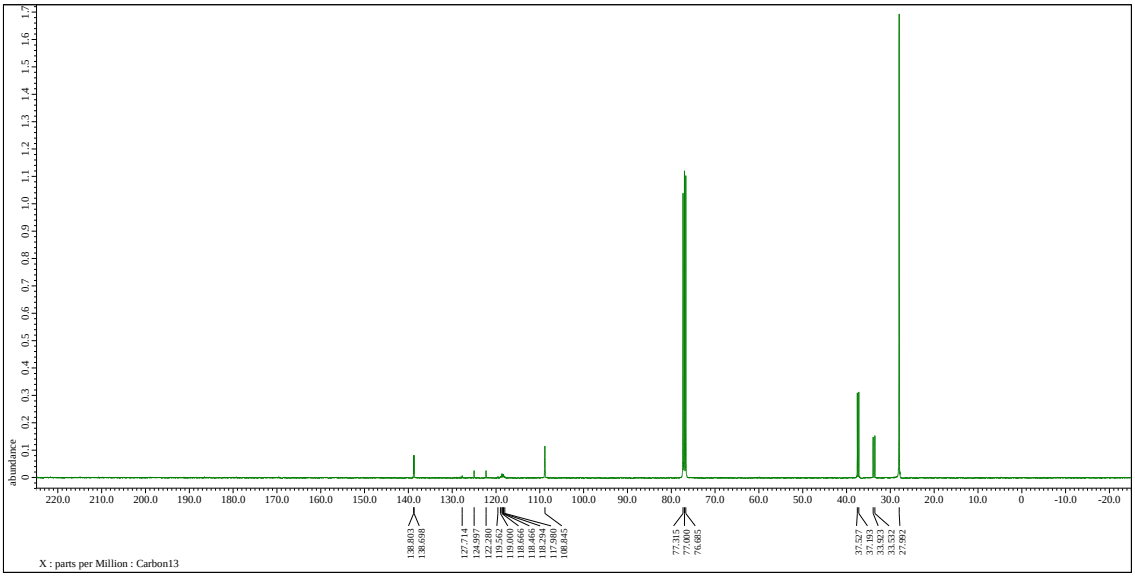

Supplementary Figure 35. $^{13}C\{^{1}H\}$ NMR of **7f**.

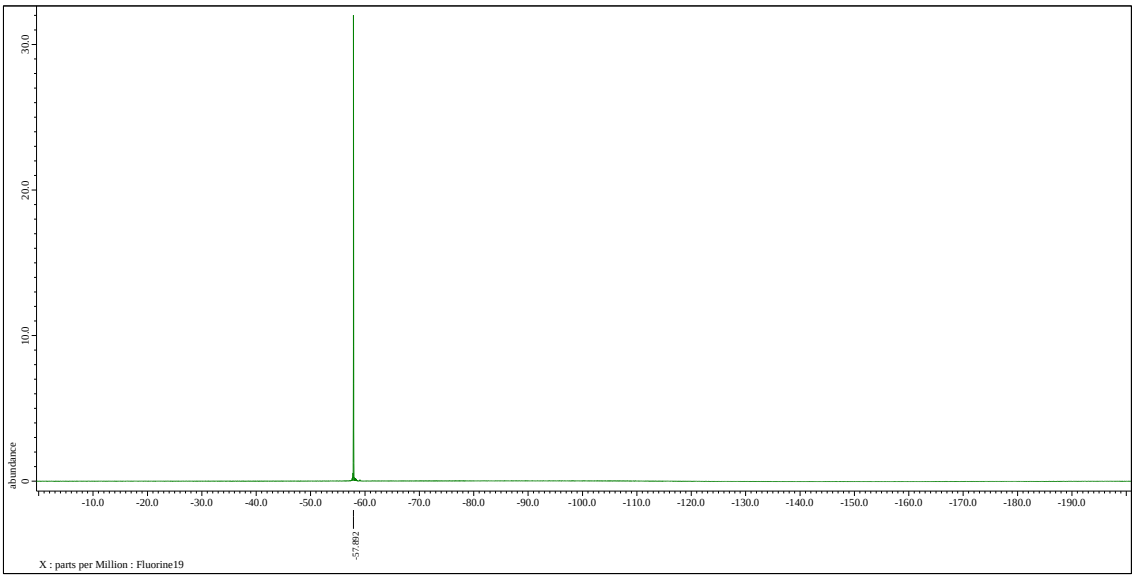

Supplementary Figure 36. ^{19}F NMR of **7f**.

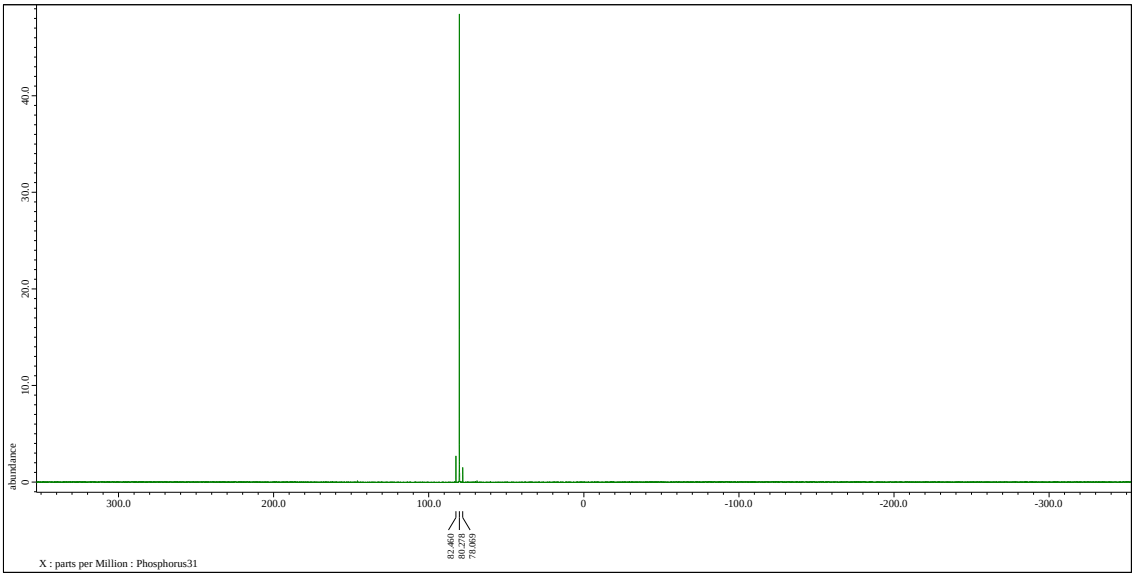

Supplementary Figure 37. $^{31}P\{^{1}H\}$ NMR of **7f**.

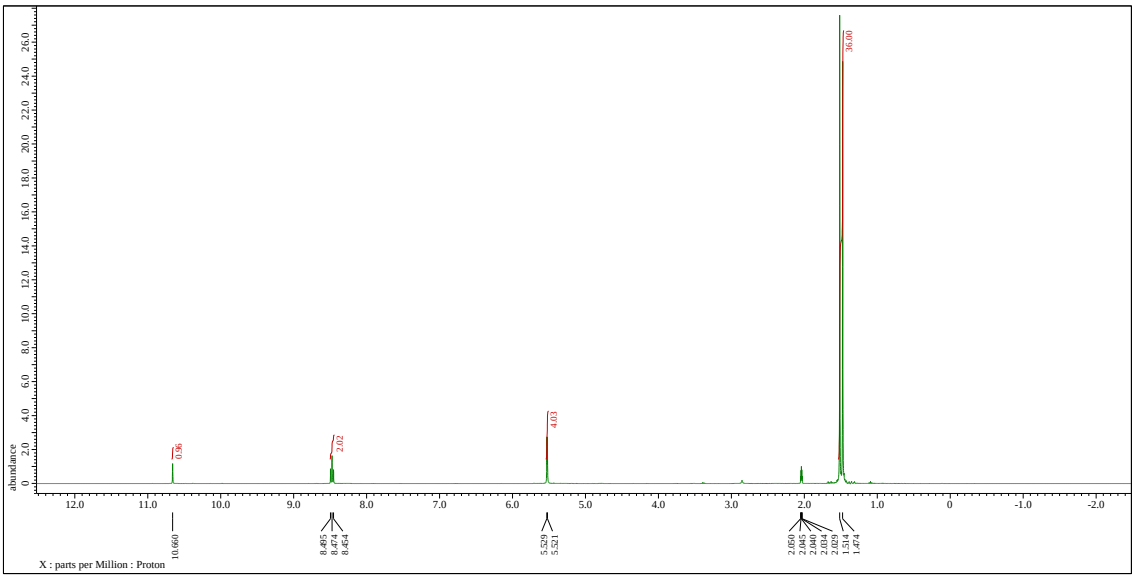

Supplementary Figure 38. ^{1}H NMR of **8c**.

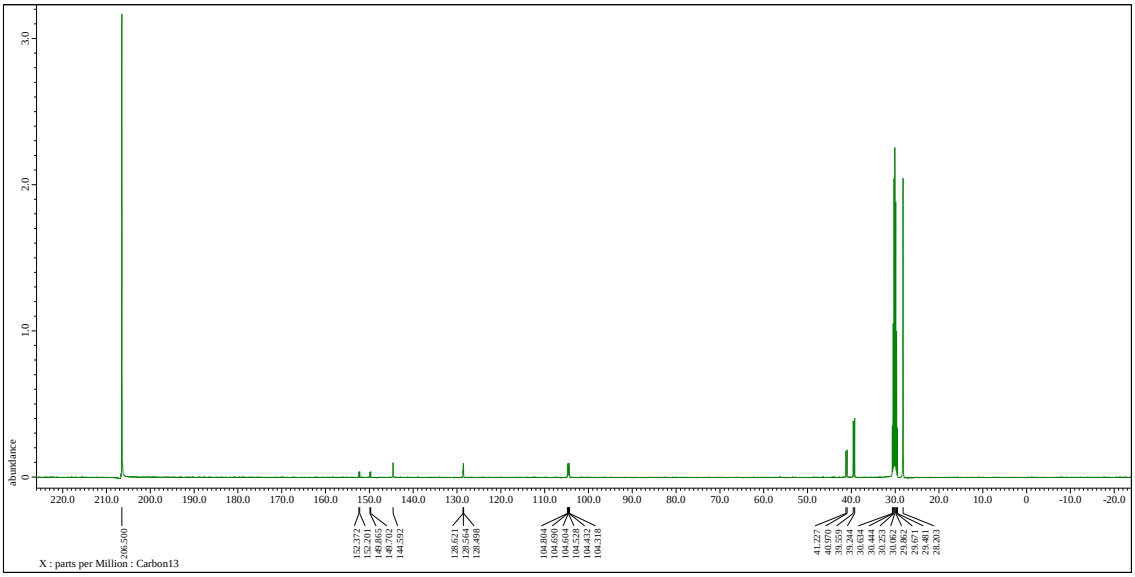

Supplementary Figure 39. $^{13}C\{^{1}H\}$ NMR of **8c**.

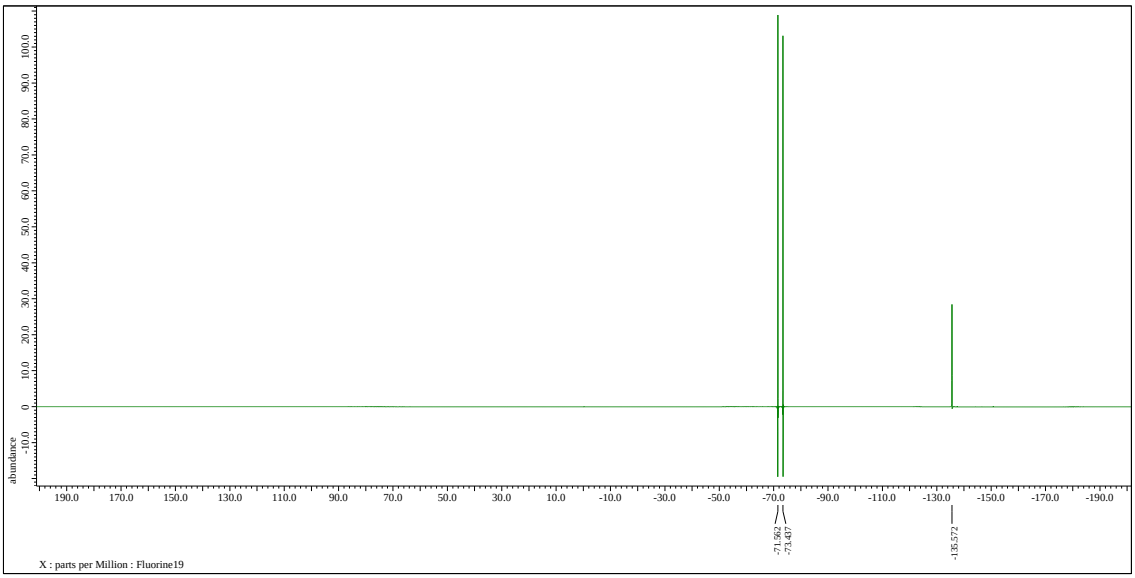

Supplementary Figure 40. ^{19}F NMR of **8c**.

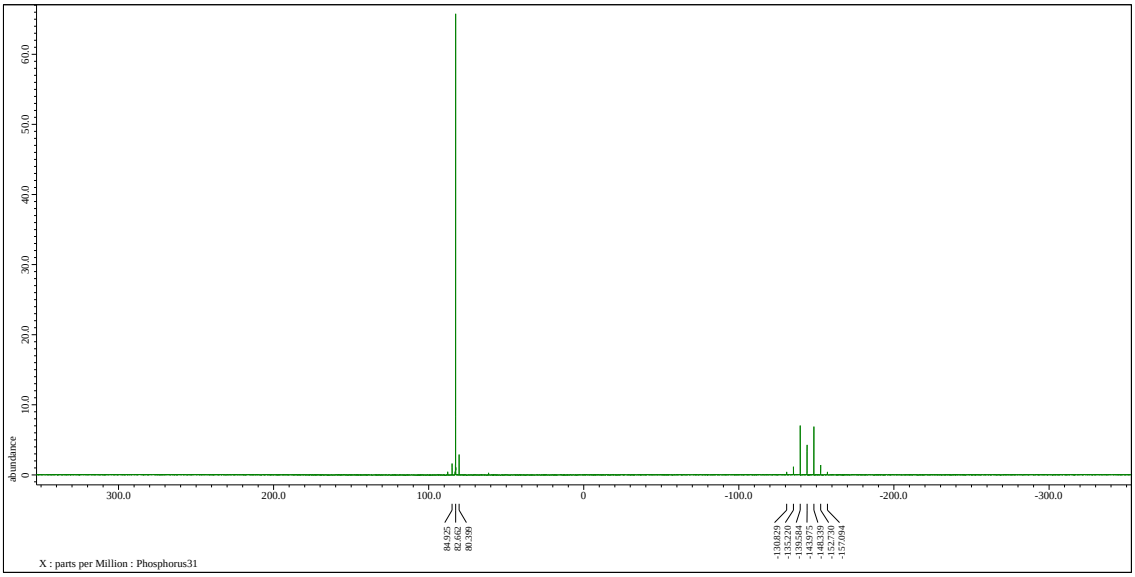

Supplementary Figure 41. $^{31}P\{^{1}H\}$ NMR of **8c**.

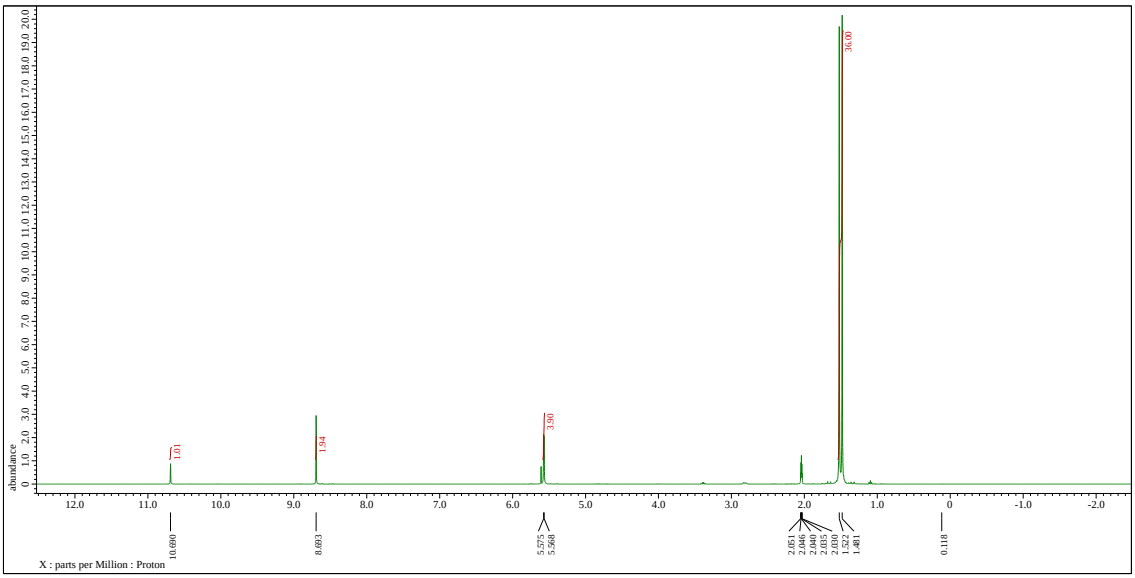

Supplementary Figure 42. ^{1}H NMR of **8d**.

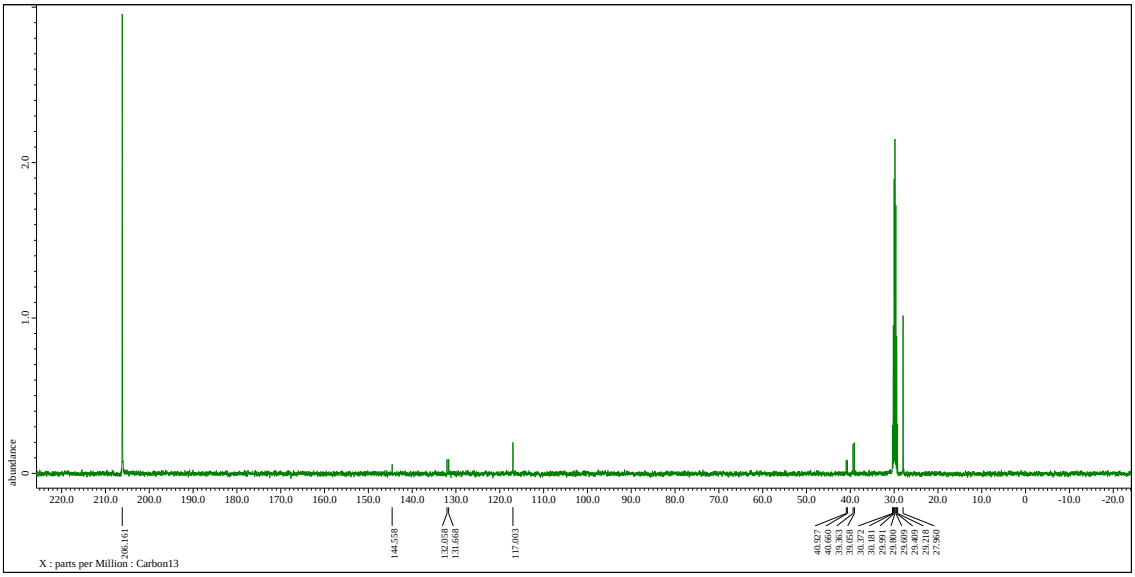

Supplementary Figure 43. $^{13}C\{^{1}H\}$ NMR of **8d**.

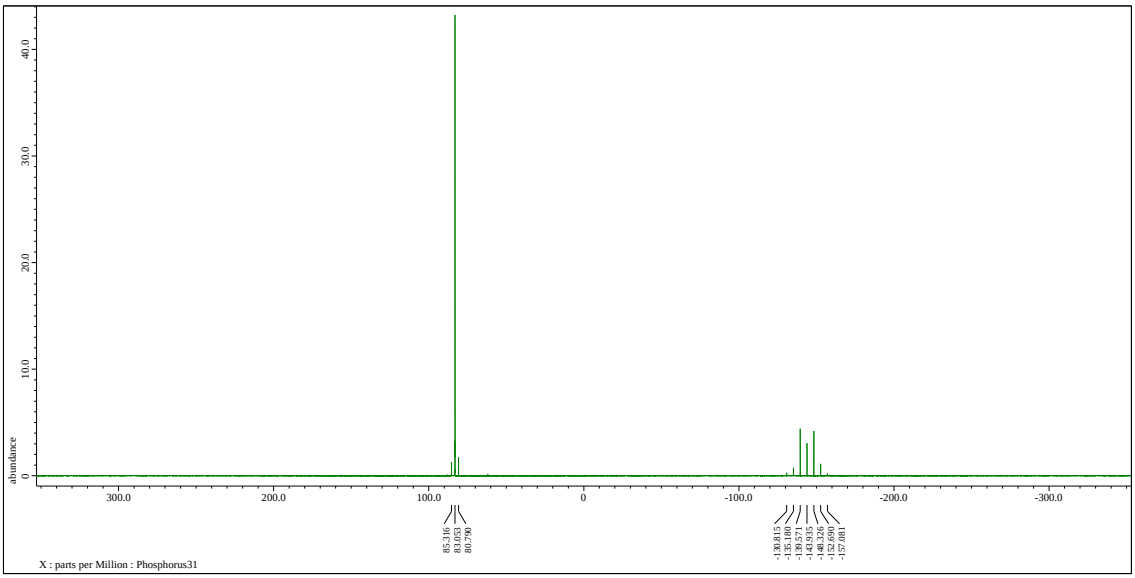

Supplementary Figure 44. $^{31}P\{^{1}H\}$ NMR of **8d**

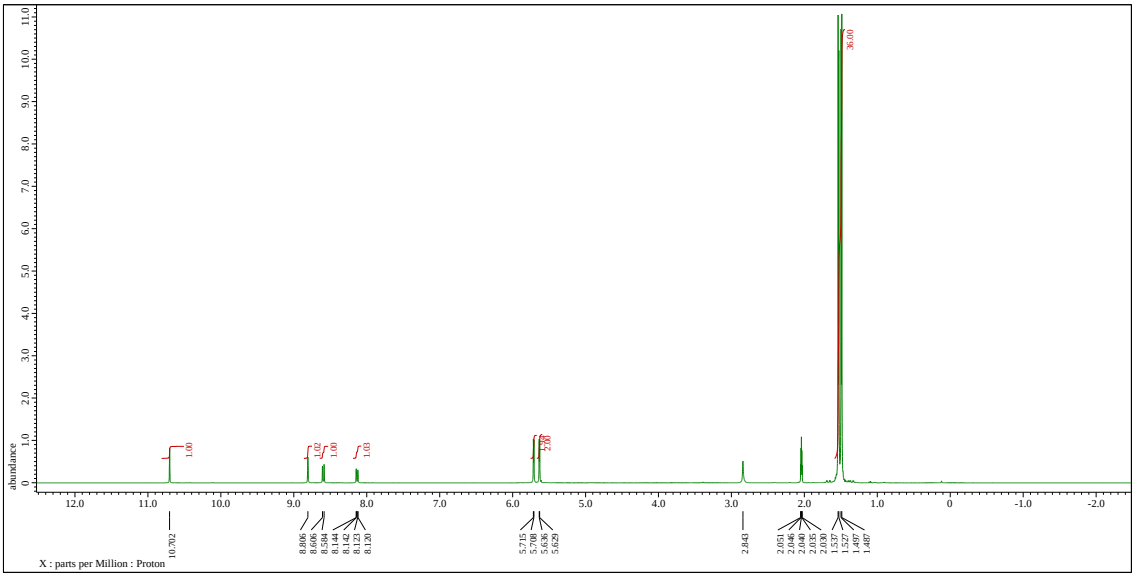

Supplementary Figure 45. ^{1}H NMR of **8e**.

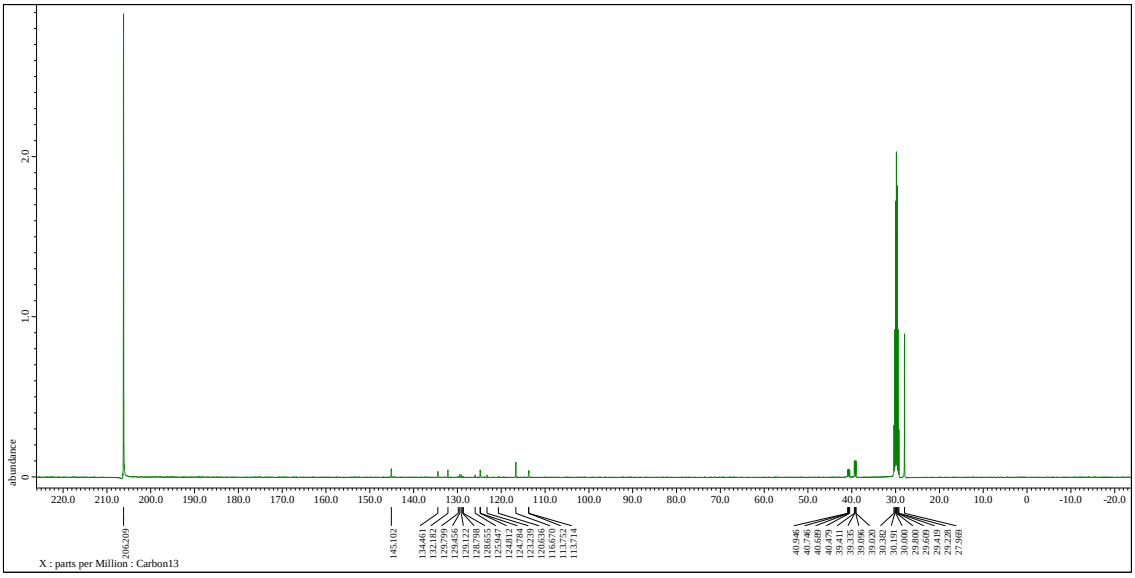

Supplementary Figure 46. $^{13}C\{^{1}H\}$ NMR of **8e**.

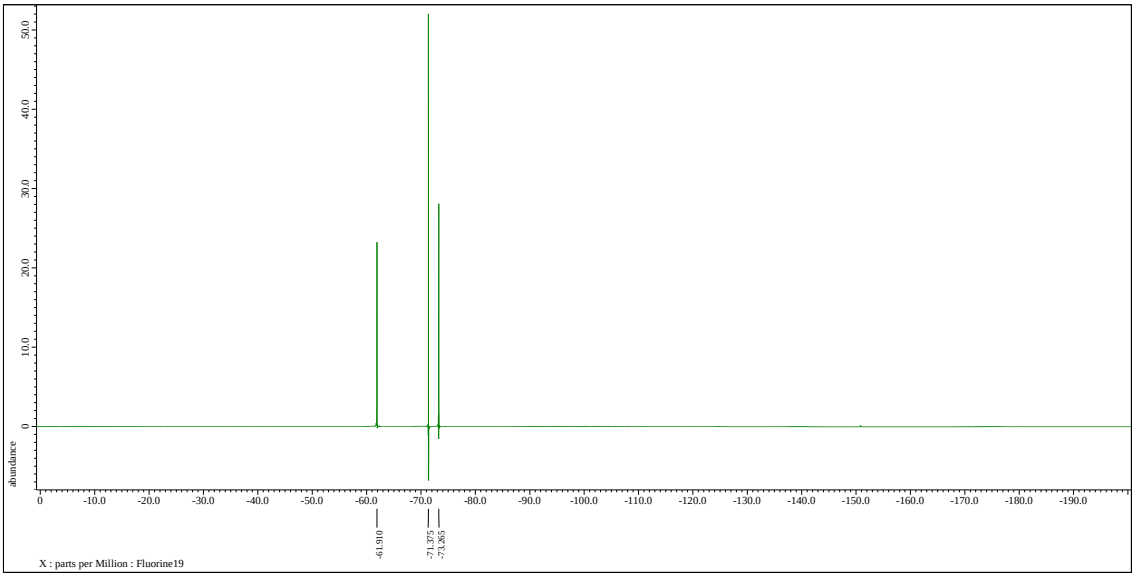

Supplementary Figure 47. ^{19}F NMR of **8e**.

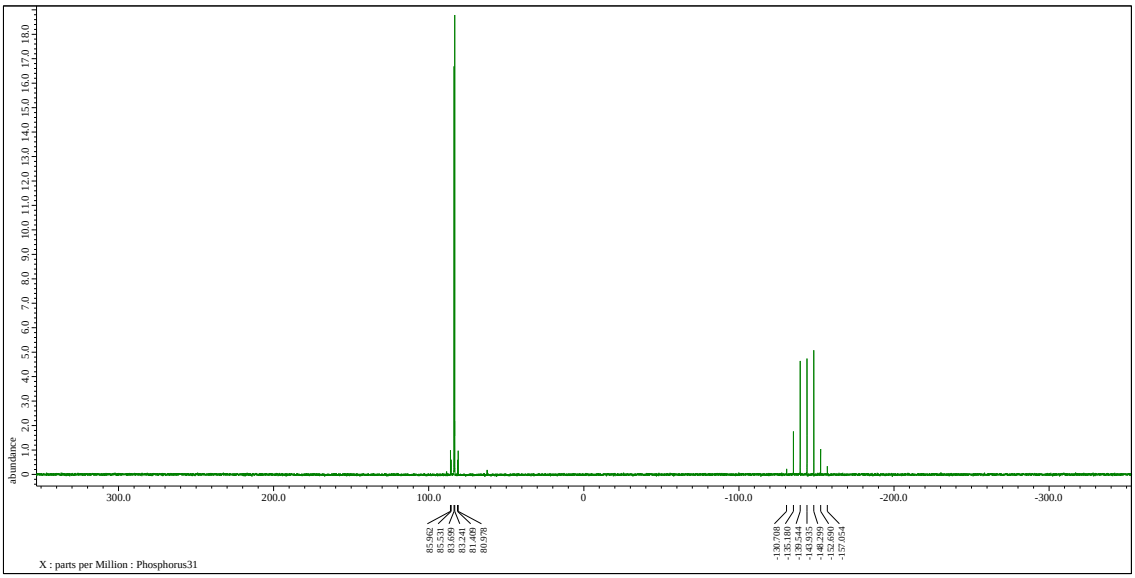

Supplementary Figure 48. $^{31}P\{^{1}H\}$ NMR of **8e**.

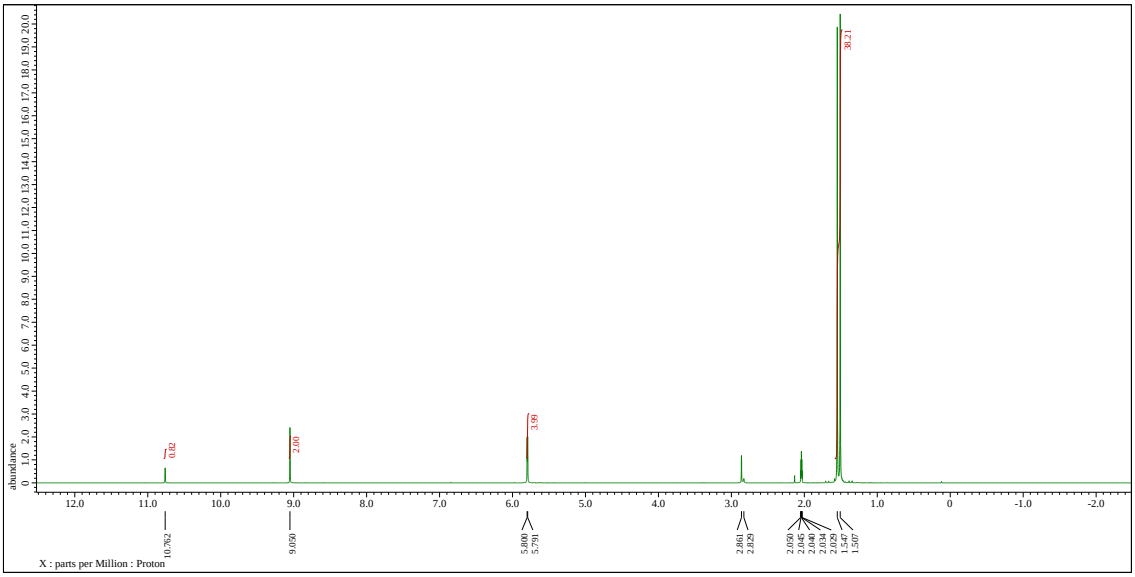

Supplementary Figure 49. ^{1}H NMR of **8f**.

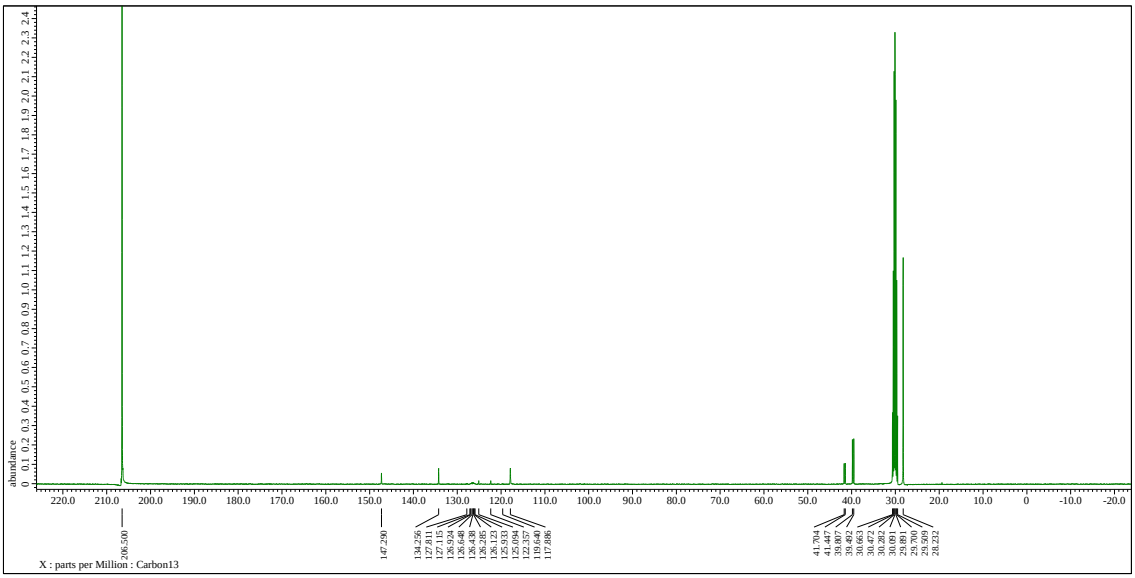

Supplementary Figure 50. ^{13}C{^{1}H} NMR of **8f**.

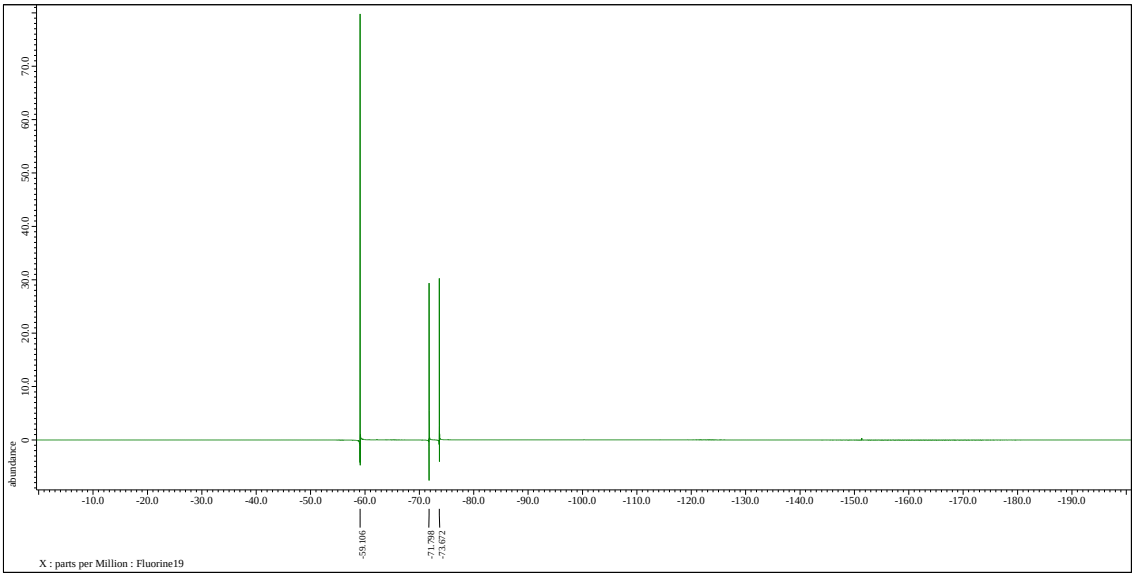

Supplementary Figure 51. ^{19}F NMR of **8f**.

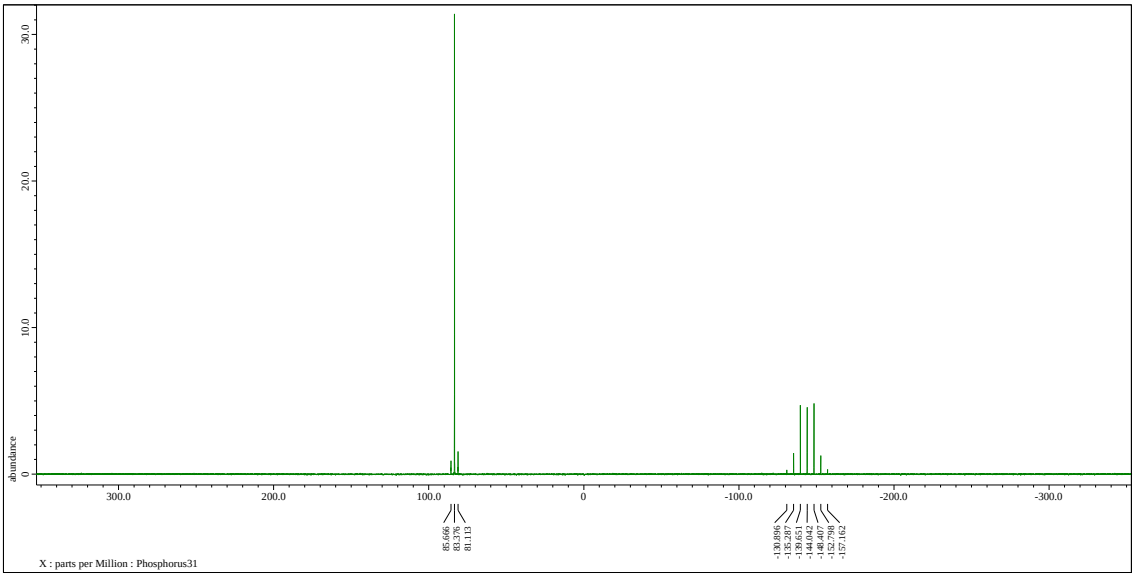

Supplementary Figure 52. $^{31}P\{^{1}H\}$ NMR of **8f**.

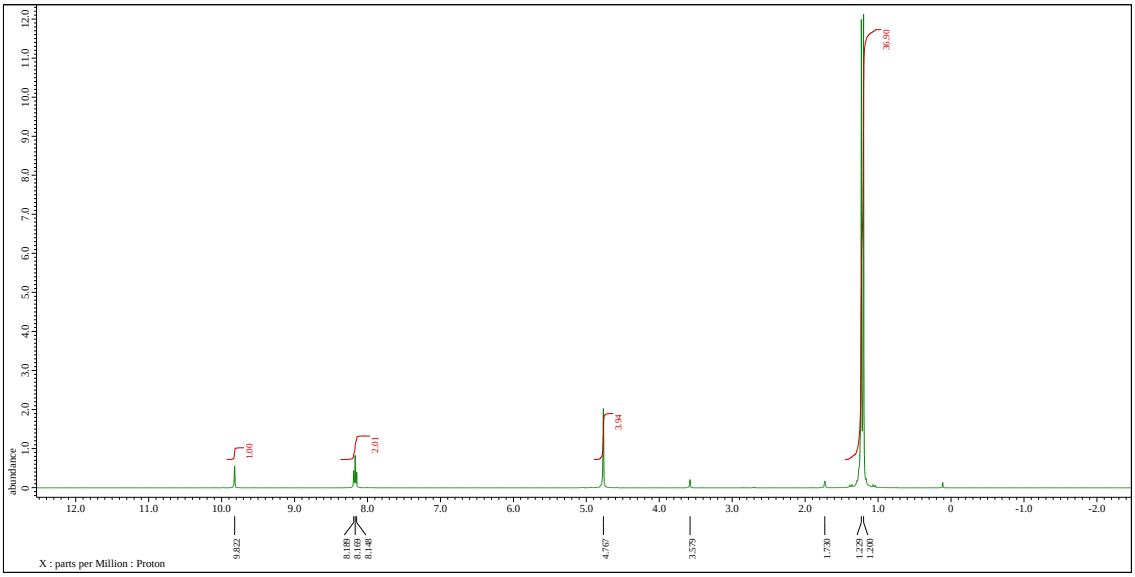

Supplementary Figure 53. ^{1}H NMR of **5c**.

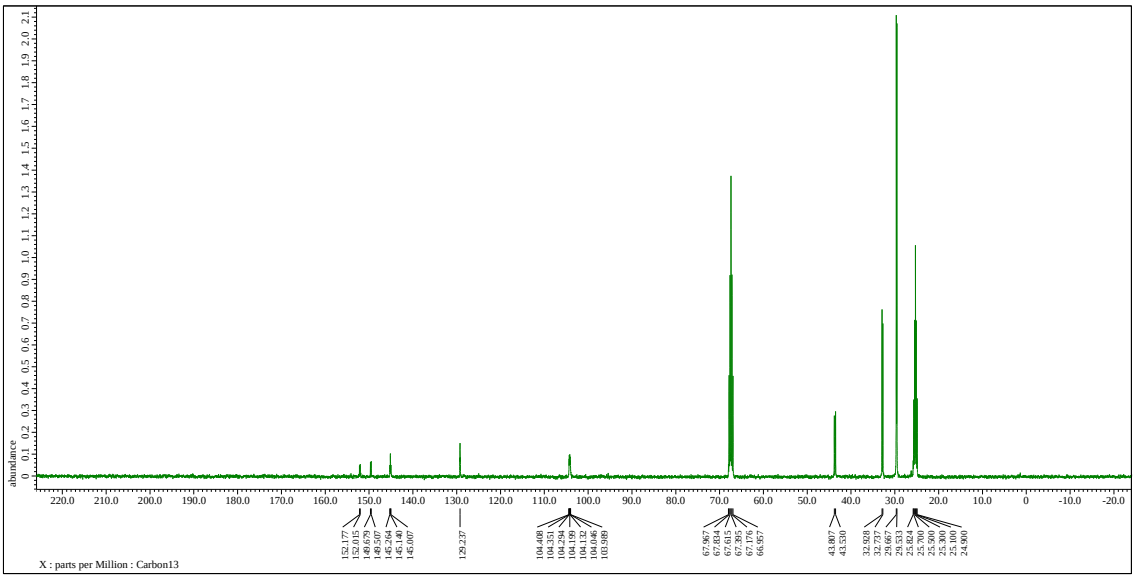

Supplementary Figure 54. ^{13}C{^{1}H} NMR of **5c**.

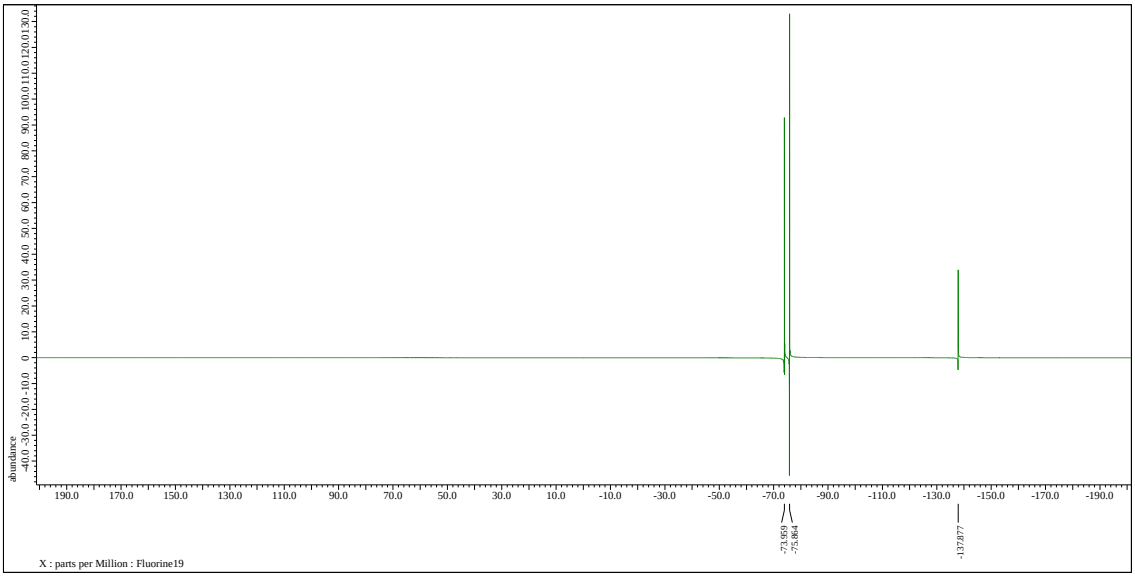

Supplementary Figure 55. ^{19}F NMR of **5c**.

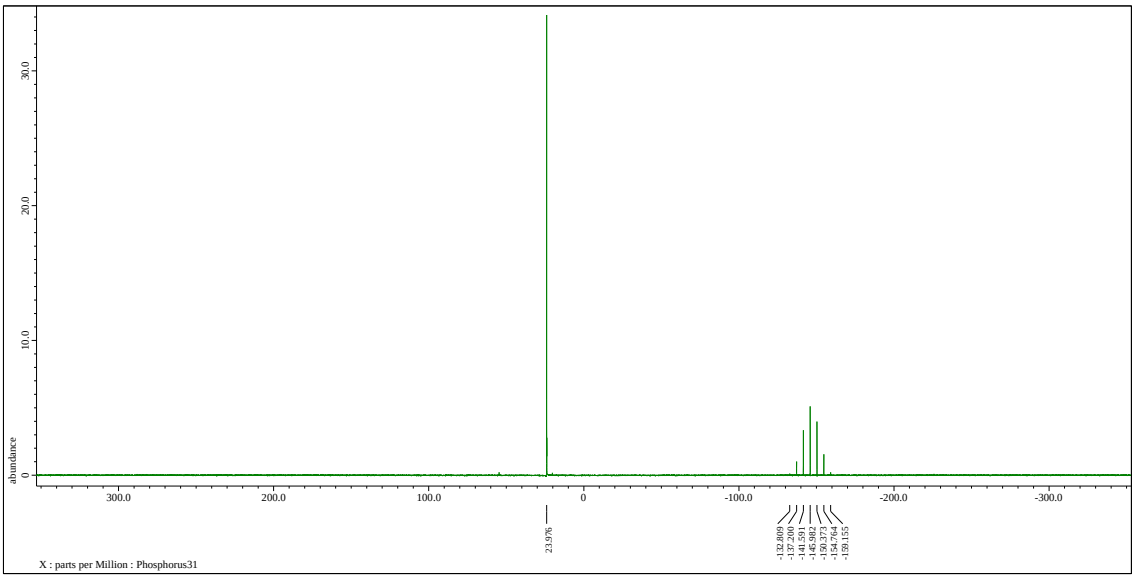

Supplementary Figure 56. $^{31}P\{^{1}H\}$ NMR of **5c**.

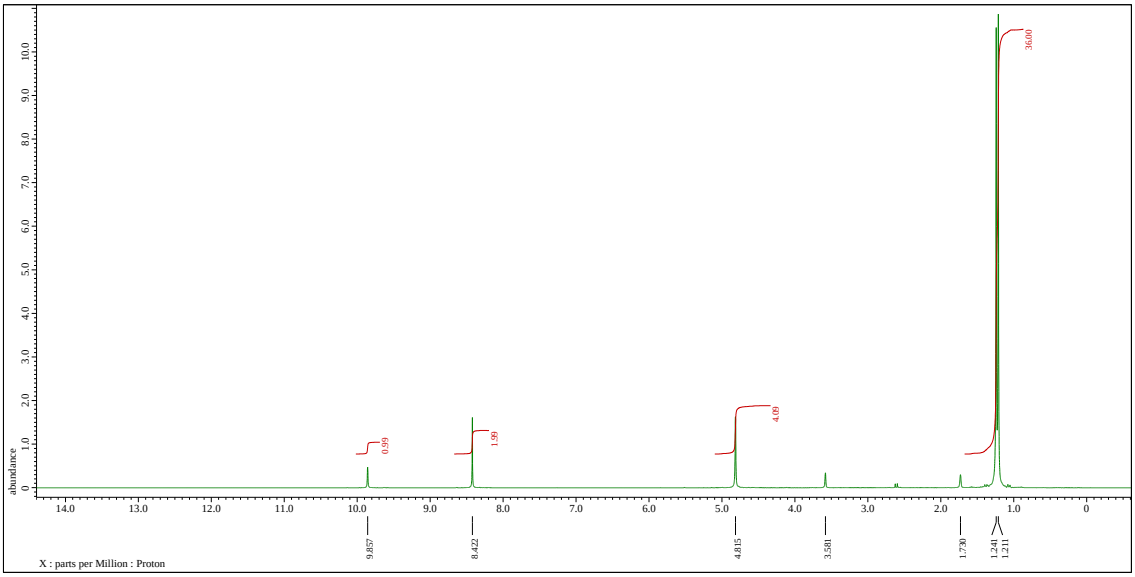

Supplementary Figure 57. ^{1}H NMR of **5d**.

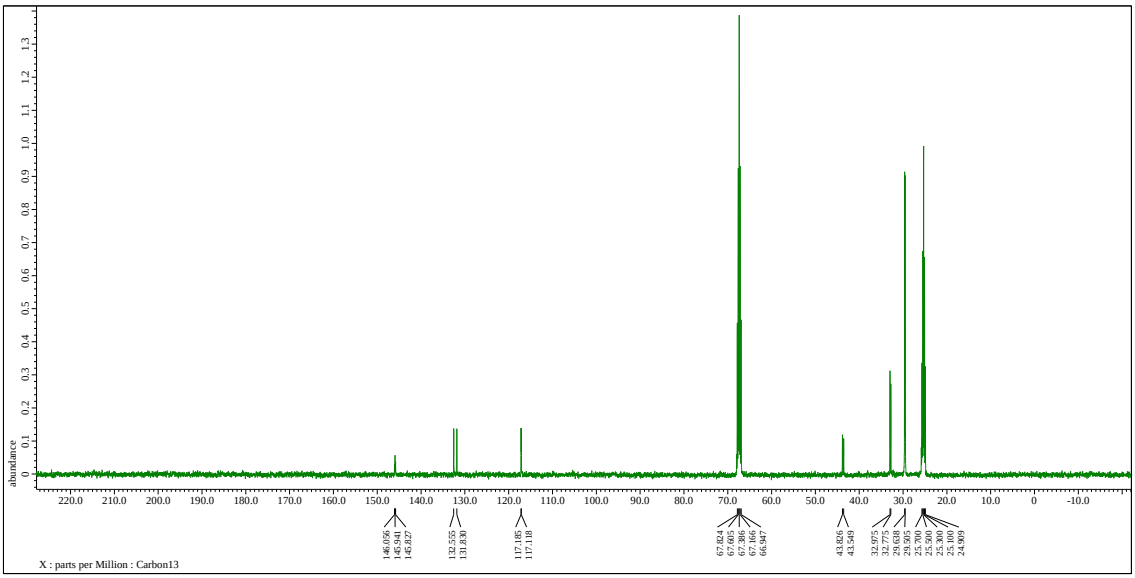

Supplementary Figure 58. ^{13}C{^{1}H} NMR of **5d**.

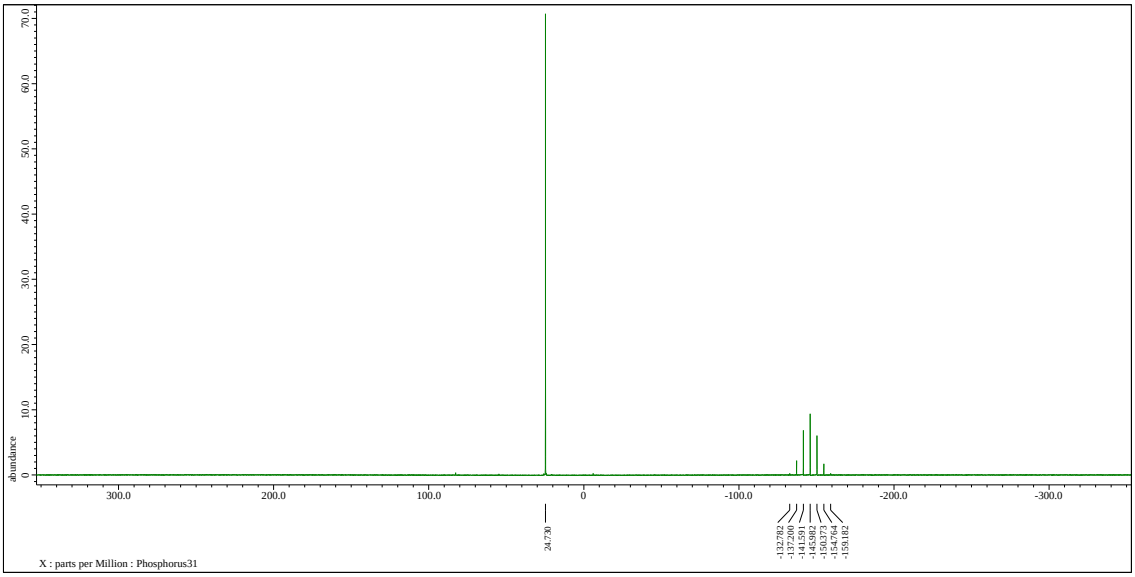

Supplementary Figure 59. $^{31}P\{^{1}H\}$ NMR of **5d**.

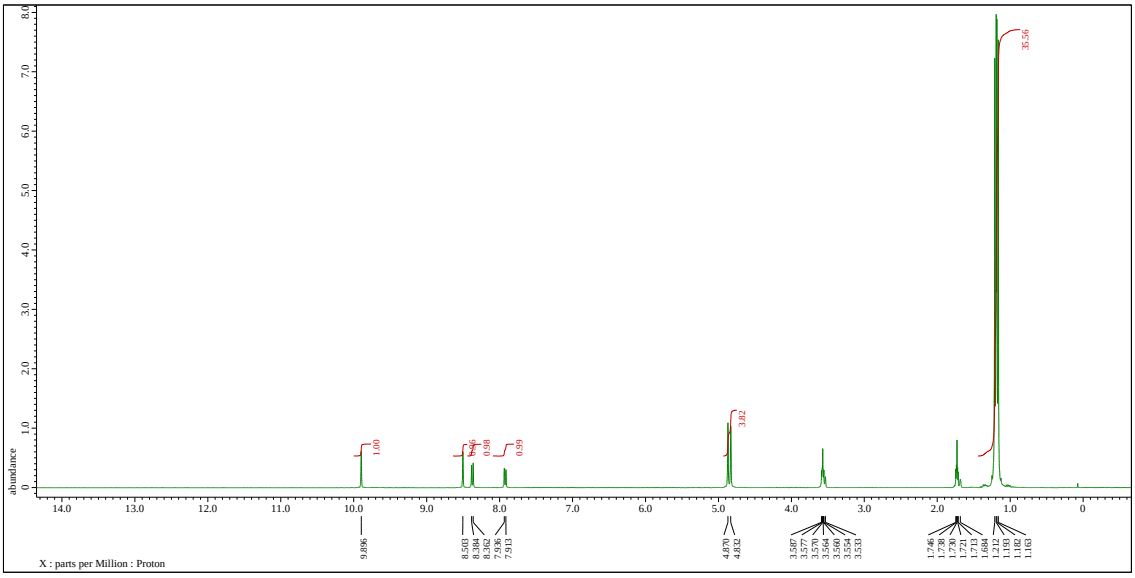

Supplementary Figure 60. ^{1}H NMR of **5e**.

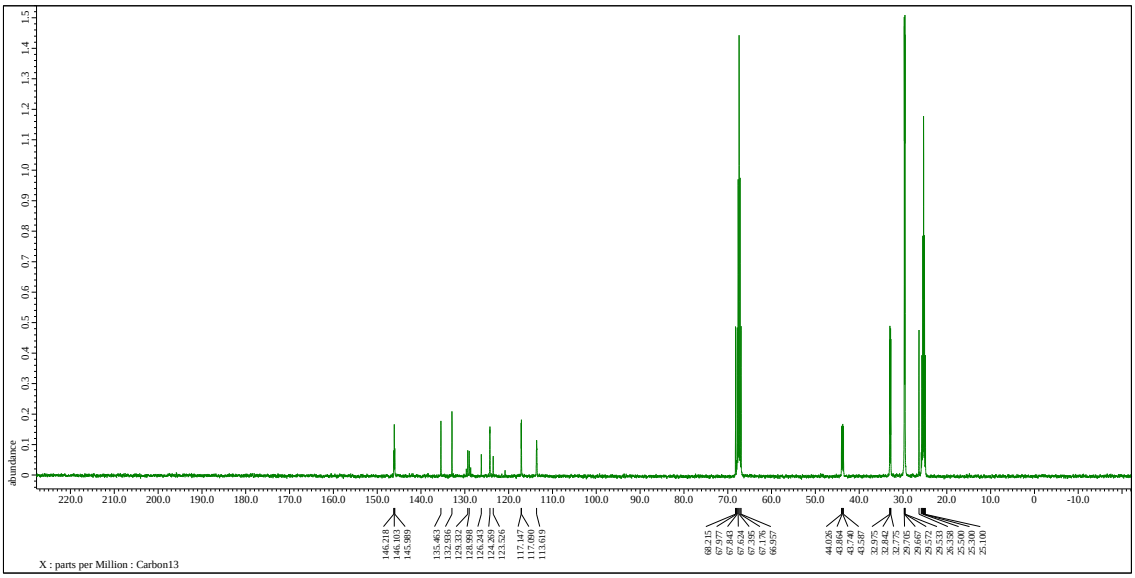

Supplementary Figure 61. $^{13}C\{^{1}H\}$ NMR of **5e**.

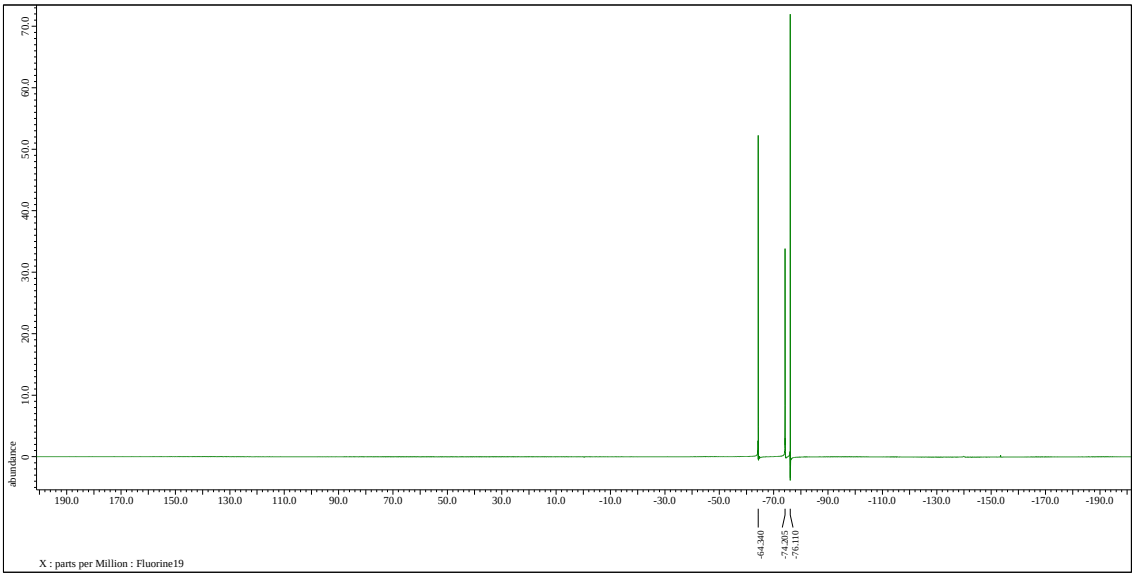

Supplementary Figure 62. ^{19}F NMR of **5e**.

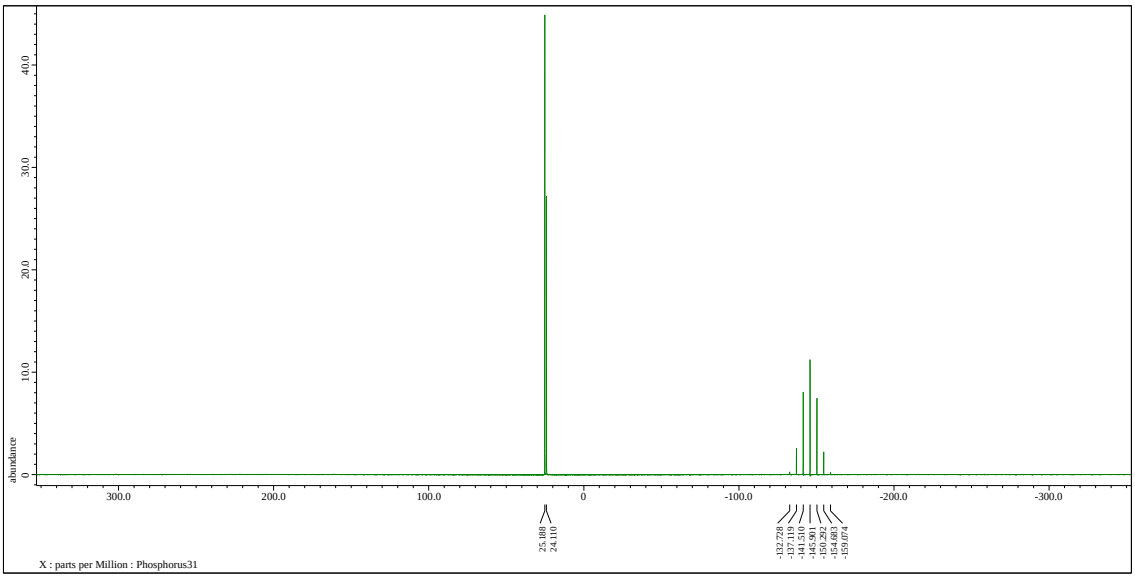

Supplementary Figure 63. $^{31}P\{^{1}H\}$ NMR of **5e**.

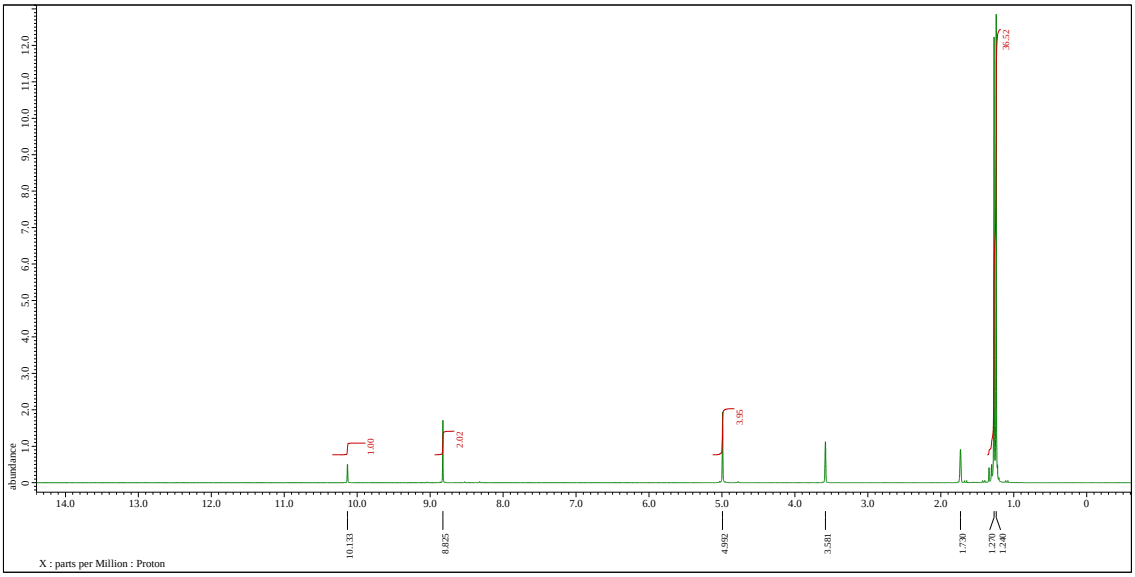

Supplementary Figure 64. ^{1}H NMR of **5f**.

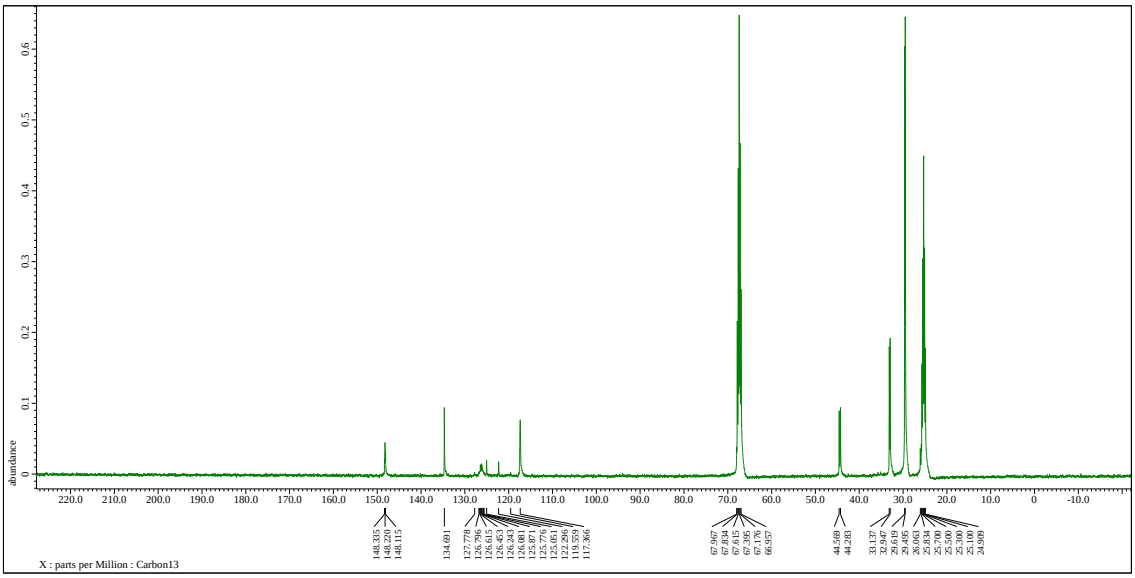

Supplementary Figure 65. $^{13}C\{^{1}H\}$ NMR of **5f**.

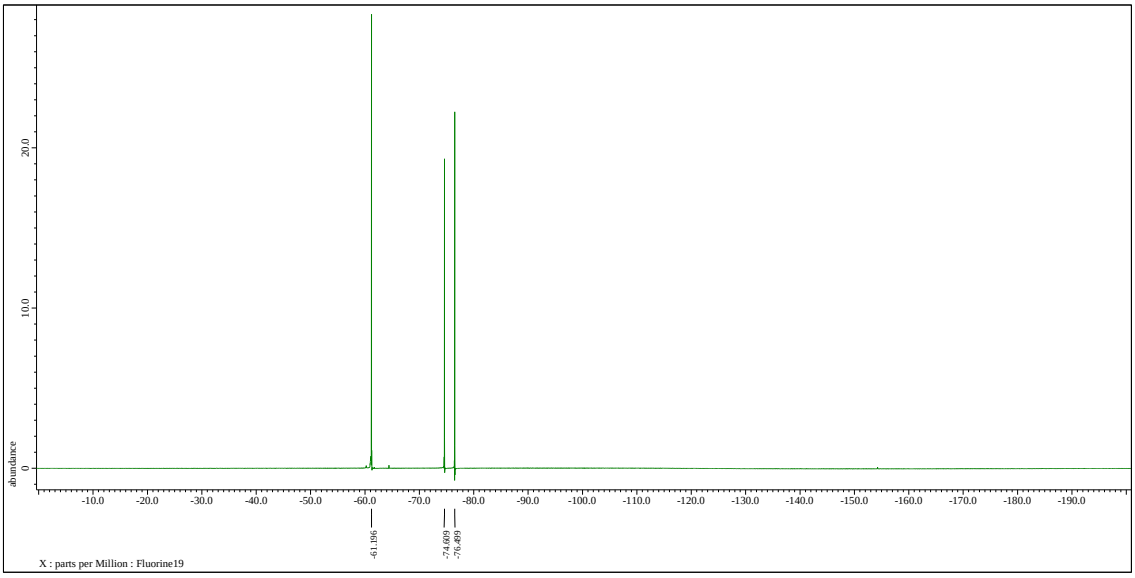

Supplementary Figure 66. ^{19}F NMR of **5f**.

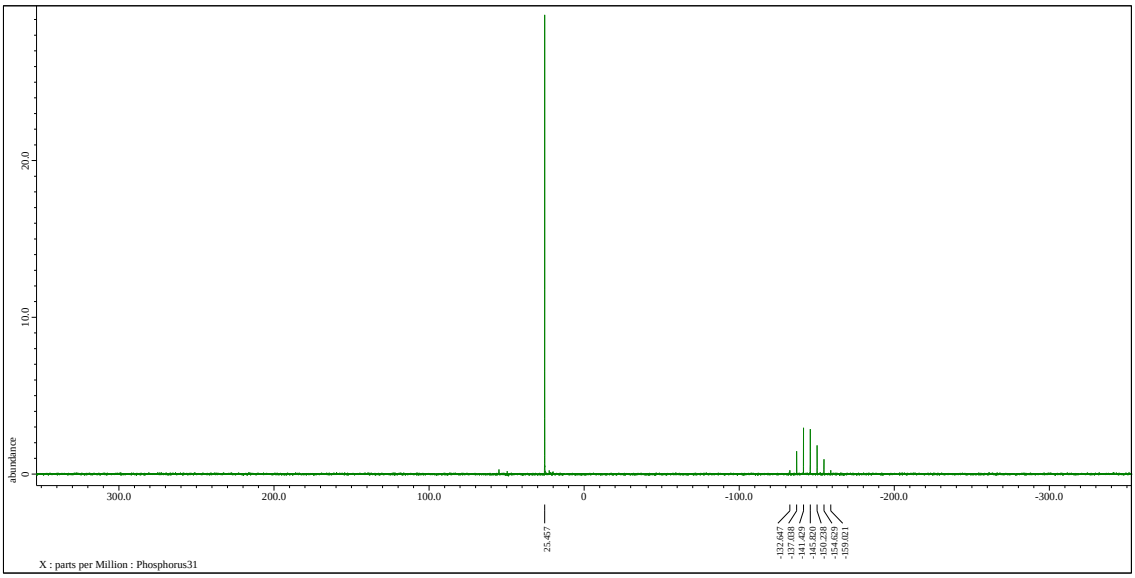

Supplementary Figure 67. $^{31}P\{^{1}H\}$ NMR of **5f**.

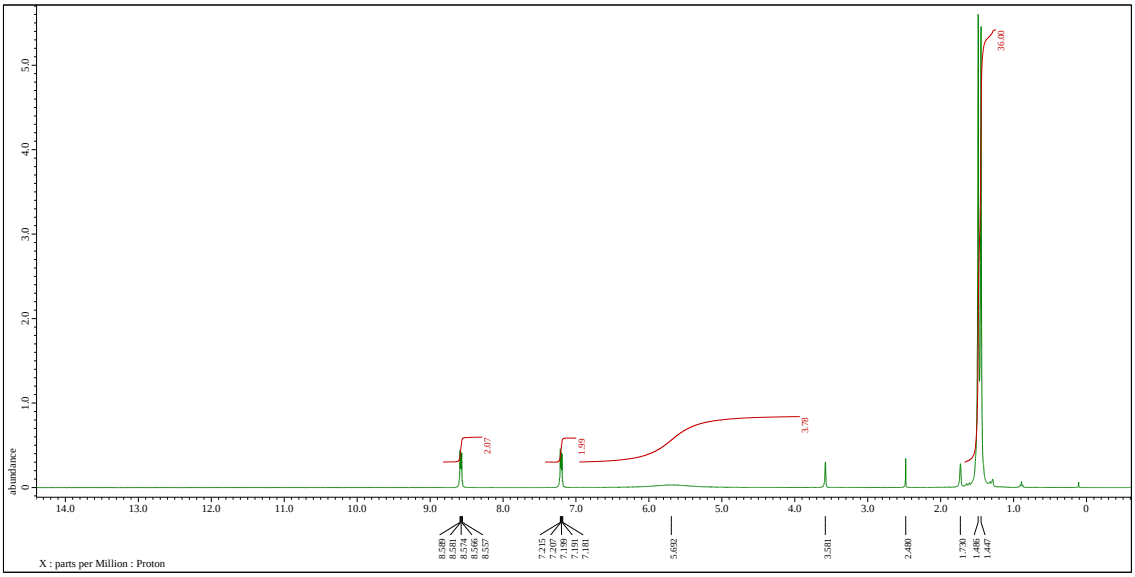

Supplementary Figure 68. ^{1}H NMR of **4a**.

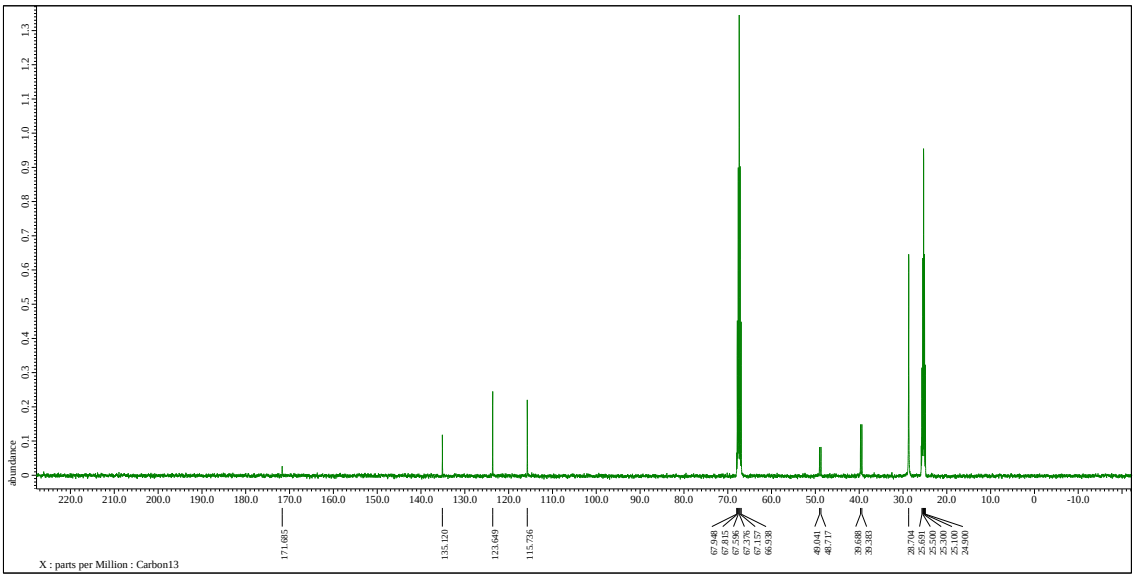

Supplementary Figure 69. $^{13}C\{^{1}H\}$ NMR of **4a**.

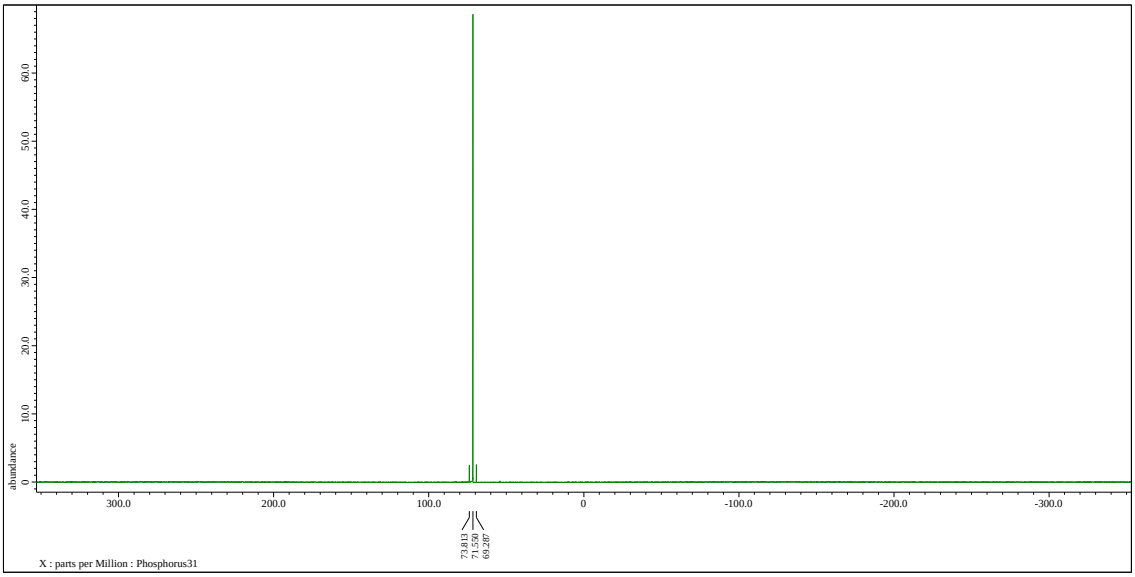

Supplementary Figure 70. $^{31}P\{^{1}H\}$ NMR of **4a**.

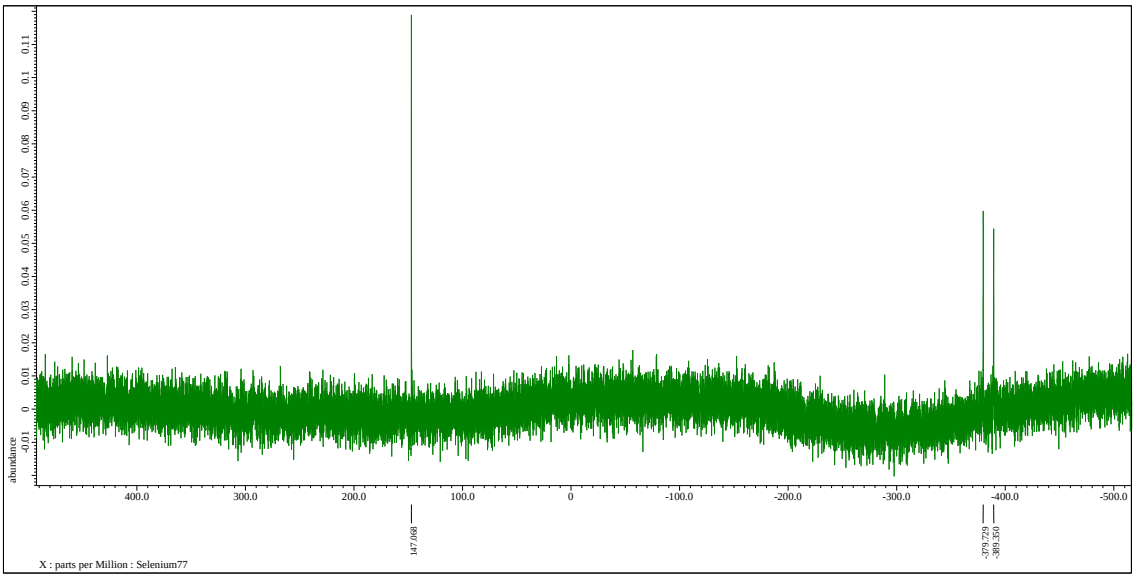

Supplementary Figure 71. $^{77}Se\{^{1}H\}$ NMR of **4a**.

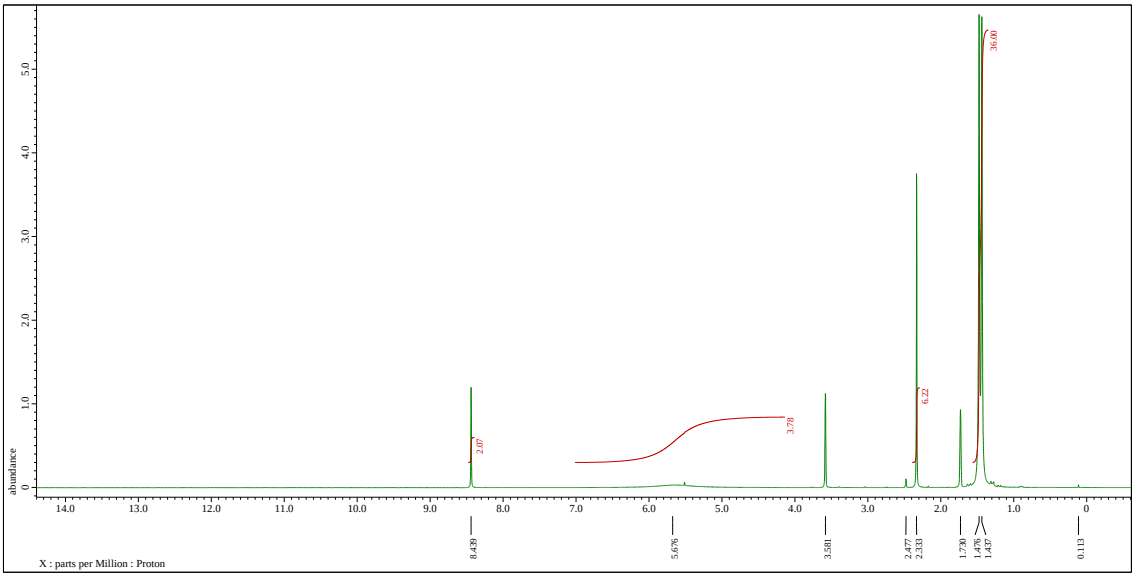

Supplementary Figure 72. ^{1}H NMR of **4b**.

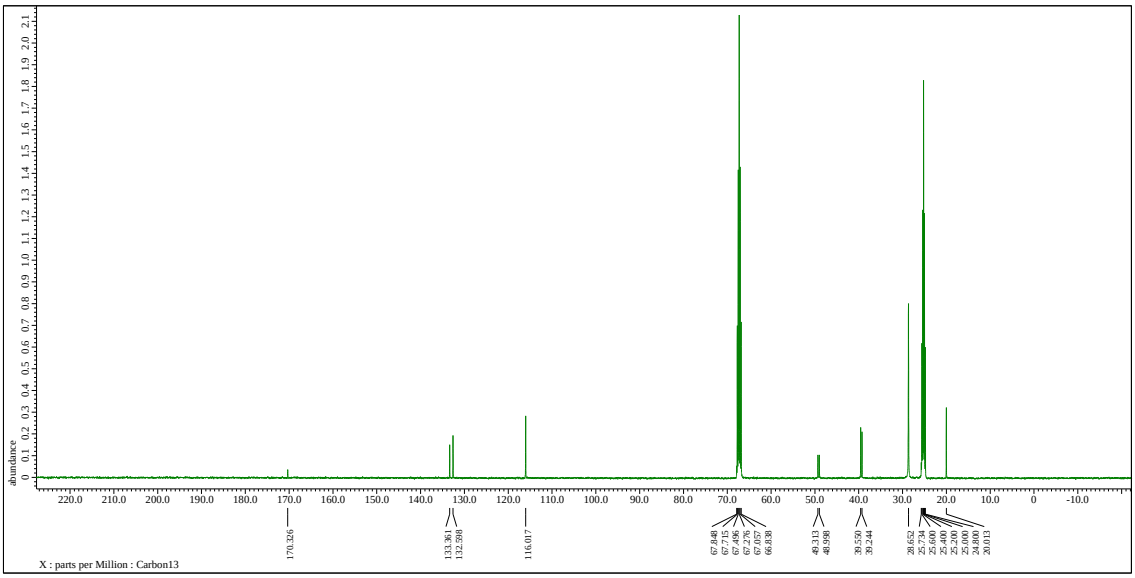

Supplementary Figure 73. $^{13}C\{^{1}H\}$ NMR of **4b**.

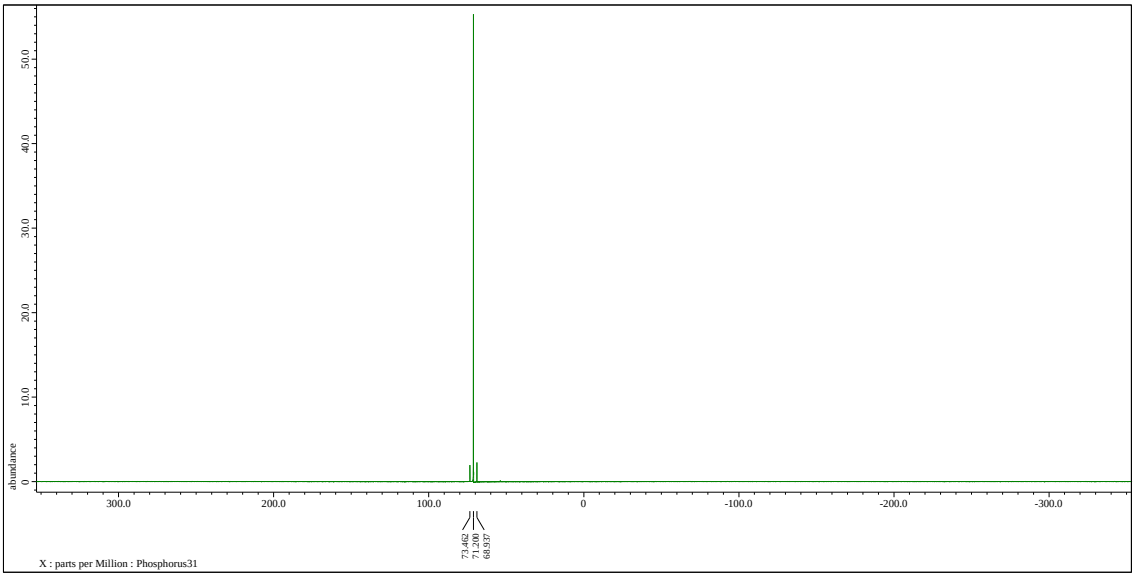

Supplementary Figure 74. $^{31}P\{^{1}H\}$ NMR of **4b**.

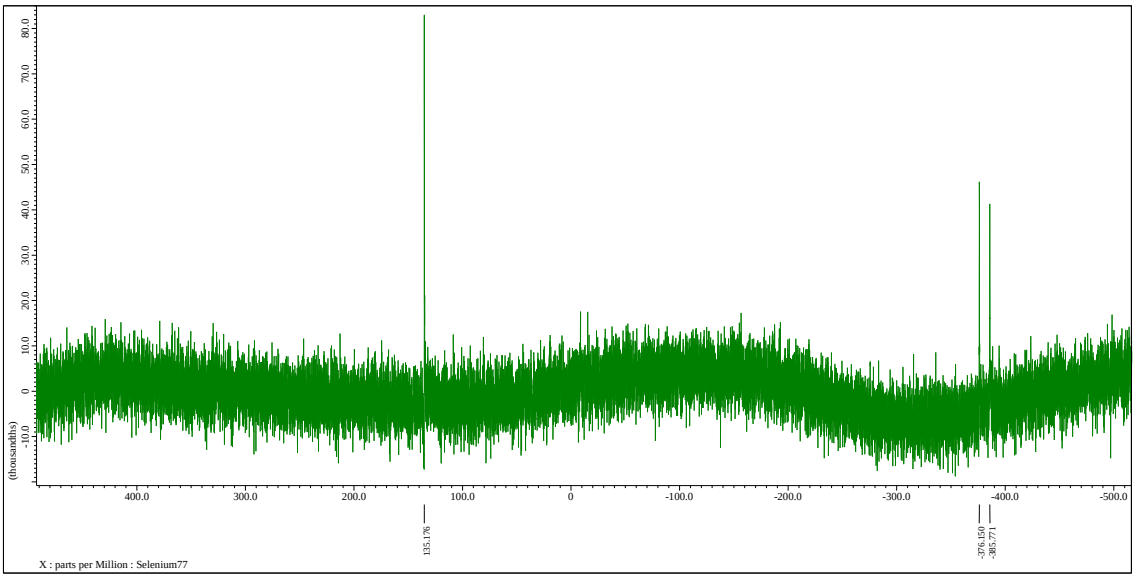

Supplementary Figure 75. $^{77}Se\{^{1}H\}$ NMR of **4b**.

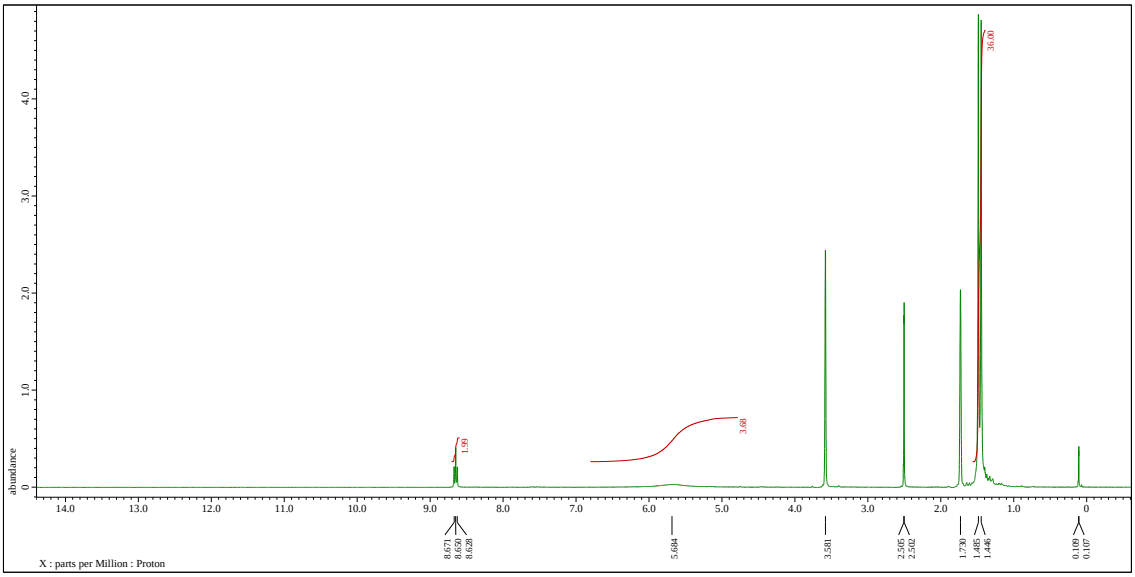

Supplementary Figure 76. ^{1}H NMR of **4c**.

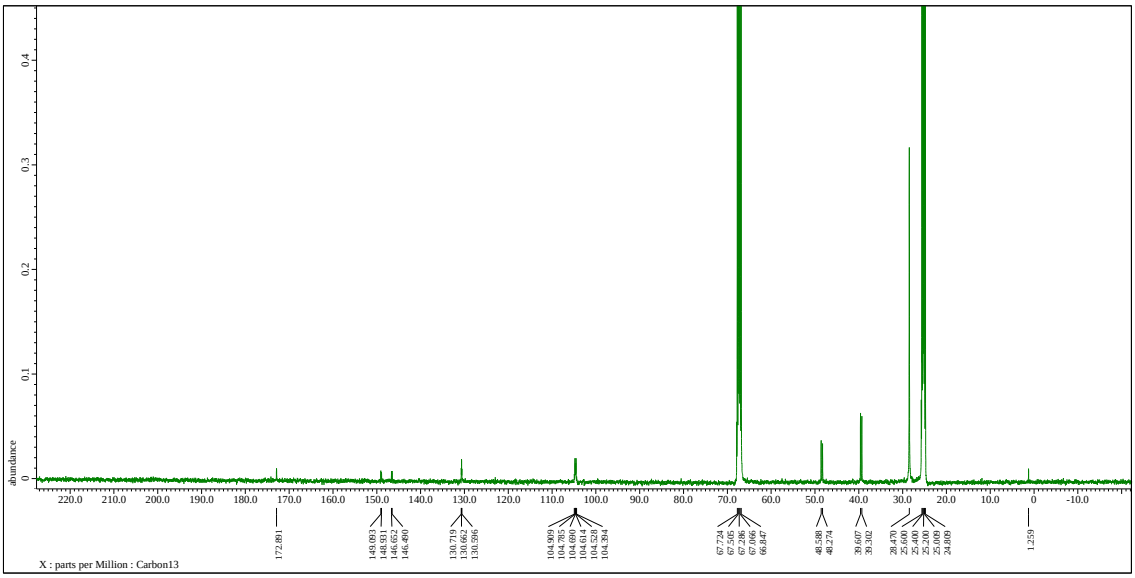

Supplementary Figure 77. $^{13}C\{^{1}H\}$ NMR of **4c**.

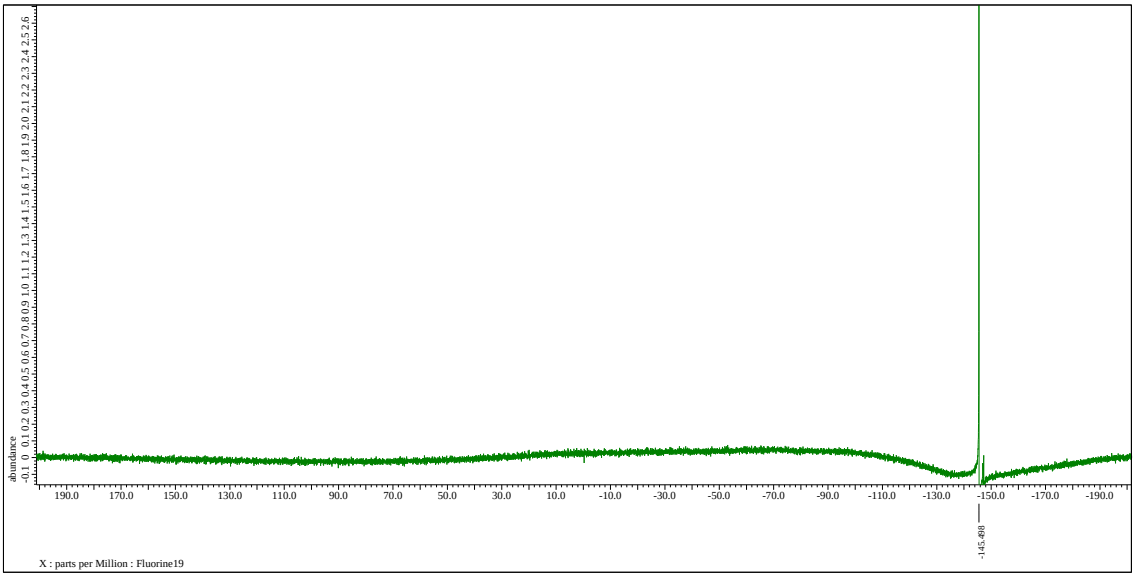

Supplementary Figure 78. ^{19}F NMR of **4c**.

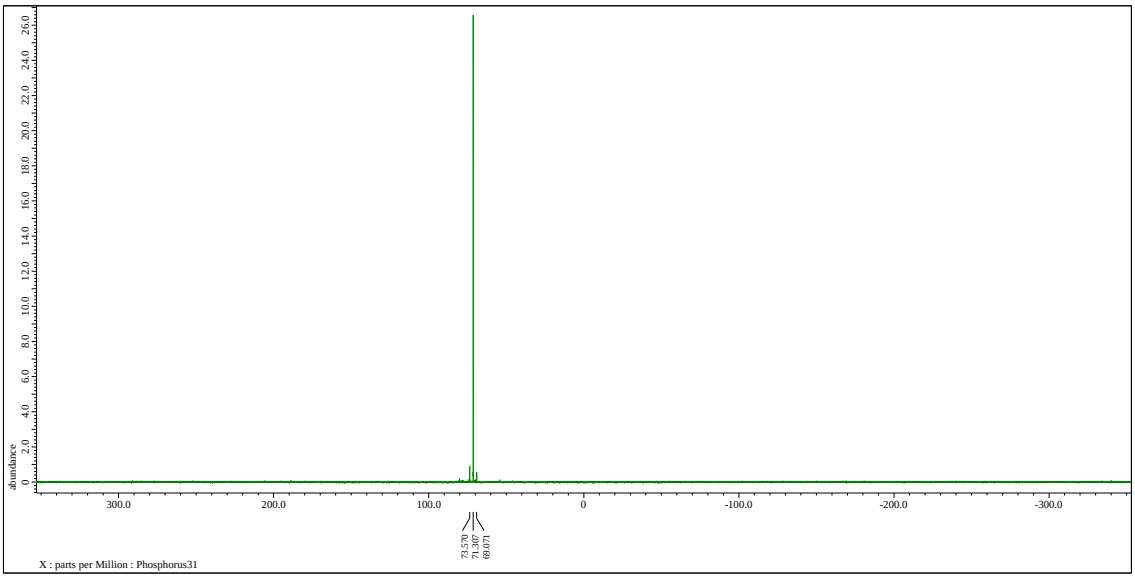

Supplementary Figure 79. $^{31}P\{^{1}H\}$ NMR of **4c**.

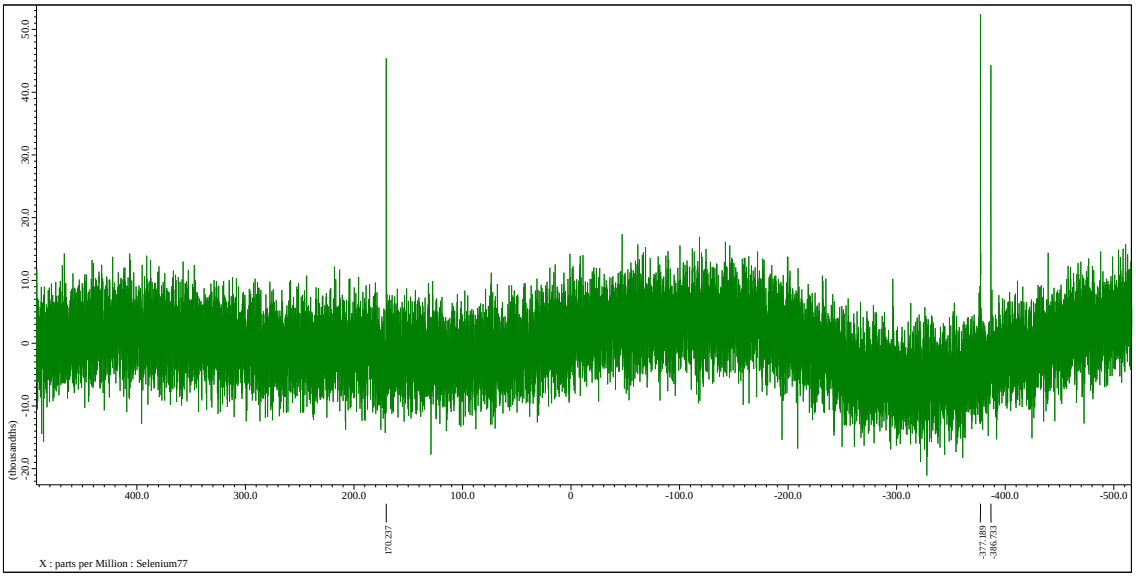

Supplementary Figure 80. $^{77}Se\{^{1}H\}$ NMR of **4c**.

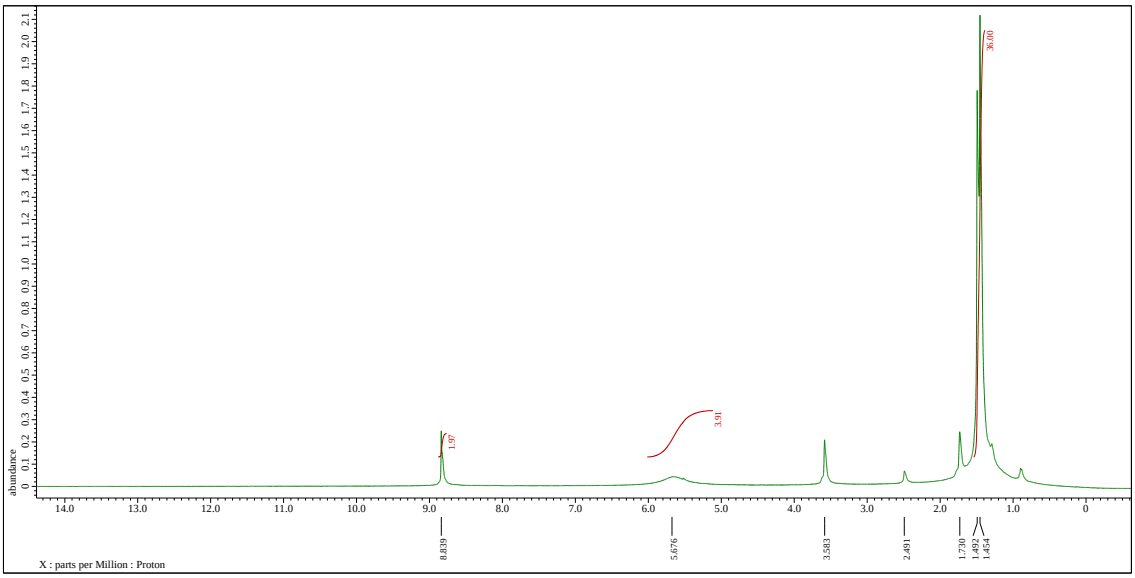

Supplementary Figure 81. ^{1}H NMR of **4d**.

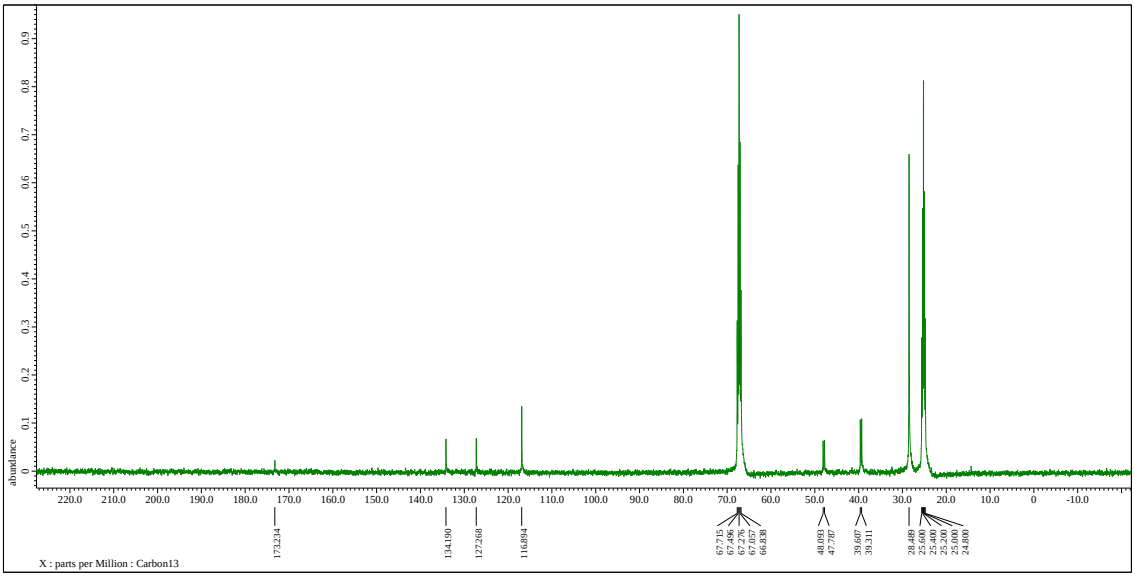

Supplementary Figure 82. ^{13}C{^{1}H} NMR of **4d**.

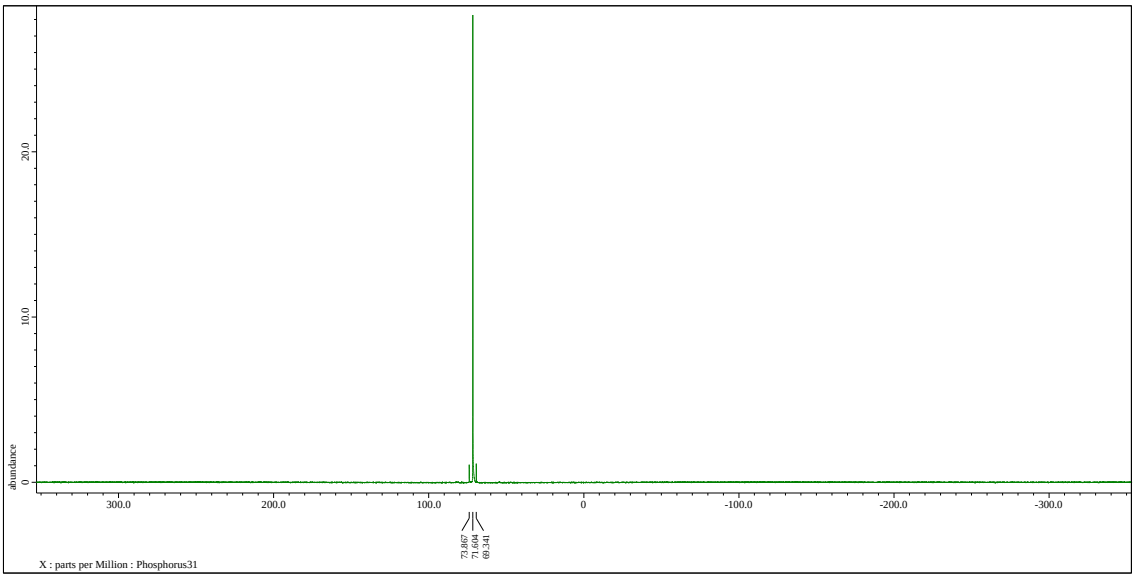

Supplementary Figure 83. $^{31}P\{^{1}H\}$ NMR of **4d**.

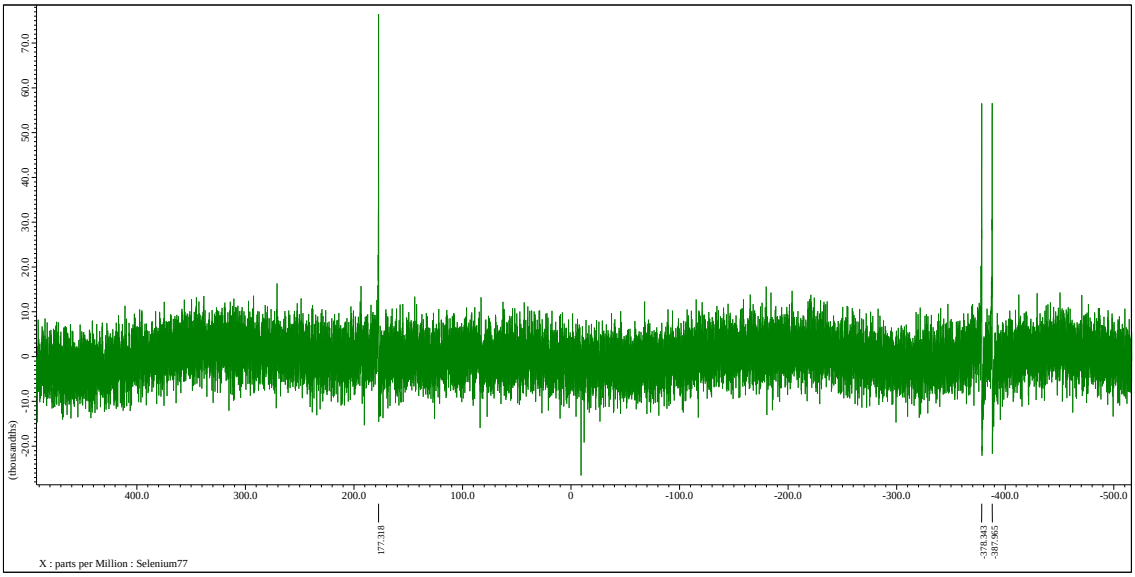

Supplementary Figure 84. $^{77}Se\{^{1}H\}$ NMR of **4d**.

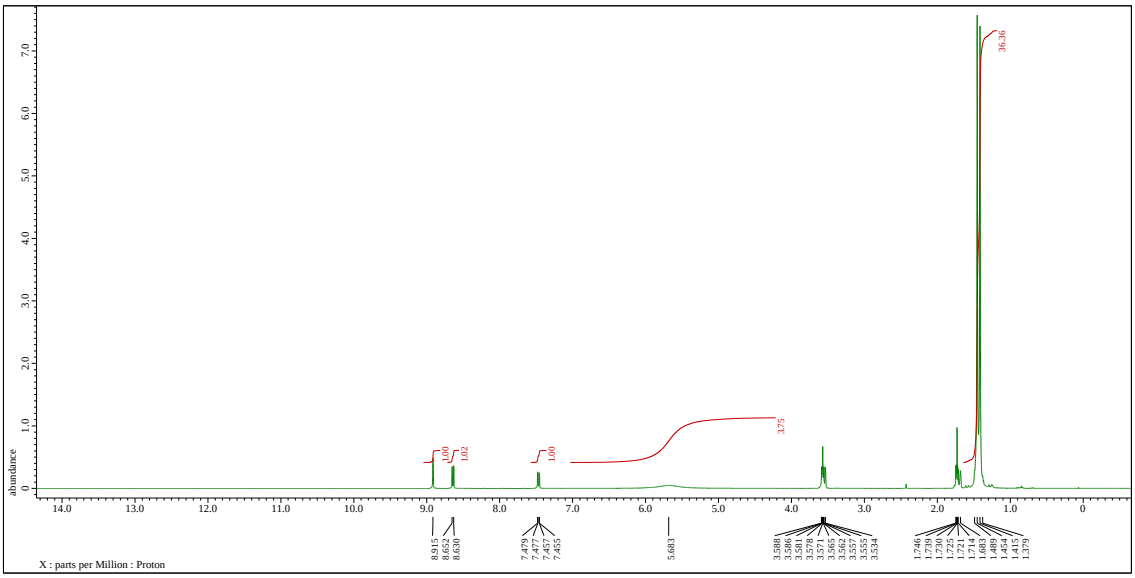

Supplementary Figure 85. ^{1}H NMR of **4e**.

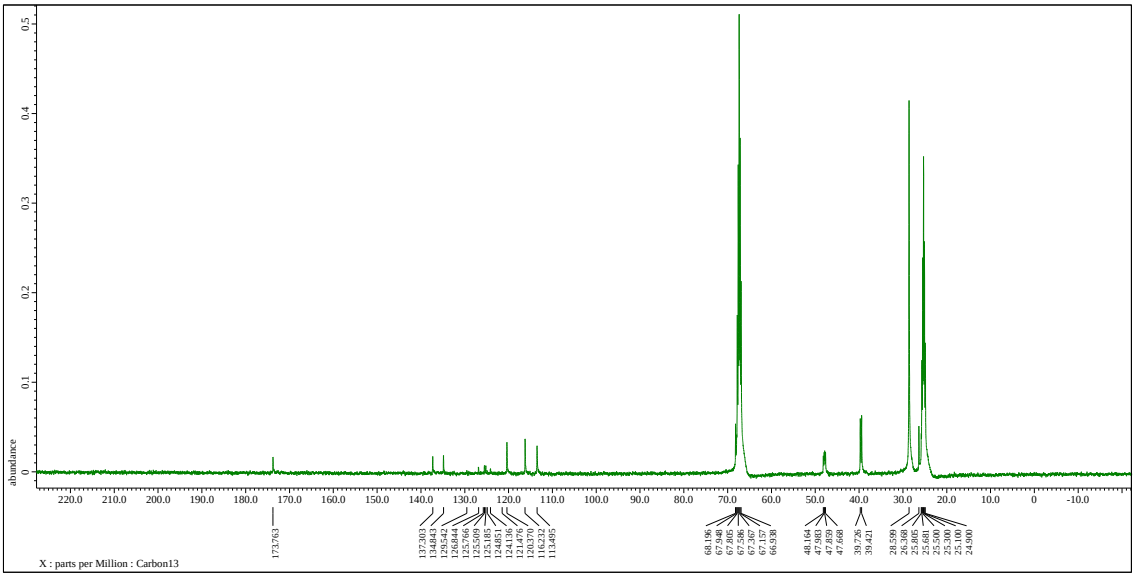

Supplementary Figure 86. $^{13}C\{^{1}H\}$ NMR of **4e**.

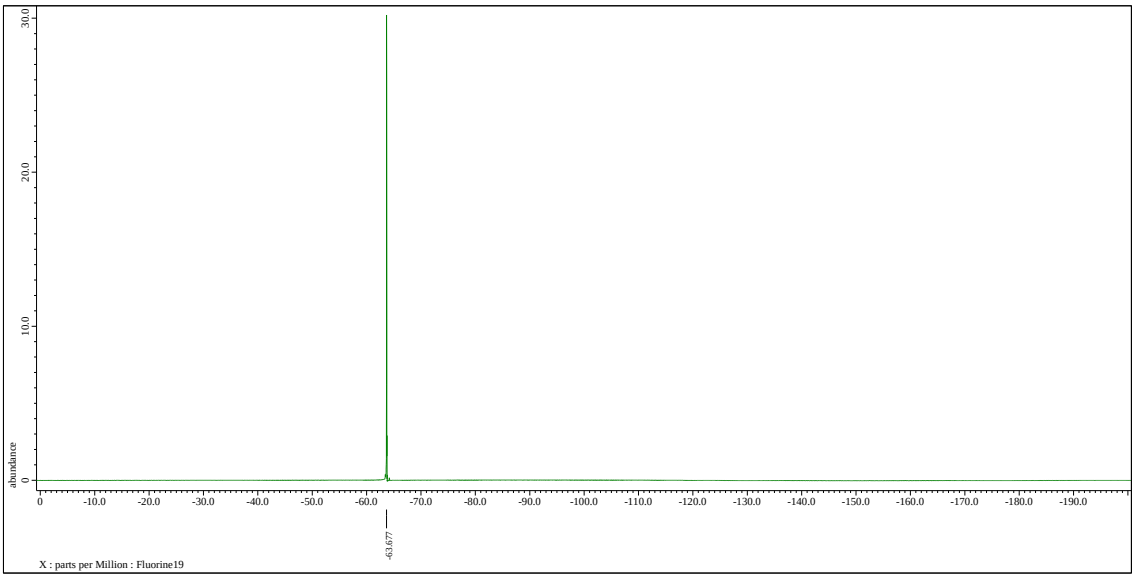

Supplementary Figure 87. ^{19}F NMR of **4e**.

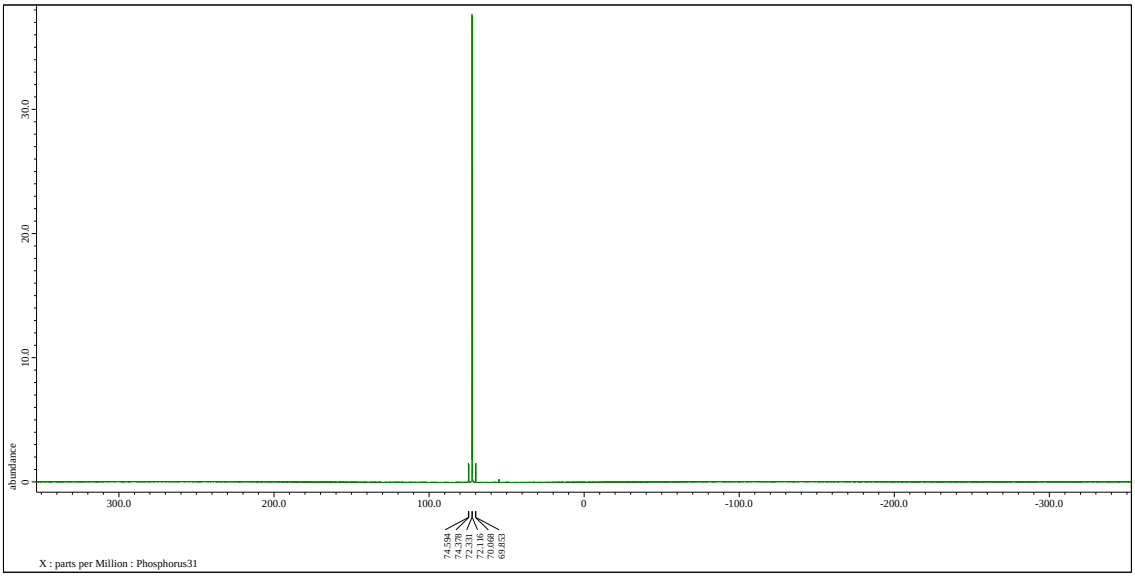

Supplementary Figure 88. $^{31}P\{^{1}H\}$ NMR of **4e**.

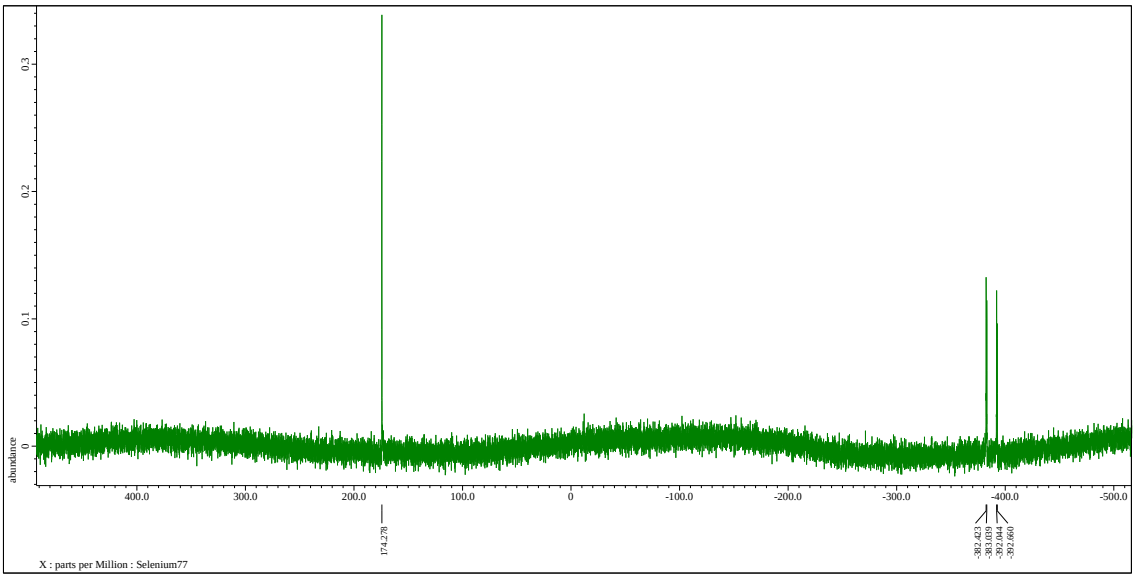

Supplementary Figure 89. $^{77}Se\{^{1}H\}$ NMR of **4e**.

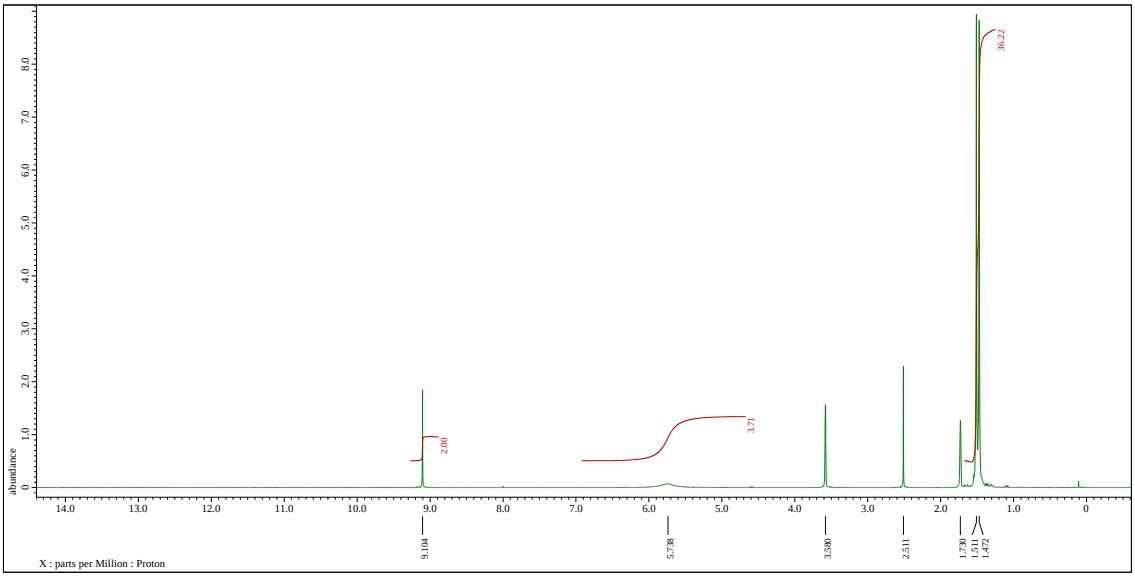

Supplementary Figure 90. ^{1}H NMR of **4f**.

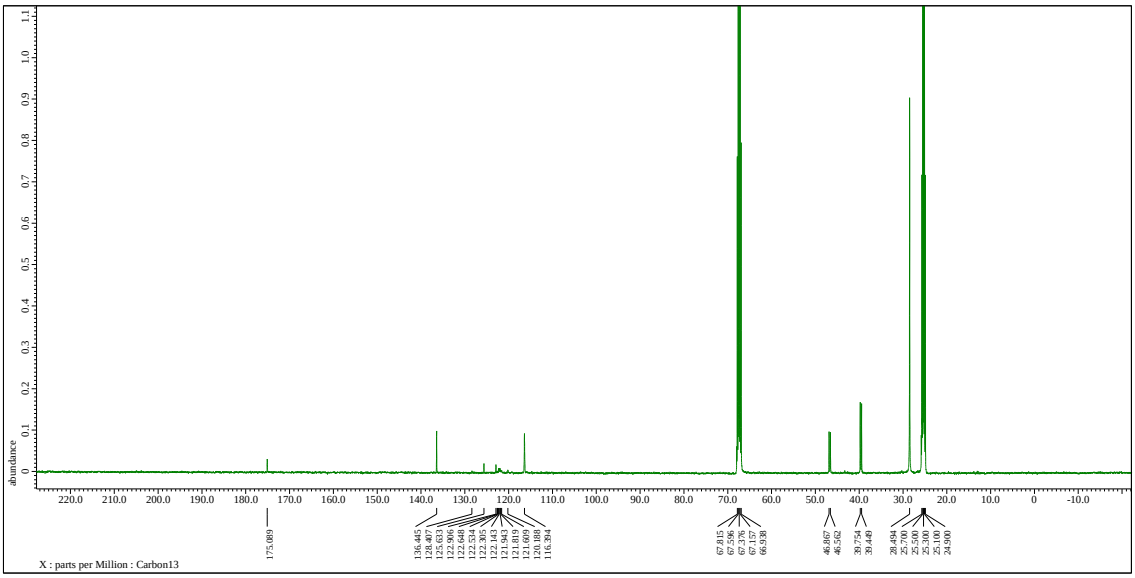

Supplementary Figure 91. $^{13}C\{^{1}H\}$ NMR of **4f**.

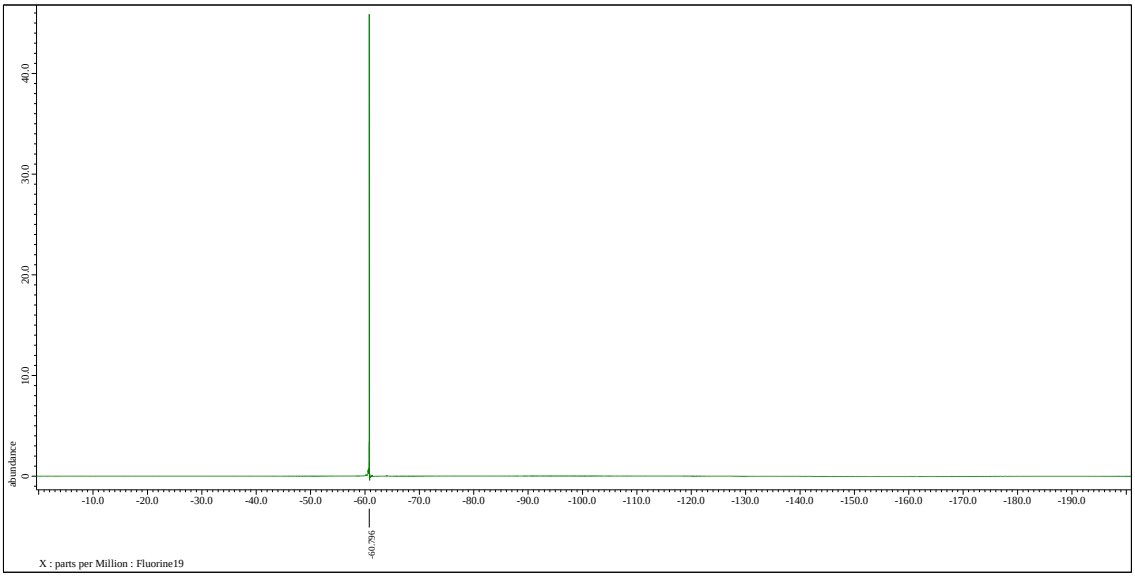

Supplementary Figure 92. ^{19}F NMR of **4f**.

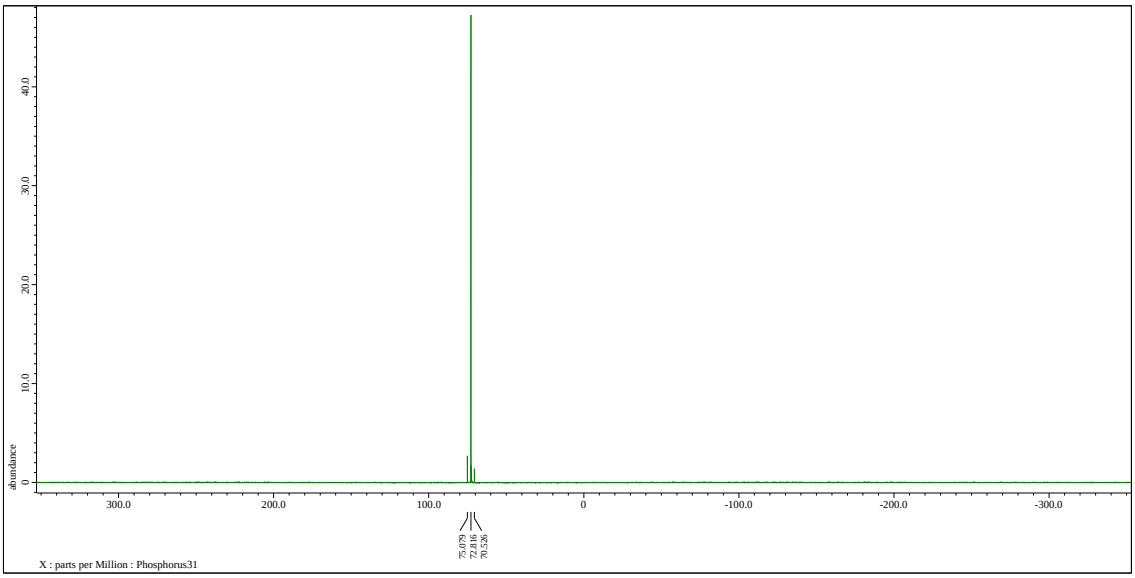

Supplementary Figure 93. $^{31}P\{^{1}H\}$ NMR of **4f**.

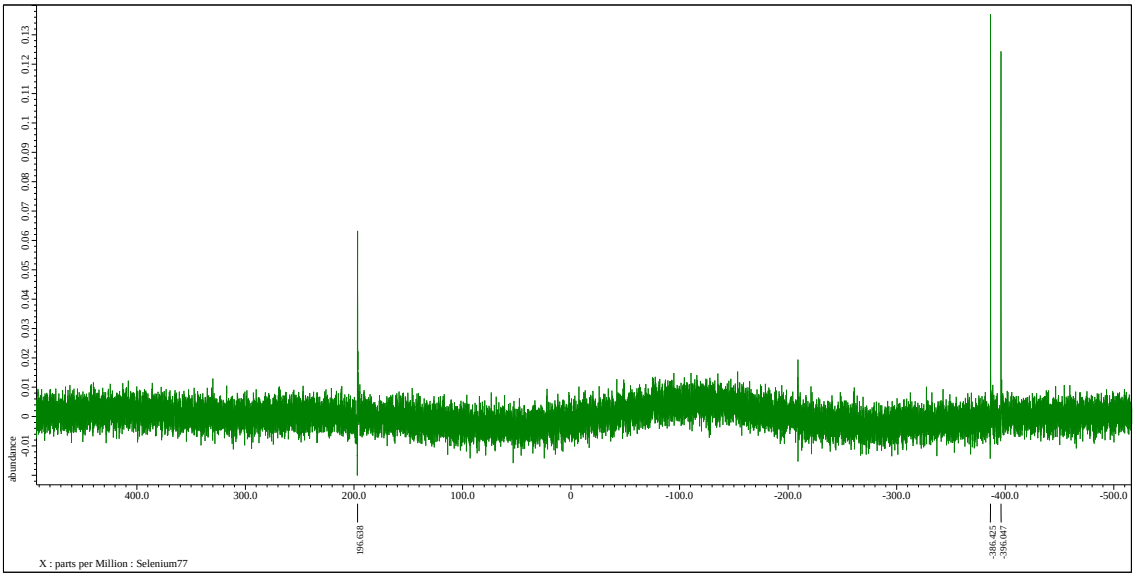

Supplementary Figure 94. $^{77}Se\{^{1}H\}$ NMR of **4f**.

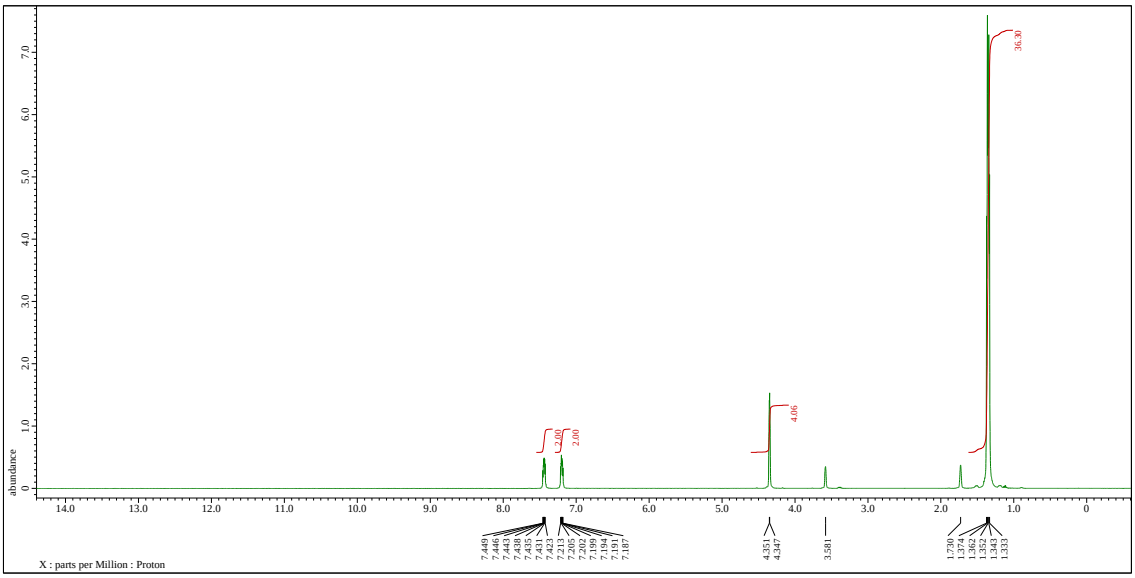

Supplementary Figure 95. ^{1}H NMR of **6a**.

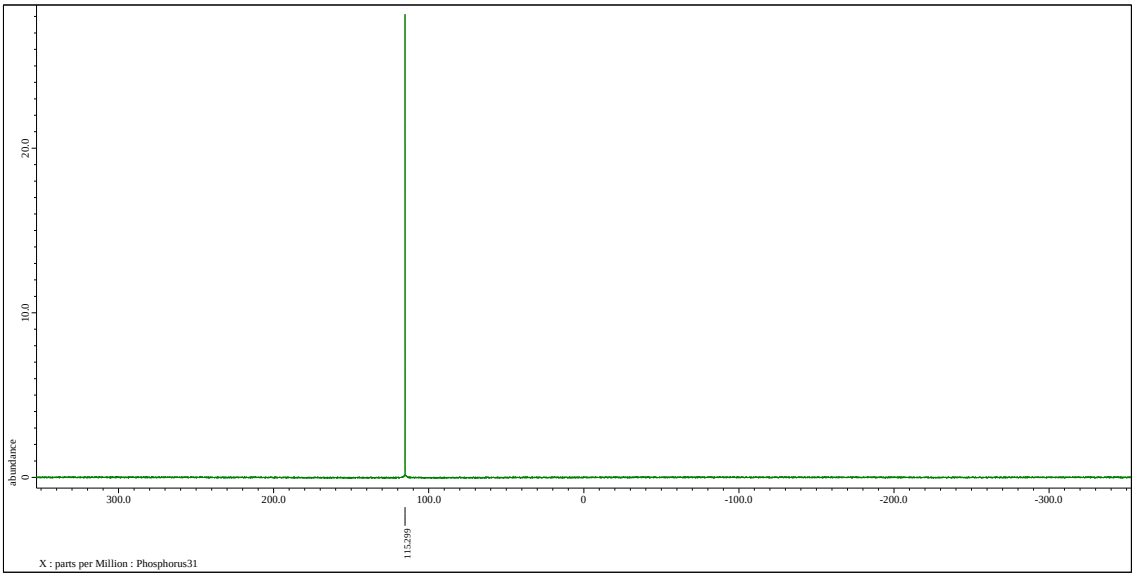

Supplementary Figure 96. $^{31}P\{^{1}H\}$ NMR of **6a**.

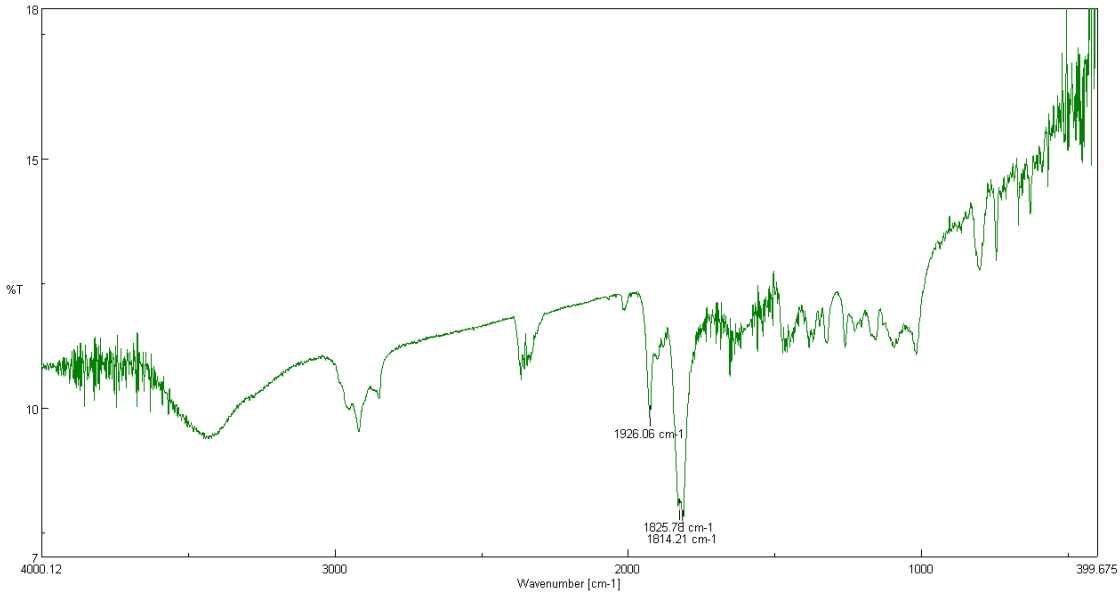

Supplementary Figure 97. IR spectrum (KBr) of **6a**.

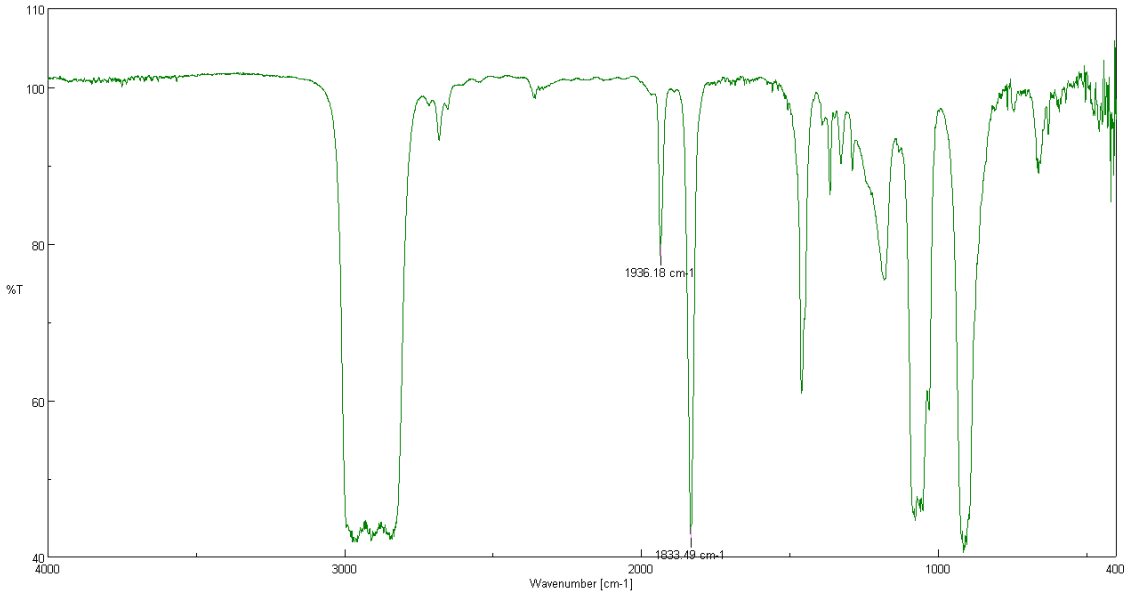

Supplementary Figure 98. IR spectrum (THF) of **6a**.

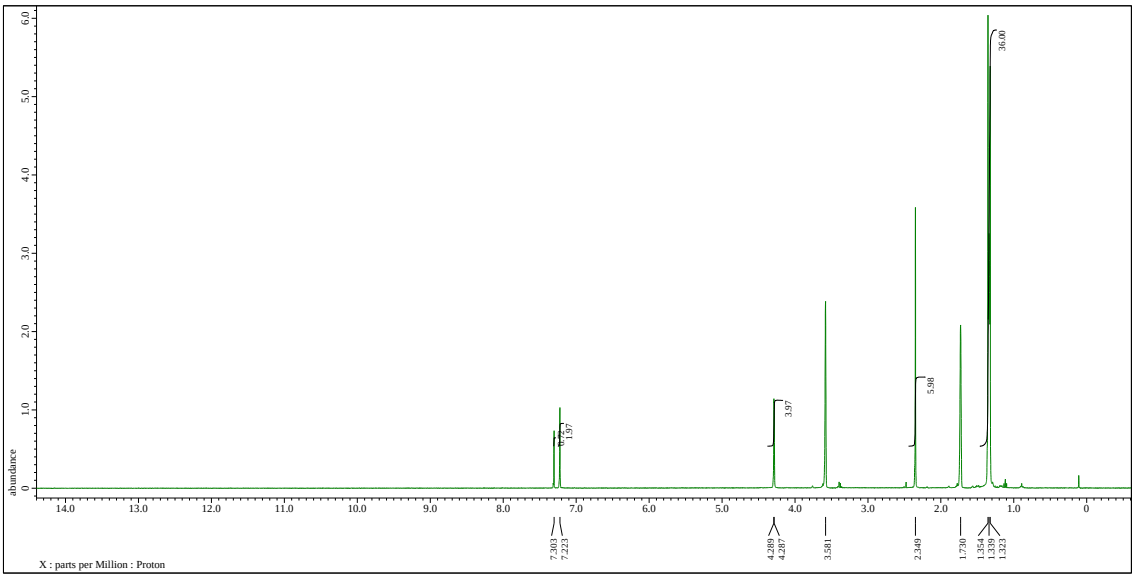

Supplementary Figure 99. ^{1}H NMR of **6b**.

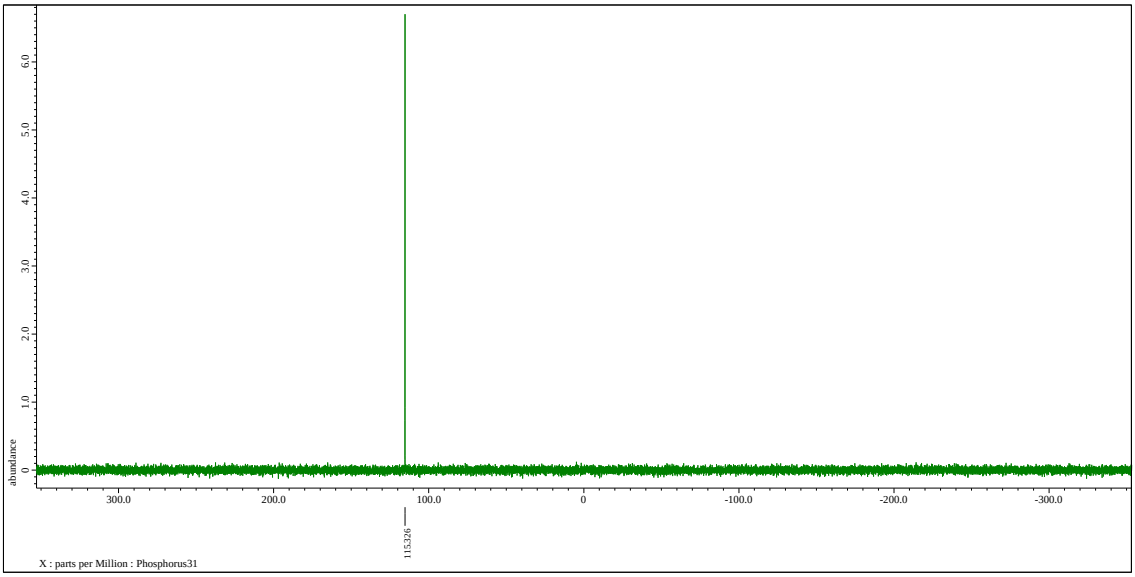

Supplementary Figure 100. $^{31}P\{^{1}H\}$ NMR of **6b**.

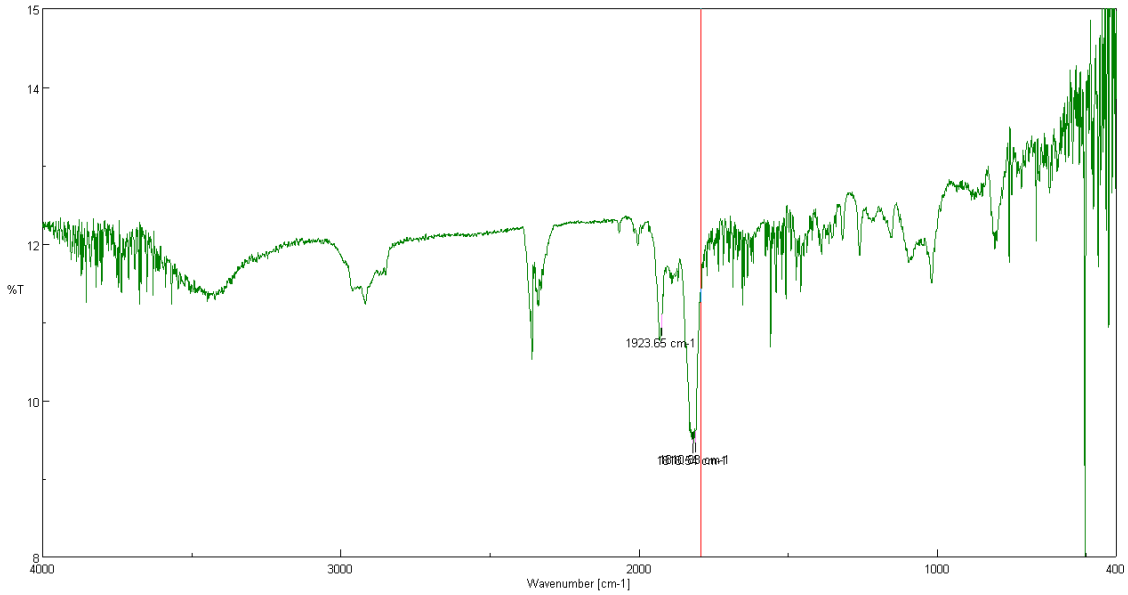

Supplementary Figure 101. IR spectrum (KBr) of **6b**.

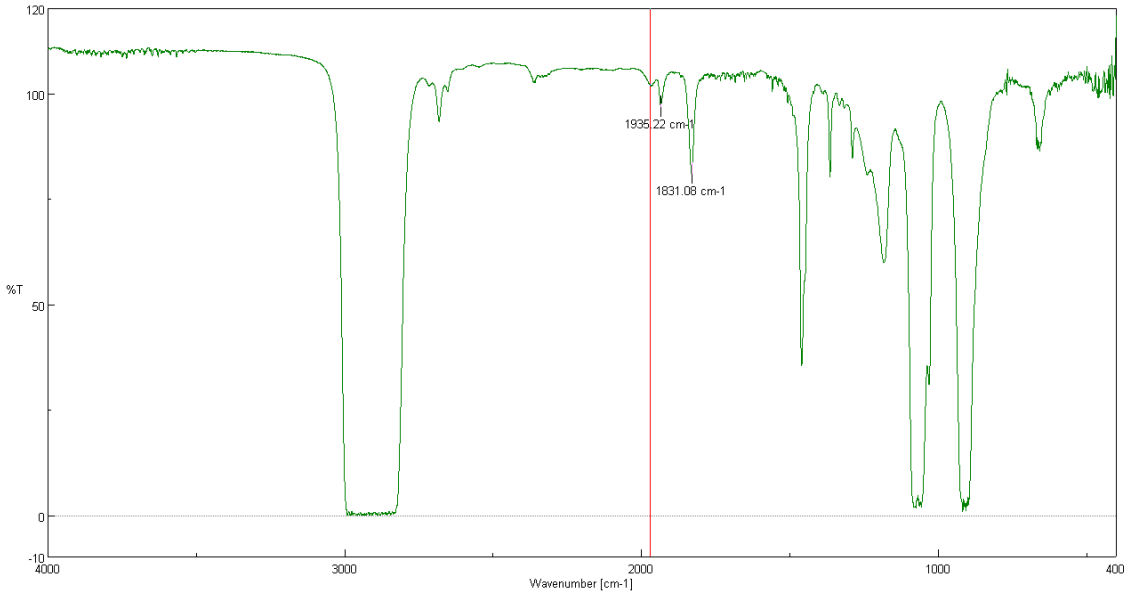

Supplementary Figure 102. IR spectrum (THF) of **6b**.

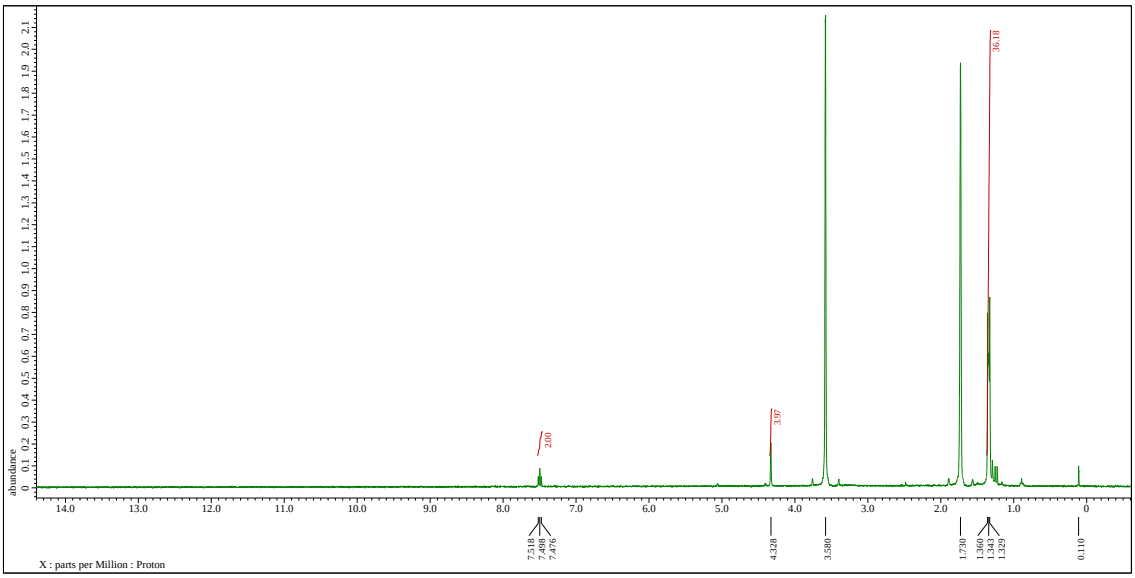

Supplementary Figure 103. ^{1}H NMR of **6c**.

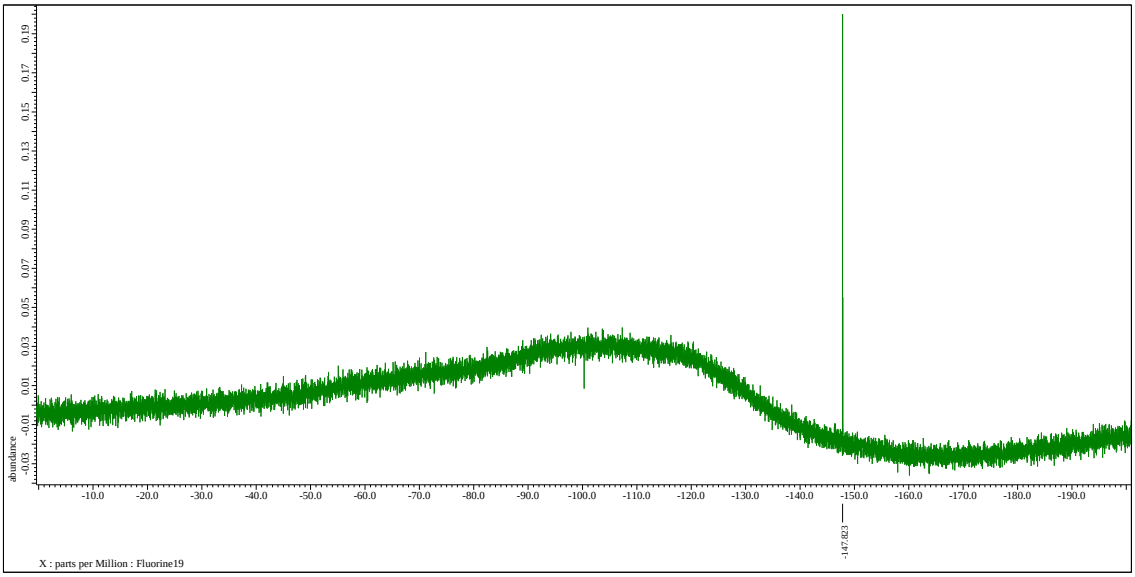

Supplementary Figure 104. ^{19}F NMR of **6c**.

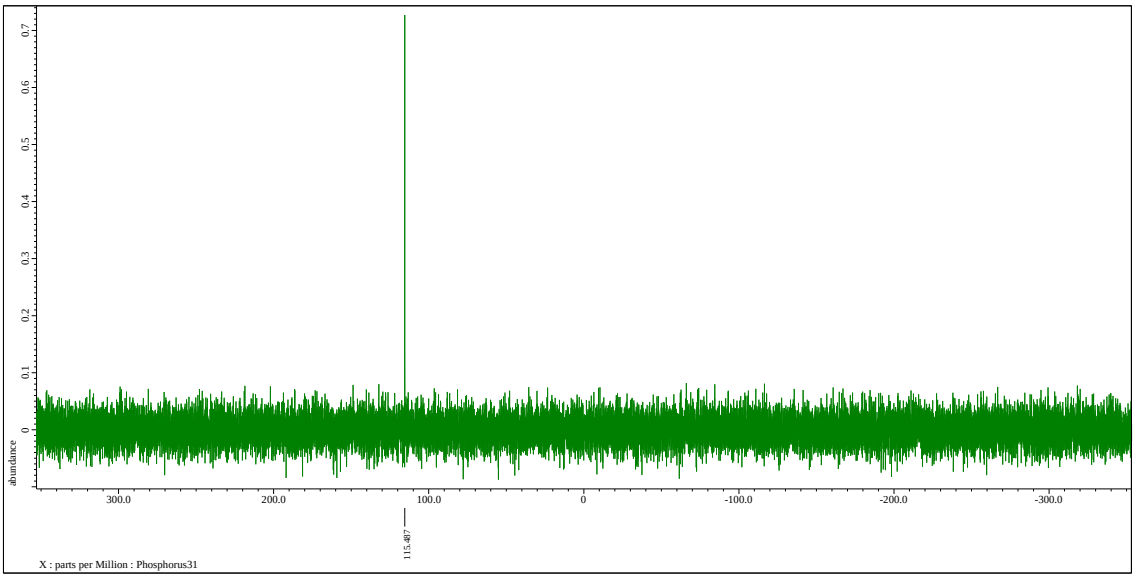

Supplementary Figure 105. $^{31}P\{^{1}H\}$ NMR of **6c**.

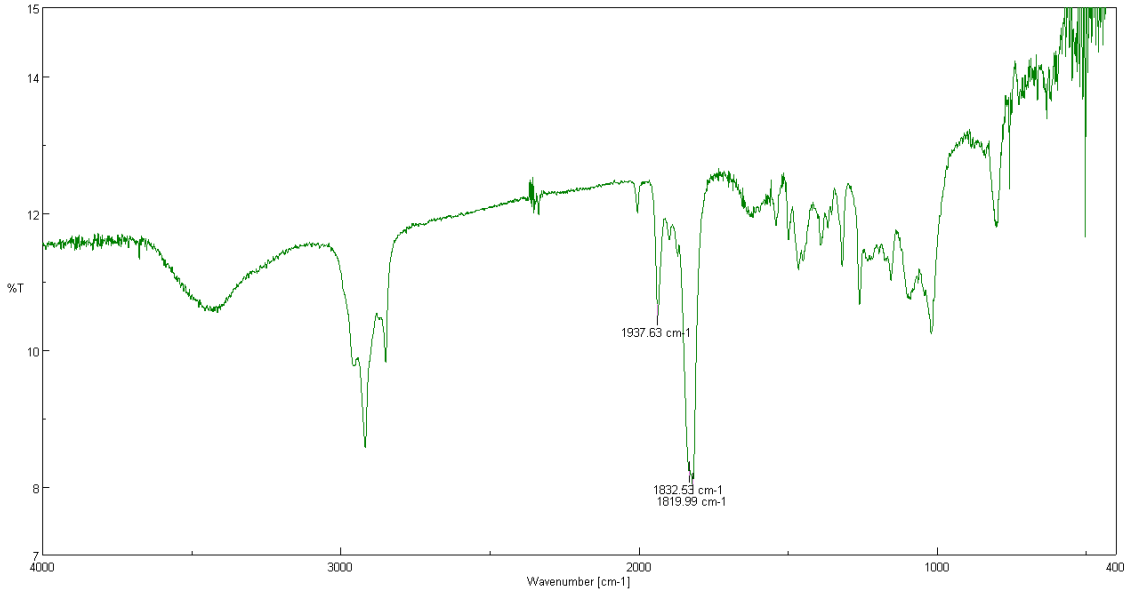

Supplementary Figure 106. IR spectrum (KBr) of **6c**.

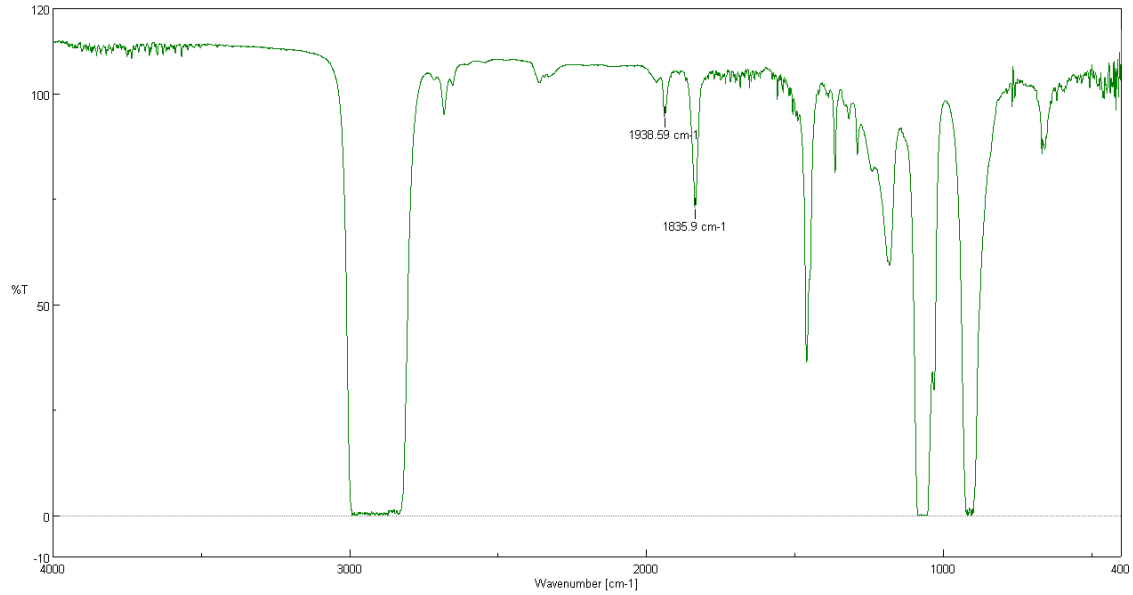

Supplementary Figure 107. IR spectrum (THF) of **6c**.

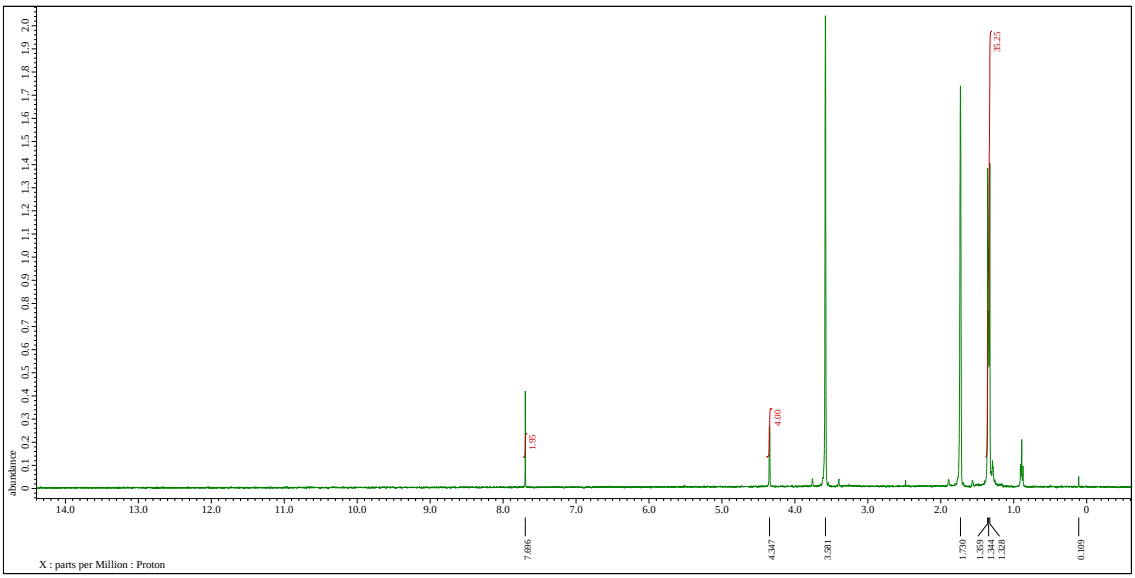

Supplementary Figure 108. ^{1}H NMR of **6d**.

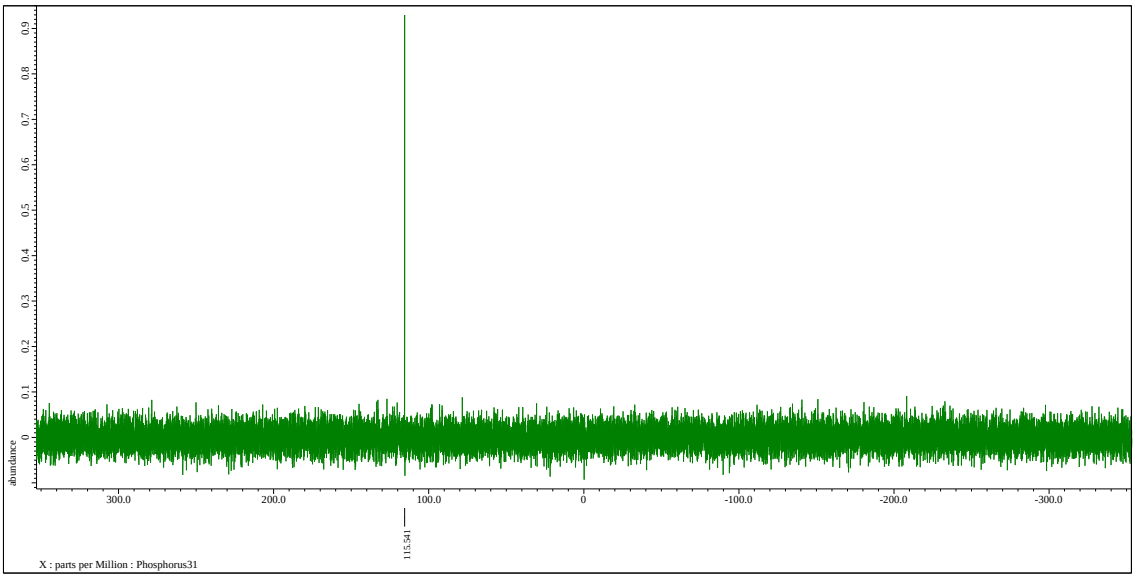

Supplementary Figure 109. $^{31}P\{^{1}H\}$ NMR of **6d**.

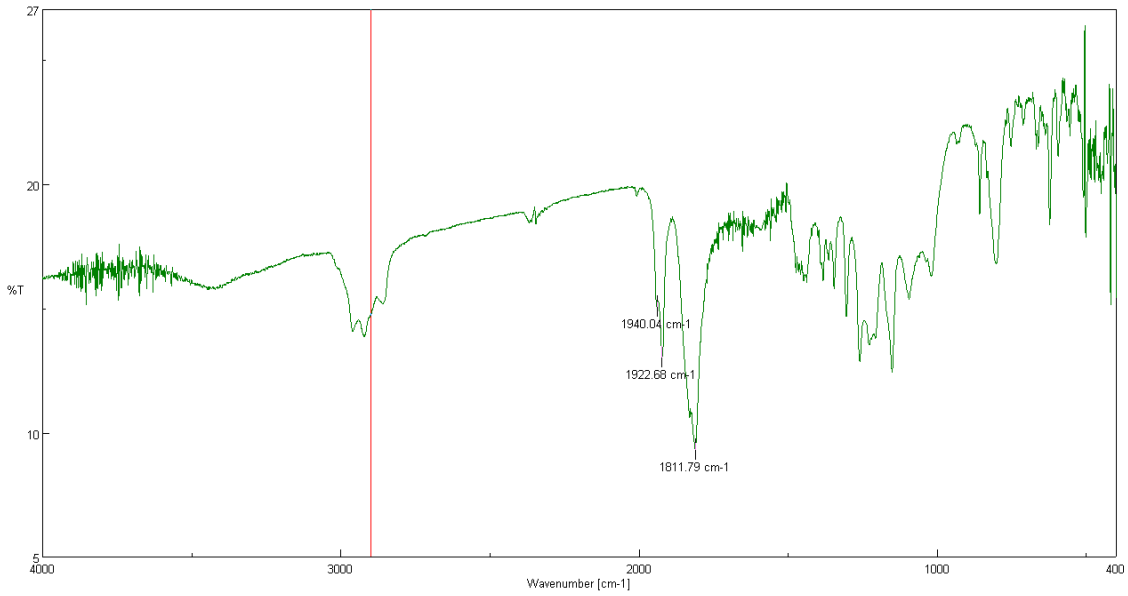

Supplementary Figure 110. IR spectrum (KBr) of **6d**.

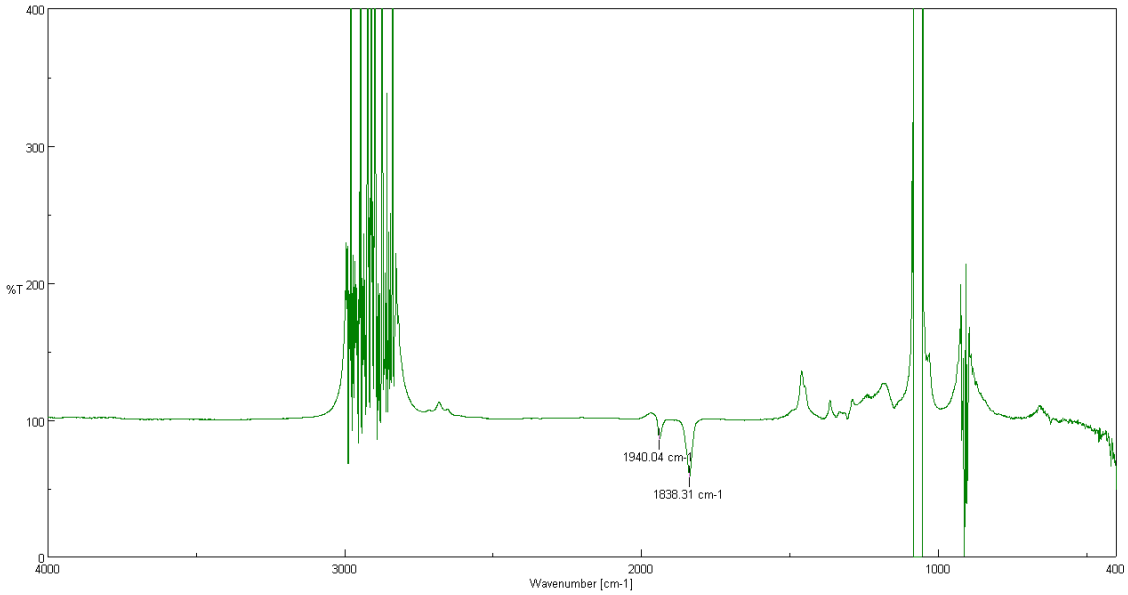

Supplementary Figure 111. IR spectrum (THF) of **6d**.

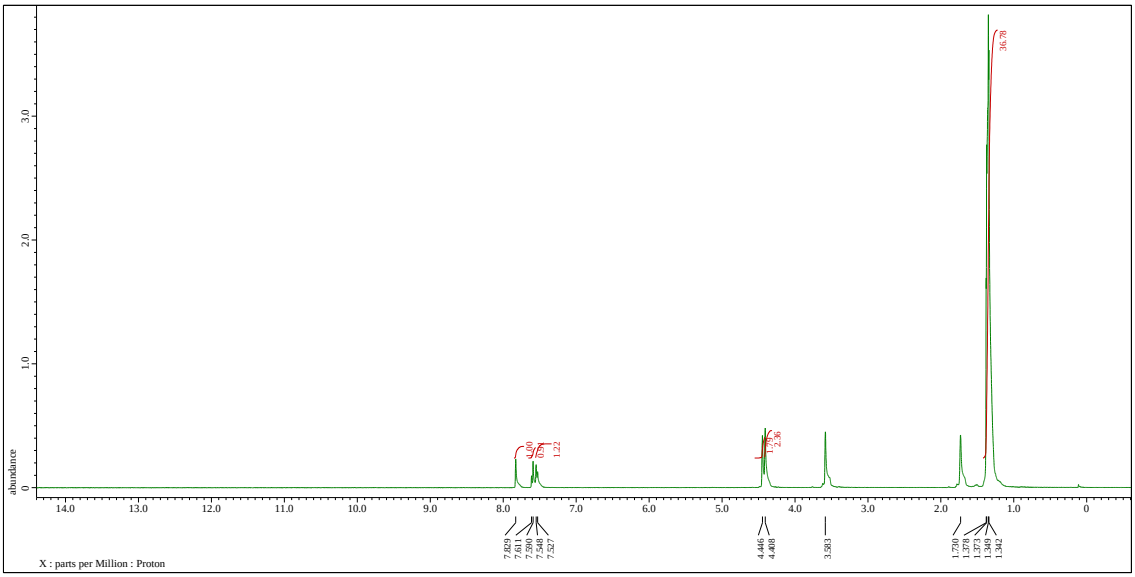

Supplementary Figure 112. ^{1}H NMR of **6e**.

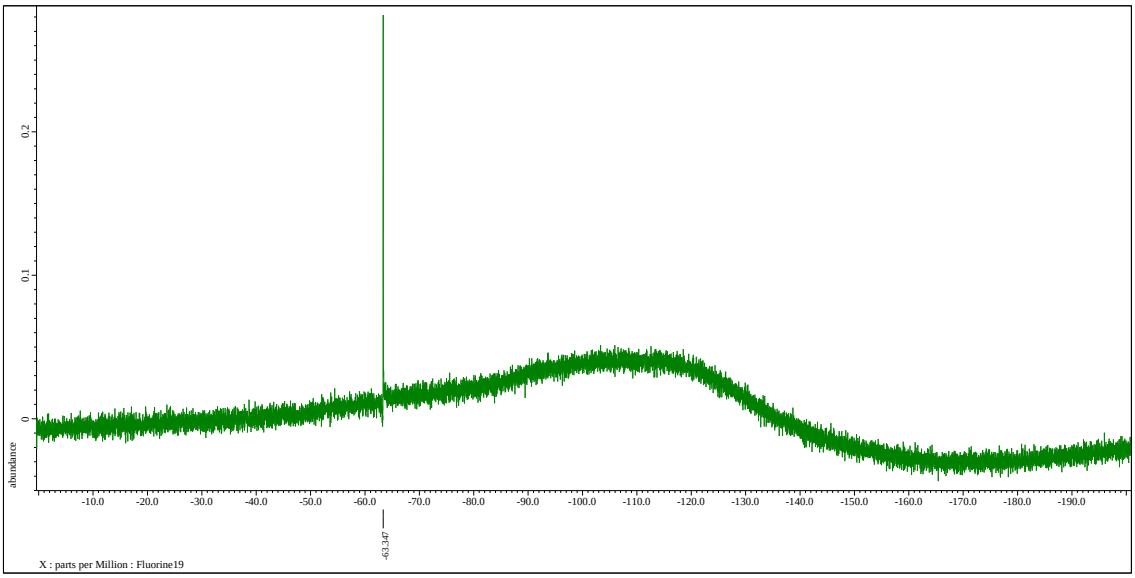

Supplementary Figure 113. ^{19}F NMR of **6e**.

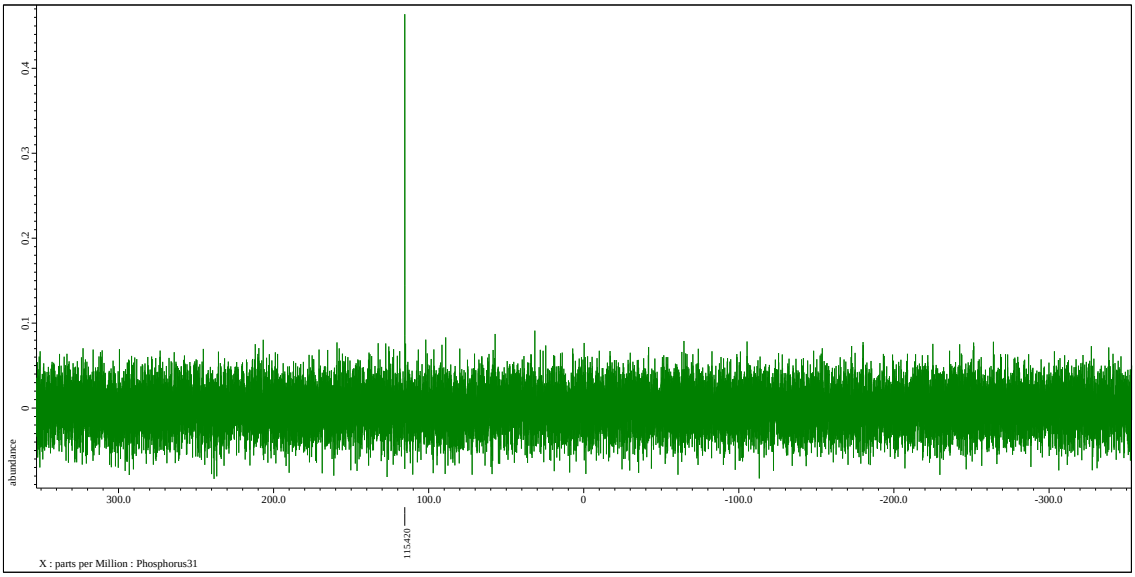

Supplementary Figure 114. $^{31}P\{^{1}H\}$ NMR of **6e**.

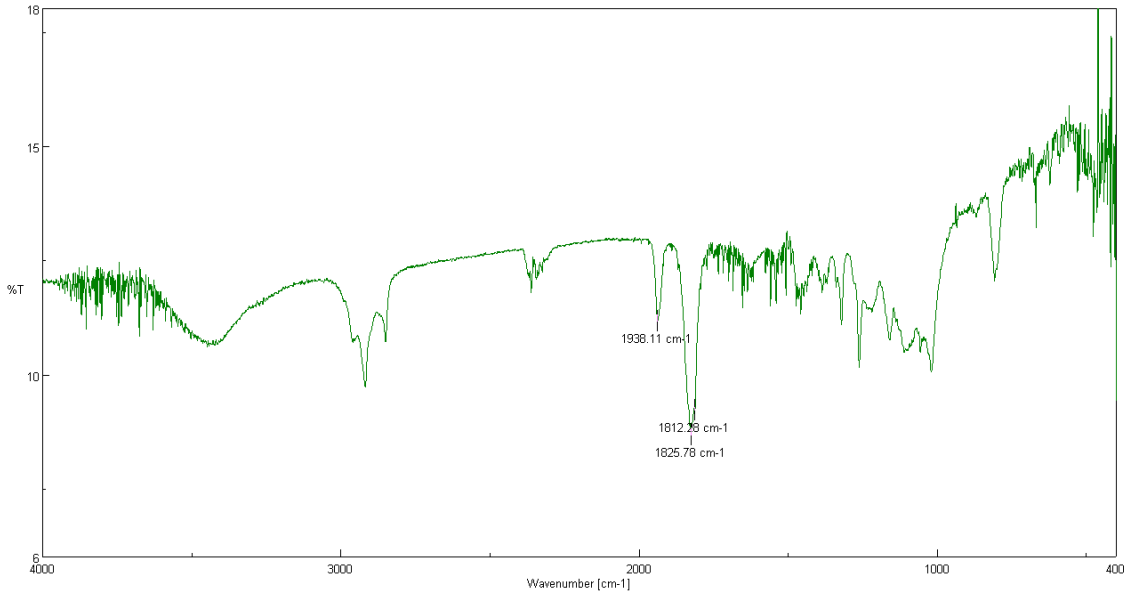

Supplementary Figure 115. IR spectrum (KBr) of **6e**.

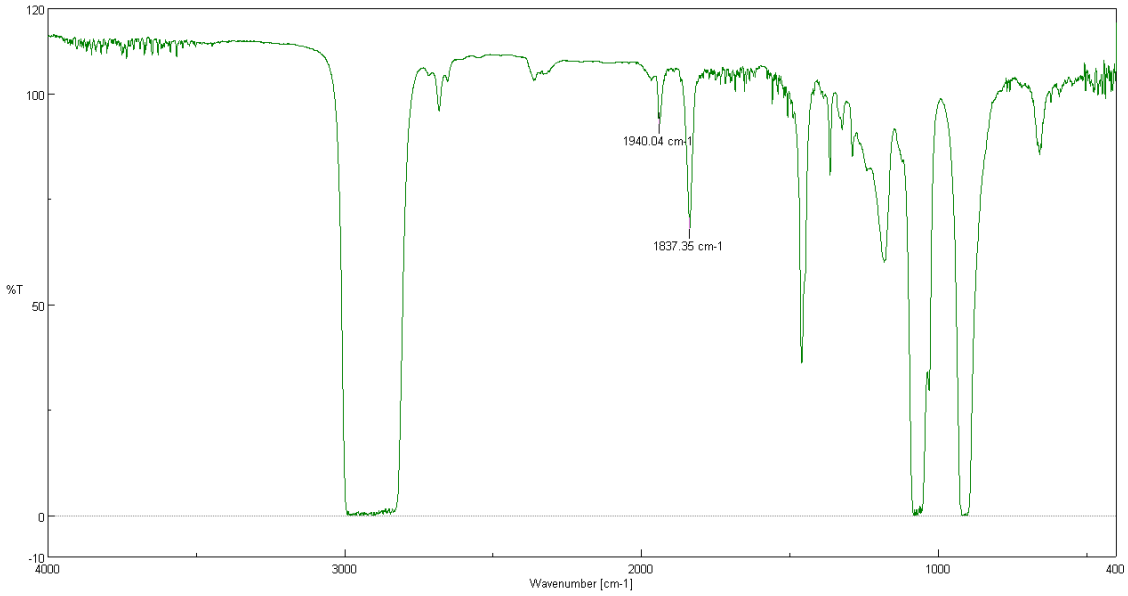

Supplementary Figure 116. IR spectrum (THF) of **6e**.

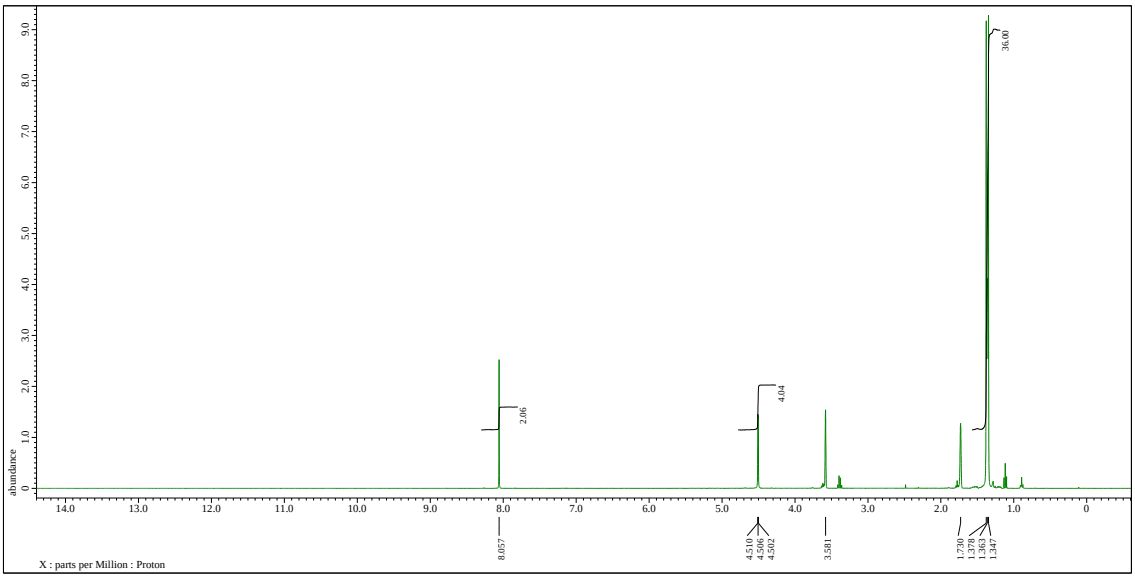

Supplementary Figure 117. ^{1}H NMR of **6f**.

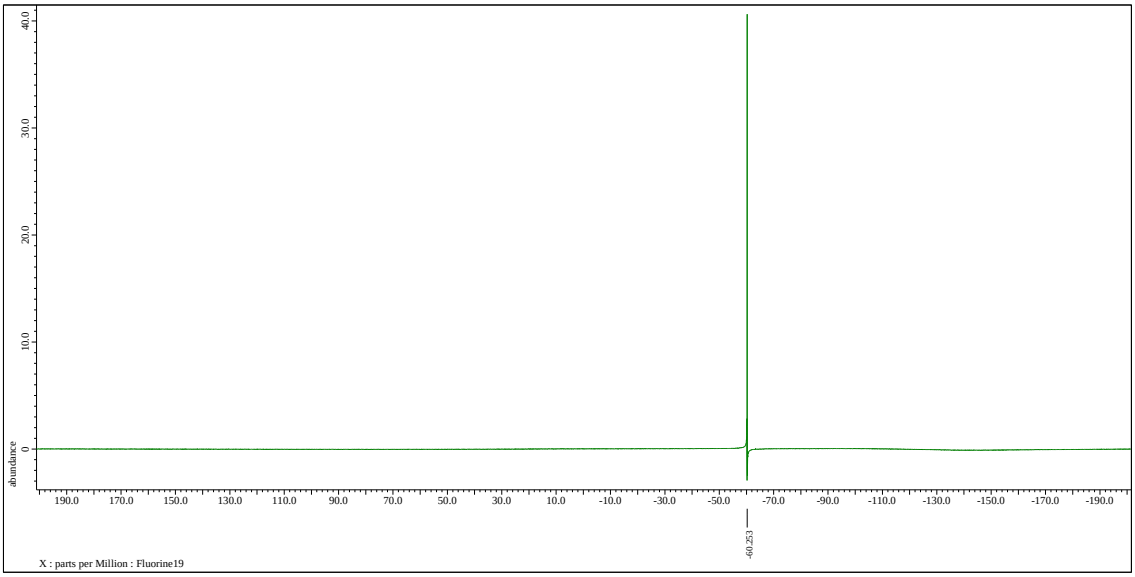

Supplementary Figure 118. ^{19}F NMR of **6f**.

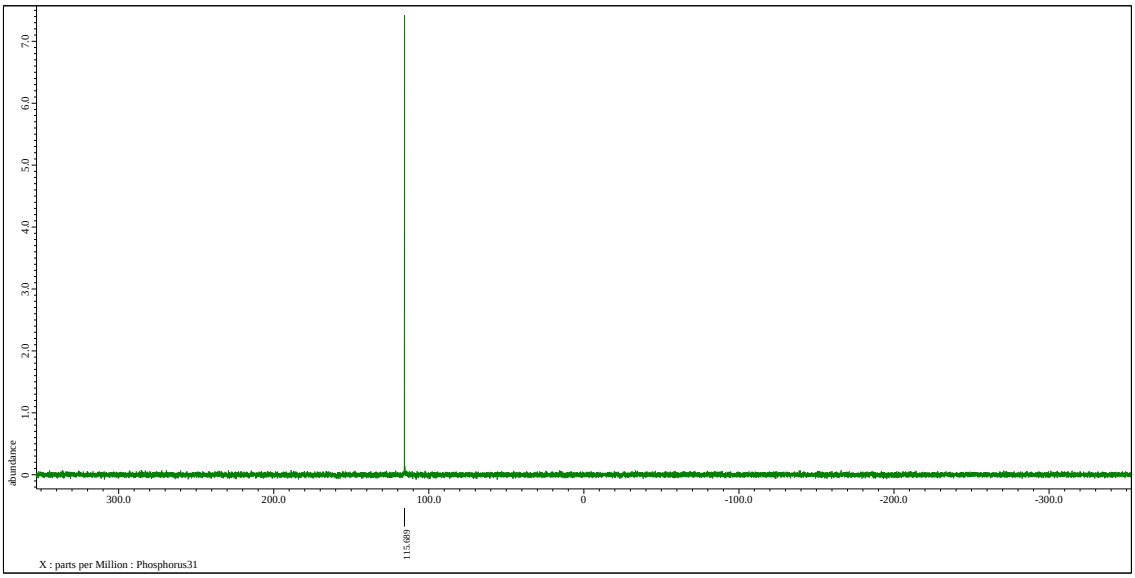

Supplementary Figure 119. $^{31}P\{^{1}H\}$ NMR of **6f**.

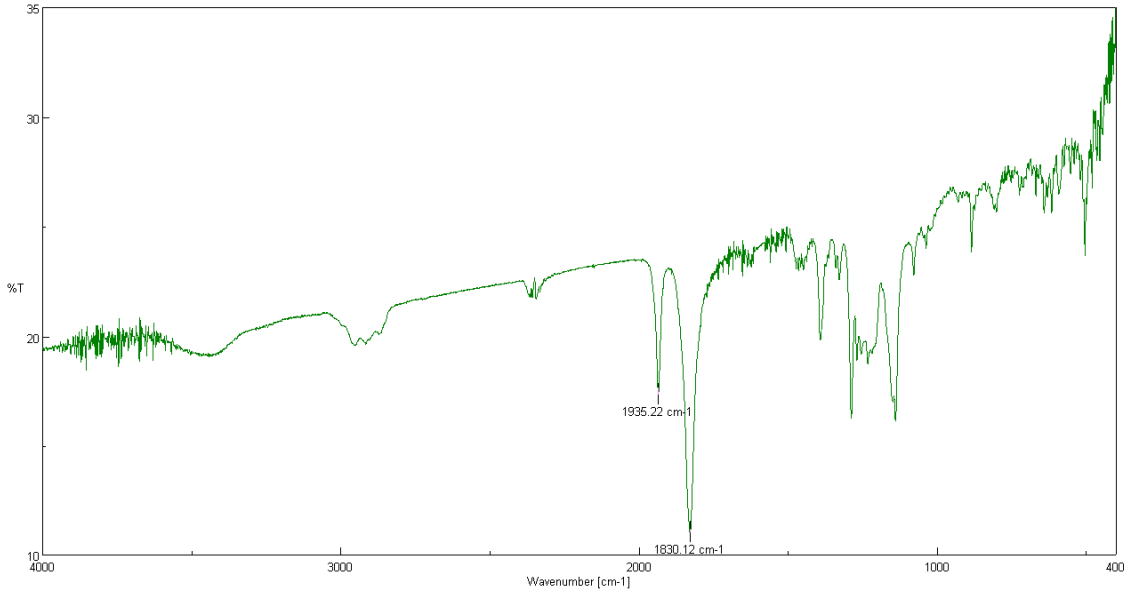

Supplementary Figure 120. IR spectrum (KBr) of **6f**.

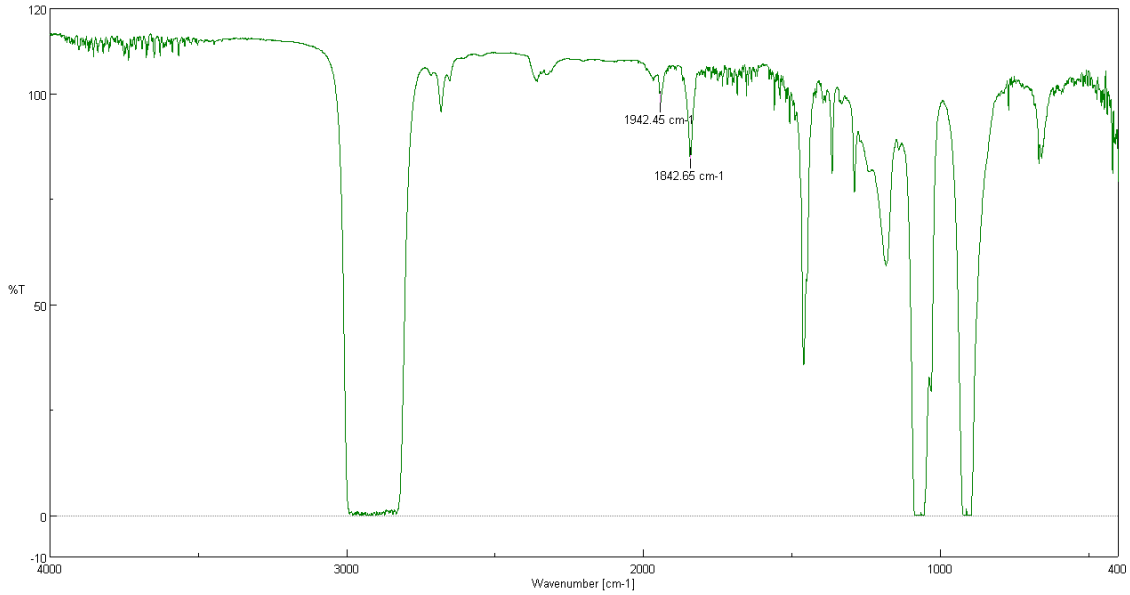

Supplementary Figure 121. IR spectrum (THF) of **6f**.

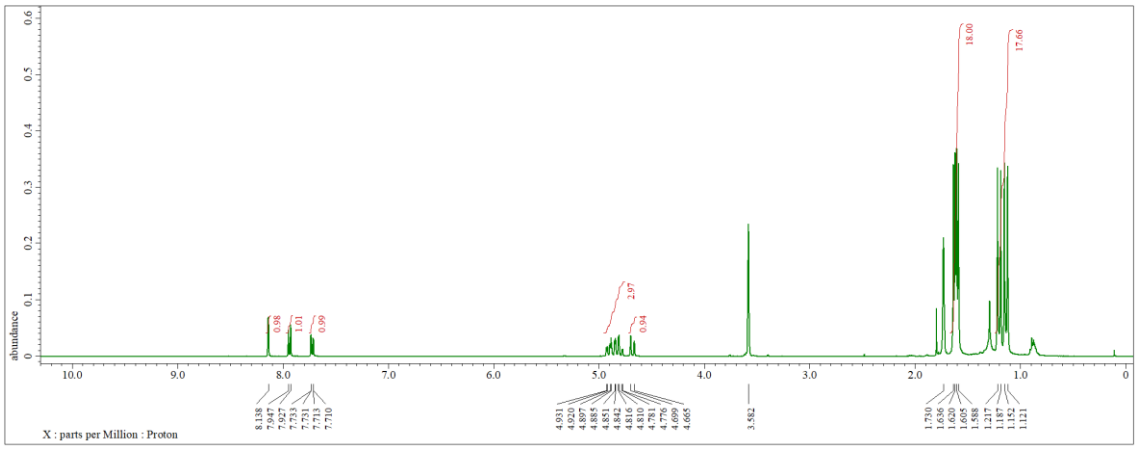

Supplementary Figure 122. ^{1}H NMR of **2e**.

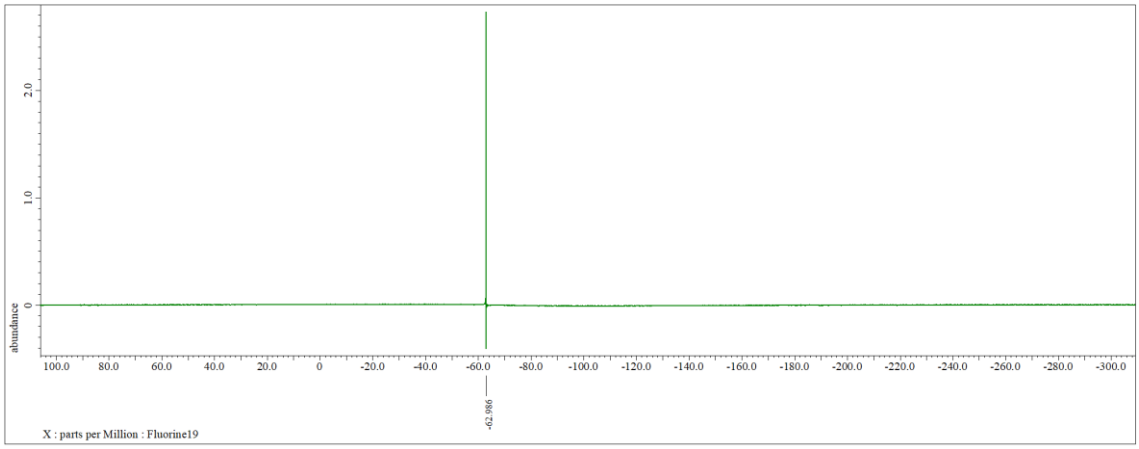

Supplementary Figure 123. ^{19}F NMR of **2e**.

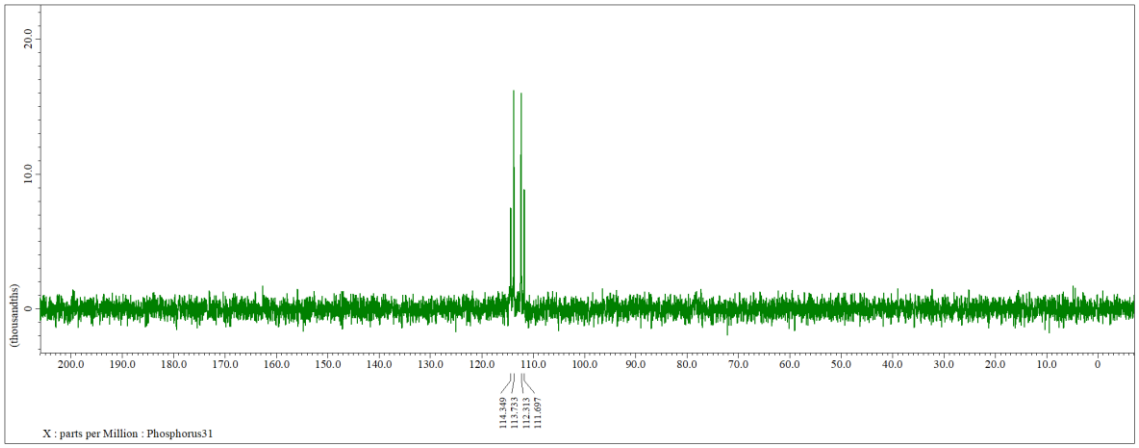

Supplementary Figure 124. ^{31}P{^{1}H} NMR of **2e**.

8. Supplementary references

S1. Bain, G. A. & Berry, J. F. Diamagnetic Corrections and Pascal's Constants. *J. Chem. Educ.* **85**, 532 (2008).

S2. Eizawa, A., Arashiba, K., Egi, A., Tanaka, H., Nakajima, K., Yoshizawa, K. & Nishibayashi, Y. Catalytic Reactivity of Molybdenum-Trihalide Complexes Bearing PCP-Type Pincer Ligands. *Chem. - Asian J.* **14**, 2091−2096 (2019).

S3. Ashida, Y., Onozuka, Y., Arashiba, K., Konomi, A., Tanaka, H., Kuriyama, S., Yamazaki, Y., Yoshizawa, K. & Nishibayashi, Y. Catalytic nitrogen fixation using visible light energy. *Nat. Commun*. **13**, 7263 (2022).

S4. Wietz, I. S. & Rabinovitz, M. The application of C_8K for organic synthesis: reduction of substituted naphthalenes. *J. Chem. Soc., Perkin Trans.* **1**, 117−120 (1993).

S5. Adhikari, D., Mossin, S., Basuli, F., Huffman, J. C., Szilagyi, R. K., Meyer, K., & Mindiola, D. J. Structural, Spectroscopic, and Theoretical Elucidation of a Redox-Active Pincer-Type Ancillary Applied in Catalysis. *J. Am. Chem. Soc.* **130**, 3676−3682 (2008).

S6. Robbins, J. L., Edelstein, N., Spencer, B. & Smart, J. C. Syntheses and electronic-structures of decamethylmetallocenes. *J. Am. Chem. Soc.* **104**, 1882−1893 (1982).

S7. Mandel, L. R., Porter, C. C., Kuehl, F. A Jr., Jensen, M. P., Schmitt, S. M., Windholz, T. B., Beattie T. R., Carty, J. A., Christensen, B. G. & Shen, T.-Y. Inhibition of adrenal phenethanolamine N-methyltransferase by substituted benzimidazoles. *J. Med. Chem.* **13**, 1043−1047 (1970).

S8. Stoffelbach, F., Saurenz, D., & Poli, R. Improved preparations of molybdenum coordination compounds from tetrachlorobis(diethyl ether)molybdenum(IV). *Eur. J. Inorg. Chem.* **2001**, 2699−2703 (2001).

S9. George, W. W. & Brian, E. H. Synthetic routes to alumina-supported molybdenum subcarbonyls. The effect of the supported complex on olefin metathesis. *Organometallics* **6**, 2494−2498 (1987).

S10. Watson, P. L., Tulip, T. H. & Williams, I. Defluorination of perfluoroolefins by divalent lanthanoid reagents: activating C–F bonds. *Organometallics* **9**, 1999–2009 (1990).

S11. Eizawa, A., Arashiba, K., Tanaka, H., Kuriyama, S., Matsuo, Y., Nakajima, K., Yoshizawa, K. & Nishibayashi, Y. Remarkable Catalytic Activity of Dinitrogen-Bridged Dimolybdenum Complexes Bearing NHC-Based PCP-Pincer Ligands toward Nitrogen Fixation. *Nat. Commun.* **8**, 14874 (2017).

S12. Weatherburn, M. W. Phenol-hypochlorite reaction for determination of ammonia. *Anal. Chem.* **39**, 971–974 (1967).

S13. CrystalStructure 4.3.1: Single Crystal Structure Analysis Software; Rigaku Corp: Tokyo, Japan, and MSC: The Woodlands, TX, 2018.

S14. Altomare, A. et al. SIR97: a new tool for crystal structure determination and refinement. *J. Appl. Crystallogr.* **32**, 115–119 (1999).

S15. Sheldrick, G. M. A short history of SHELX. *Acta Crystallogr. A* **64**, 112–122 (2008).

S16. Sheldrick, G. M. SHELXT: Integrating space group determination and structure solution. *Acta Crystallogr. A* **70**, C1437 (2014).

S17. Sheldrick, G. M. Crystal structure refinement with SHELXL. *Acta Crystallogr. C* **71**, 3–8 (2015).

S18. Spek, A. L. PLATON SQUEEZE: a tool for the calculation of the disordered solvent contribution to the calculated structure factors. *Acta Crystallogr. C* **71**, 9 (2015).

S19. Gaussian 09, Revision E.01, Frisch, M. J.; Trucks, G. W.; Schlegel, H. B.; Scuseria, G. E.; Robb, M. A.; Cheeseman, J. R.; Scalmani, G.; Barone, V.; Mennucci, B.; Petersson, G. A.; Nakatsuji, H.; Caricato, M.; Li, X.; Hratchian, H. P.; Izmaylov, A. F.; Bloino, J.; Zheng, G.; Sonnenberg, J. L.; Hada, M.; Ehara, M.; Toyota, K.; Fukuda, R.; Hasegawa, J.; Ishida, M.; Nakajima, T.; Honda, Y.; Kitao, O.; Nakai, H.; Vreven, T.; Montgomery, J. A., Jr.; Peralta, J. E.; Ogliaro, F.; Bearpark, M.; Heyd, J. J.; Brothers, E.; Kudin, K. N.; Staroverov, V. N.; Keith, T.; Kobayashi, R.; Normand, J.; Raghavachari, K.; Rendell, A.; Burant, J. C.; Iyengar, S. S.; Tomasi, J.; Cossi, M.; Rega, N; Millam, J. M.; Klene, M.; Knox, J. E.; Cross, J. B.; Bakken, V.; Adamo, C.; Jaramillo, J.; Gomperts, R.; Stratmann, R. E.; Yazyev, O.; Austin, A. J.; Cammi, R.; Pomelli, C.; Ochterski, J. W.; Martin, R. L.; Morokuma, K.; Zakrzewski, V. G.; Voth, G. A.; Salvador, P.; Dannenberg, J. J.; Dapprich, S.; Daniels, A. D.; Farkas, O.; Foresman, J. B.; Ortiz, J. V.; Cioslowski, J.; Fox, D. J. Gaussian, Inc., Wallingford CT, 2013.

S20. Becke, A. D. Density-functional exchange-energy approximation with correct asymptotic behavior. *Phys. Rev. A* **38**, 3098–3100 (1988).

S21. Becke, A. D. Density-functional thermochemistry. III. The role of exact exchange. *J. Chem. Phys.* **98**, 5648–5652 (1993).

S22. Lee, C.; Yang, W.; Parr, R. G. Development of the Colle-Salvetti correlation-energy formula into a functional of the electron density. *Phys. Rev. B* **37**, 785–789 (1988).

S23. Vosko, S. H.; Wilk, L.; Nusair, M. J. Accurate spin-dependent electron liquid correlation energies for local spin density calculations: a critical analysis. *Can. J. Phys.* **58**, 1200–1211 (1980).

S24. Grimme, S.; Antony, J.; Ehrlich, S.; Krieg, H. A consistent and accurate ab initio parametrization of density functional dispersion correction (DFT-D) for the 94 elements H-Pu. *J. Phys. Chem.* **132**, 154104 (2010).

S25. Dolg, M.; Wedig, U.; Stoll, H.; Preuß, H. Energy-adjusted ab initio pseudopotentials for the first row transition elements. *J. Chem. Phys*. **86**, 866–872 (1987).

S26. Andrae, D.; Häußermann, U.; Dolg, M.; Stoll, H.; Preuß, H. Energy-adjustedab initio pseudopotentials for the second and third row transition elements. *Theor. Chim. Acta.* **77**, 123–141 (1990).

S27. Ditchfield, R.; Hehre, W. J.; Pople, J. A. Self-consistent molecular-orbital methods. IX. An extended Gaussian-type basis for molecular-orbital studies of organic molecules. *J. Chem. Phys*. **54**, 724–728 (1971).

S28. Hehre, W. J.; Ditchfield, R.; Pople, J. A. Self-consistent molecular orbital methods. XII. Further extensions of Gaussian-type basis sets for use in molecular orbital studies of organic molecules. *J. Chem. Phys.* **56**, 2257–2261 (1972).

S29. Hariharan, P. C.; Pople, J. A. The influence of polarization functions on molecular orbital hydrogenation energies. *Theor. Chem. Acc.* **28**, 213–222 (1973).

S30. Francl, M. M.; Pietro, W. J.; Hehre, W. J.; Binkley, J. S.; Gordon, M. S.; DeFrees, D. J.; Pople, J. A. Self-consistent molecular orbital methods. XXIII. A polarization-type basis set for second-row elements. *J. Chem. Phys*. **77**, 3654–3665 (1982).

S31. Krishnan, R.; Binkley, J. S.; Seeger, R.; Pople, J. A. Self-consistent molecular orbital methods. XX. A basis set for correlated wave functions. *J. Chem. Phys.* **72**, 650–654 (1980).

S32. McLean, A. D.; Chandler, G. S. Contracted Gaussian basis sets for molecular calculations. I. Second row atoms, Z=11–18. *J. Chem. Phys.* **72**, 5639–5648 (1980).

S33. Clark, T.; Chandrasekhar, J.; Spitznagel, G. W.; Schleyer, P. v. R. Efficient diffuse function-augmented basis sets for anion calculations. III. The 3-21+G basis set for first-row elements, Li–F. *J. Comput. Chem.* **4**, 294–301 (1983).

S34. Tomasi, J.; Mennucci, B.; Cammi, R. Quantum mechanical continuum solvation models. *Chem. Rev*. **105**, 2999–3094 (2005).